

UNIVERSIDADE DE SOROCABA
PRÓ-REITORIA DE PÓS-GRADUAÇÃO, PESQUISA, EXTENSÃO E INOVAÇÃO
PROGRAMA DE PÓS-GRADUAÇÃO EM CIÊNCIAS FARMACÊUTICAS

Thais Francine Ribeiro Alves

***Scaffold* acelular baseado em hidrogel com potencial na engenharia de tecido
do miocárdio: Desenvolvimento, Avaliação Mecânica e Biológica**

Sorocaba/SP

2019

Thais Francine Ribeiro Alves

***Scaffold* acelular baseado em hidrogel com potencial na engenharia de tecido do miocárdio: Desenvolvimento, Avaliação Mecânica e Biológica**

Hydrogel-based acellular scaffold with potential in the engineering of myocardial tissue: Development, Mechanical and Biological Evaluation

Tese apresentada ao Programa de Pós-Graduação em Ciências Farmacêuticas da Universidade de Sorocaba, como exigência parcial para obtenção do título de Doutora em Ciências Farmacêuticas.

Orientador: Prof. Dr. Marco Vinícius Chaud

Sorocaba/SP

2019

Ficha Catalográfica

A482s Alves, Thaís Francine Ribeiro
Scaffold acelular baseado em hidrogel com potencial na engenharia de tecido do miocárdio : desenvolvimento, avaliação mecânica e biológica / Thaís Francine Ribeiro Alves. -- 2019.
133 f. : il.

Orientador: Prof. Dr. Marco Vinícius Chaud.
Tese (Doutorado em Ciências Farmacêuticas) - Universidade de Sorocaba, Sorocaba, SP, 2019.

1. Infarto do miocárdio. 2. Materiais biomédicos. 3. Polímeros na medicina. I. Chaud, Marco Vinícius. II. Universidade de Sorocaba. III. Título.

Thais Francine Ribeiro Alves

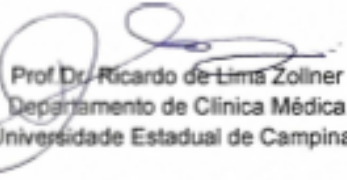
Scaffold acelular baseado em hidrogel com potencial na engenharia de tecido do miocárdio: Desenvolvimento, Avaliação Mecânica e Biológica

Tese apresentada ao Programa de Pós-Graduação em Ciências Farmacêuticas da Universidade de Sorocaba, como exigência parcial para obtenção do título de Doutora em Ciências Farmacêuticas.

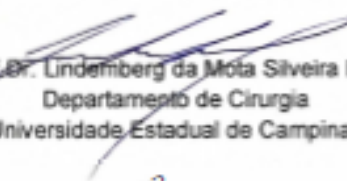
Banca examinadora:



Prof. Dr. Marco Vinicius Chaud
Universidade de Sorocaba



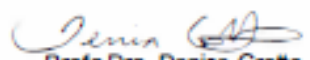
Prof. Dr. Ricardo de Lima Zolner
Departamento de Clínica Médica
Universidade Estadual de Campinas



Prof. Dr. Lindemberg da Mota Silveira Filho
Departamento de Cirurgia
Universidade Estadual de Campinas



Prof. Dr. Alexandro Barbosa de Souza
Departamento de Engenharia de Biomateriais e Bioprocessos
Universidade Estadual de Campinas



Profa. Dra. Denise Grotto
Universidade de Sorocaba

Dedico este trabalho à minha família, esposo e amigos
por estarem ao meu lado em todos os momentos.

AGRADECIMENTOS

Este espaço é dedicado àqueles que, de alguma forma, contribuíram para que esta dissertação fosse realizada. Não sendo possível nomear a todos, há, no entanto alguns a quem não posso deixar de manifestar o meu apreço e agradecimento sincero.

Agradeço a Deus que esteve sempre ao meu lado durante esta caminhada, que muita das vezes não foi nada fácil. Porém, Ele me deu duas características que estão inseridas em minha alma: persistência e determinação! Contudo, não teria chegado até aqui sem a ajuda de alguns anjos que Ele me enviou, a saber:

A meus pais, José e Susana, meu infinito agradecimento. Sempre acreditaram em minha capacidade e me acharam A MELHOR de todas, mesmo não sendo. Isso só me fortaleceu e me fez tentar não ser A MELHOR, mas a fazer o melhor de mim. Obrigada pelo amor incondicional!

Ao meu esposo Danilo, ouvinte atento de algumas dúvidas, inquietações, desânimos e sucessos, pelo apoio, pela confiança e pela valorização sempre tão entusiasta do meu trabalho, dando-me, desta forma, coragem para ultrapassar a culpa pelo tempo que a cada dia lhe subtraía.

Aos meus irmãos, Maria Eduarda e Mateus que sempre se orgulharam de mim e confiaram em meu trabalho. Obrigada pela confiança!

Ao meu orientador Prof. Dr. Marco Vinicius Chaud que acreditou em meu potencial de uma forma a que eu não acreditava ser capaz de corresponder. Sempre disponível e disposto a ajudar, querendo que eu aproveitasse cada segundo dentro do mestrado para absorver todo conhecimento possível. Você foi e é referência profissional e pessoal para meu crescimento. Obrigada por estar ao meu lado e acreditar tanto em mim!

As minhas eternas amigas Francielle Cristina Corrêa Neves Lopes, Katiusca da Silva Pontes e Juliana Ferreira Souza.

Aos profs. Dra. Denise Grotto, Dra. Renata Lima, Dr. Norberto Aranha, Dr. José Martins de Oliveira Junior e Dr. Daniel Komatsu por todo apoio e colaboração!

À Uniso por ter me acolhido durante a graduação e por possibilitar a realização do mestrado.

À Capes pelo incentivo financeiro.

RESUMO

A doença cardiovascular é um dos problemas de saúde mais graves do mundo, e gera um alto nível de mortalidade a cada ano. A medicina regenerativa é um campo emergente que visa melhorar ou reparar o desempenho de um tecido danificado ou de um órgão. Os *scaffolds* são estruturas tridimensionais (3D) e porosas, os quais podem ser produzidos utilizando biopolímeros capazes de mimetizar a matriz extracelular (MEC). Para gerar estrutura lamelar densa e porosa foram utilizados polímeros biomiméticos associado a técnica de compressão plástica. As misturas poliméricas de colágeno, quitosana, fibroína de seda, ácido hialurônico, agente reticulante e com ou sem adição de polianilina, obtido por compressão plástica, foram usadas para obter os dispositivos tridimensionais poroso, anisotrópico e miméticos a matriz extracelular. Desta forma, considerando as estruturas anisotrópicas, as propriedades fisiomecânicas, a compatibilidade celular e a ação protetora contra espécies reativas de oxigênio, os *scaffolds* obtidos neste estudo podem fornecer um caminho para melhorar a remodelação inversa do tecido cardíaco, após o infarto agudo do miocárdio.

Palavras-chave: infarto agudo do miocárdio; engenharia de tecidos; *scaffolds* cardíacos; *scaffold* lamelar denso; *scaffolds* condutivos.

ABSTRACT

Cardiovascular disease is one of the most serious health problems in the world, and generates a high level of mortality each year. Regenerative medicine is an emerging field that aims to improve or repair the performance of a damaged tissue or an organ. Scaffolds are three-dimensional (3D) and porous structures, which can be produced using biopolymers capable of mimicking the extracellular matrix (ECM). To generate a dense and porous lamellar structure, biomimetic polymers were used, associated with a plastic compression technique. Polymeric mixtures of collagen, chitosan, silk fibroin, hyaluronic acid, crosslinking agent and with or without addition of polyaniline, obtained by plastic compression, were used to obtain the three-dimensional porous, anisotropic and mimetic extracellular matrix devices. Thus, considering the anisotropic structures, biomechanical properties, cellular compatibility and protective action against reactive oxygen species, the scaffolds obtained in this study may provide a way to improve the inverse remodeling of cardiac tissue after acute myocardial infarction.

Key words: acute myocardial infarction; fabric engineering; scaffolds; scaffold lamella dense; scaffolds.

LISTA DE ILUSTRAÇÕES

Capítulo 2: “Dense lamellar scaffold as biomimetic materials for reverse engineering of myocardial tissue: preparation, characterization and physiomechanical”

Figure 1 - Dense lamellar scaffold obtained by plastic compression.....	46
Figure 2 - Physiomechanical properties of dense lamellar scaffolds.....	47
Figure 3 - Swelling efficiency profile of dense lamellar scaffolds.....	48
Figure 4 - Morphometric characteristic of dense lamellar scaffolds evaluated by computerized microtomography.....	49
Figure 5 - Scanning electron microscopy of dense lamellar scaffolds.....	50
Figure 6 - Differential scanning calorimetry of COL, CH, SF (panel A), and scaffolds samples (panel B).....	51
Figure 7 - Infrared spectra of COL, CH, SF (panel A) and scaffolds samples (panel B).....	52
Figure 8 - Results of MTT analyses, exposure to control and COL-CH-SF scaffold in H9c2 cells for 24h.....	53
Figure 9 - Results regarding cell growth (H9c2) after exposure to COL-CH-SF.....	53

Capítulo 3: “Design and evaluating of biomimetically inspired dense lamellar scaffold obtained by plastic compression: Development, physiomechanical characterization, and in vitro cellular activities”

Figure 1 - Physiomechanical properties of PA-scaffold and GA-scaffold.....	77
Figure 2 - PBS uptake (A) and retained (B) by scaffold at 37 °C according to cross-linking agent.....	80
Figure 3 - Weight loss (A) and pH value (B) of the scaffolds in PBS at 37 °C according to cross-linking agent.....	81

Figure 4 - SEM of PA- scaffold (A-B) and GA-scaffold (C-D).....	82
Figure 5 - DSC thermogram of excipients, PA-scaffold, and GA-scaffold.....	85
Figure 6 - FTIR spectra of excipients, PA-scaffold, and GA-scaffold.....	86
Figure 7 - Antioxidant activity as a function of time of the scaffolds.....	88
Figure 8 - Results of MTT analyses, exposure to GA-scaffold, PA-scaffold, and scaffold without cross-linking agent in H9c2 cells for 24h.....	89
Figure 9 - Cell growth curve (H9c2) after exposure to GA-scaffold, PA-scaffold, and scaffold without crosslinking agent at 48 and 72h.....	89
Figure 10 - Cell growth curve (H9c2) after exposure to GA-scaffold, PA-scaffold, and scaffold without crosslinking agent at 48 and 72h.....	90

Capítulo 4: “Biomimetic dense lamellar scaffold based on a complex of the polyaniline (PANI) and biopolymers for electroactive and physiomechanical stimulation of the myocardial”

Figure 1 – Illustration of water-soluble PANi-PVP. Route 1 depicts that the polymer in acid medium can be activated by breaking hydrogen bonds. Route 2 depicts that the increase of solubility occurs by steric stabilization.....	101
Figure 2 - UV-Visible spectra of water-soluble polyaniline in emeraldine salt form (A). Residual aniline over 13 hours (B)	110
Figure 3 – FTIR spectra of excipients and PA-scaffold.....	111
Figure 4 – DSC thermogram of excipients and PANi-scaffold.....	113
Figure 5 – Physiomechanical properties of PANi-scaffold.....	114
Figure 6 - Fluid uptake of scaffolds (%) fluid retained both by the whole scaffold structure (A), and by the scaffold material itself (B) in PBS at 37 °C.....	116
Figure 7 - Weight loss (A) and pH value (B) of the scaffolds in PBS at 37 °C according to cross-linking agent.....	117
Figure 8 – Surface Zeta Potential of PANi-scaffold.....	119
Figure 9 – SEM of PANi- scaffold (A-B)	120
Figure 10 – Antioxidant Activity of PANi-scaffold.....	122

Figure 11 – Results of MTT analyses, exposure to PANi-scaffold, and scaffold without crosslinking agent in H9c2 cells for 24h.....	122
Figure 12 – Cell growth curve (H9c2) after exposure to PANi-scaffold, and scaffold without crosslinking agent at 48 and 72h.....	123

LISTA DE TABELAS

Capítulo 2: “Dense lamelar scaffold as biomimetic materials for reverse engineering of myocardial tissue: preparation, characterization and physiomechanical”

Table 1 - Mechanical properties of Young’s modulus of scaffolds.....47

Table 2 - Morphological characteristics of scaffolds.....49

Capítulo 3: “Design and evaluating of biomimetically inspired dense lamellar scaffold obtained by plastic compression: Development, physiomechanical characterization, and in vitro cellular activities”

Table 1 - Formulation of PA-scaffold and GA-scaffold.....71

Table 2 - Morphological characteristics of scaffolds.....82

Capítulo 4: “Biomimetic dense lamellar scaffold based on a complex of the polyaniline (PANi) and biopolymers, collagen, silk fibroin, and hyaluronic acid for electroactive and physiomechanical stimulation of the myocardial”

Table 1 - Formulation of PA-scaffold and GA-scaffold.....102

Table 2 - Morphological characteristics of scaffolds.....117

LISTA DE EQUAÇÕES

Capítulo 3: “Design and evaluating of biomimetically inspired dense lamellar scaffold obtained by plastic compression: Development, physiomechanical characterization, and in vitro cellular activities”

Equation 1 – Fluid uptake of scaffold (%).....	73
Equation 2 – Weight loss (%).....	73
Equation 3 – Specific permeability.....	74
Equation 4 – Antioxidant activity (%).....	75

Capítulo 4: “Biomimetic dense lamellar scaffold based on a complex of the polyaniline (PANi) and biopolymers, collagen, silk fibroin, and hyaluronic acid for electroactive and physiomechanical stimulation of the myocardial”

Equation 1 - Fluid uptake of scaffold (%).....	105
Equation 2 - Weight loss (%).....	105
Equation 3 - Specific permeability.....	106
Equation 4 - Electrical conductivity.....	107
Equation 5 - Antioxidant activity (%).....	108

SUMÁRIO

1	INTRODUÇÃO	16
2	OBJETIVO	19
2.1	Geral	19
2.2	Específico	19
CAPÍTULO I		20
1	REVISÃO BIBLIOGRÁFICA	21
1.1	Infarto agudo do miocárdio	21
1.2	Regeneração de tecidos	23
1.3	<i>Scaffolds</i>	24
1.4	Biomateriais	25
1.4.1	Polímeros Naturais	26
1.4.2	Polímeros Sintéticos	29
1.4.3	Polímeros condutores	29
1.4.4	Agentes reticulantes	30
2	Perspectivas Futuras	32
3	Referências	33
CAPÍTULO II		38
ARTIGO 1 – “DENSE LAMELAR SCAFFOLD AS BIOMIMETIC MATERIALS FOR REVERSE ENGINEERING OF MYOCARDIAL TISSUE: PREPARATION, CHARACTERIZATION AND PHYSIOMECHANICAL”		39
1.1	Abstract	39
1.2	Introduction	40
1.3	Materials and methods	42
1.3.1	Materials	42
1.3.2	Preparation of Fibroin Solution	42
1.3.3	Preparation of chitosan hydrogel	42
1.3.4	Preparation of collagen-chitosan hydrogel	42
1.3.5	Preparation of collagen-chitosan-fibroin hydrogel	43
1.3.6	Preparation of dense lamellar scaffolds	43
1.3.7	Physiomechanical and Mucoadhesive Properties	43
1.3.8	Swelling efficiency	44
1.3.9	Porosity, interconnectivity and pore size	44
1.3.10	Scanning electron microscopy (SEM)	45
1.3.11	Differential scanning calorimetry (DSC)	45
1.3.12	Fourier transform infrared spectroscopy (FTIR)	45
1.3.13	Cell viability	45
1.3.14	Image cytometer	46
1.4	Results	46
1.4.1	Physiomechanical and Mucoadhesive Properties	46
1.4.2	Swelling efficiency	48

1.4.3 Porosity, interconnectivity and pore size.....	48
1.4.4 Differential scanning calorimetry (DSC).....	50
1.4.5 Fourier transform infrared spectroscopy (FTIR).....	51
1.4.6 Cell viability.....	52
1.4.7 Image cytometer.....	53
1.5 Discussion.....	54
1.6 Conclusion.....	59
1.7 References.....	60

CAPÍTULO III.....	64
--------------------------	-----------

ARTIGO 2 – “DESIGN AND EVALUATING OF BIOMIMETICALLY INSPIRED DENSE LAMELLAR SCAFFOLD OBTAINED BY PLASTIC COMPRESSION: DEVELOPMENT, PHYSIOMECHANICAL CHARACTERIZATION, AND IN VITRO CELLULAR ACTIVITIES” (SUBMITTED).....	65
---	-----------

1.1 Abstract.....	65
1.2 Introduction.....	67
1.3 Materials and methods.....	70
1.3.1 Materials.....	70
1.3.2 Extraction of Fibroin.....	70
1.3.3 Preparation of hydrogel crosslinked with Proanthocyanidin or Glutaraldehyde 70	
1.3.4 Preparation of dense lamellar scaffolds.....	71
1.3.5 Physiomechanical and Mucoadhesive Properties.....	72
1.3.6 Swelling efficiency.....	72
1.3.7 <i>In vitro</i> disintegration study.....	73
1.3.8 Porosity, interconnectivity and pore size.....	73
1.3.9 Permeability Measurement.....	74
1.3.10 Scanning electron microscopy (SEM).....	74
1.3.11 Differential scanning calorimetry (DSC).....	75
1.3.12 Fourier transform infrared spectroscopy (FTIR).....	75
1.3.13 <i>In vitro</i> antioxidant activity.....	75
1.3.14 Cell viability	75
1.3.15 Image cytometer.....	76
1.4 Results and Discussion.....	76
1.4.1 Physiomechanical and Mucoadhesive Properties.....	76
1.4.2 Swelling efficiency.....	79
1.4.3 <i>In vitro</i> disintegration study.....	80
1.4.4 Porosity, interconnectivity and pore size.....	81
1.4.5 Permeability Measurement.....	82
1.4.6 Scanning electron microscopy (SEM).....	83
1.4.7 Differential scanning calorimetry (DSC).....	84
1.4.8 Fourier transform infrared spectroscopy (FTIR).....	85
1.4.9 <i>In vitro</i> antioxidant activity.....	87
1.4.10 Cell viability	88
1.4.11 Cytometer Image.....	89
1.5 Conclusion.....	91
1.6 References.....	92

CAPÍTULO IV.....	97
-------------------------	-----------

ARTIGO 3 – “BIOMIMETIC DENSE LAMELLAR SCAFFOLD BASED ON A COLLOIDAL COMPLEX OF THE POLYANILINE (PANI) AND BIOPOLYMERS FOR ELECTROACTIVE AND PHYSIOMECHANICAL STIMULATION OF THE MYOCARDIAL.”	98
1.1 Abstract	98
1.2 Introduction	99
1.3 Materials and Methods	100
1.3.1 Materials.....	100
1.3.2 Preparation of PANi-PVP water-soluble.....	101
1.3.3 Preparation of Fibroin Solution.....	102
1.3.4 Preparation of hydrogel with PANi.....	102
1.3.5 Preparation of dense lamellar scaffolds.....	103
1.3.6 Fourier transform infrared spectroscopy (FTIR).....	103
1.3.7 Differential scanning calorimetry.....	103
1.3.8 Physiomechanical and mucoadhesive properties.....	103
1.3.9 Swelling efficiency.....	104
1.3.10 <i>In vitro</i> disintegration study.....	105
1.3.11 Morphometric characteristics.....	105
1.3.12 Permeability measurement.....	106
1.3.13 Surface zeta potential.....	106
1.3.14 Scanning electron microscopy.....	107
1.3.15 Electrical conductivity.....	107
1.3.16 <i>In vitro</i> antioxidant activity.....	107
1.3.17 Cell viability	108
1.3.18 Image cytometer.....	108
1.4 Results and Discussion	109
1.4.1 Preparation of PANi-PVP water-soluble.....	109
1.4.2 Fourier transform infrared spectroscopy (FTIR).....	110
1.4.3 Differential scanning calorimetry (DSC).....	111
1.4.4 Physiomechanical and Mucoadhesive Properties.....	113
1.4.5 Swelling efficiency.....	115
1.4.6 <i>In vitro</i> disintegration study.....	116
1.4.7 Porosity, interconnectivity and pore size.....	117
1.4.8 Permeability Measurement.....	118
1.4.9 Surface zeta potential.....	118
1.4.10 Scanning electron microscopy (SEM).....	119
1.4.11 Electrical conductivity.....	120
1.4.12 <i>In vitro</i> antioxidant activity.....	121
1.4.13 Cell viability.....	122
1.4.14 Image cytometer.....	123
1.5 Conclusion	123
1.6 Final Remarks and Future View	126
1.7 References	126
CONSIDERAÇÕES FINAIS	130
PRÓXIMAS ETAPAS	132
ANEXO A – ARTIGOS SUBMETIDOS	133

1 INTRODUÇÃO

O presente trabalho foi redigido na forma de capítulos, contendo revisão bibliográfica (Capítulo I), artigo científico publicado em 2018: “*Dense Lamellar Scaffold as Biomimetic Materials for Reverse Engineering*” (Capítulo II), artigo científico submetido: “*Design and evaluating of biomimetically inspired dense lamellar scaffold obtained by plastic compression: Development, biomechanical characterization, and in vitro cellular activities*” (Capítulo III) e artigo científico submetido: “*Biomimetic dense lamellar scaffold based on a complex of the polyaniline (PANI) and biopolymers for electroactive and biomechanical stimulation of the myocardial*” (Capítulo IV), e conclusão do estudo (Capítulo V).

O Capítulo I aborda a revisão bibliográfica sobre o tema deste trabalho. A doença cardiovascular é um dos problemas de saúde mais graves do mundo, e gera um alto nível de mortalidade a cada ano. A medicina regenerativa é um campo emergente que visa melhorar ou reparar o desempenho de um tecido danificado ou de um órgão. Os *scaffolds* são estruturas tridimensionais (3D) e porosas, os quais podem ser produzidos utilizando biopolímeros capazes de mimetizar a matriz extracelular (MEC). Os *scaffolds* devem ser capazes de suportar mecanicamente o tecido nativo durante o reparo, mas também desempenham um papel importante no fornecimento de sinais essenciais para influenciar a atividade das células.

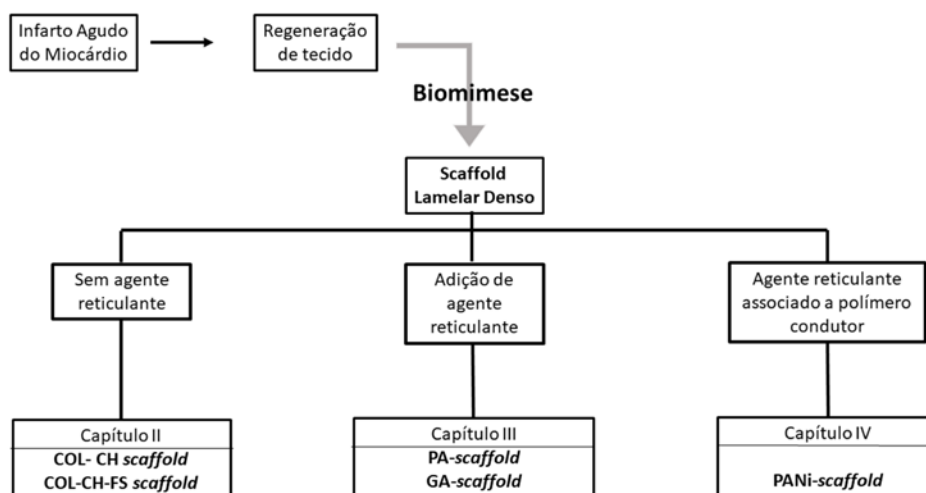
O Capítulo II aborda um estudo de desenvolvimento de *scaffolds* lamelares densos com materiais biomiméticos, obtidos pela técnica de compressão plástica, para a regeneração tecidual do miocárdio. Para gerar estrutura lamelar densa e porosa foram utilizados polímeros biomiméticos associado a técnica de compressão plástica. As misturas poliméricas de colágeno, quitosana e fibroína de seda foram usadas para obter os dispositivos tridimensionais poroso, anisotrópico e anatômico semelhantes a matriz extracelular. As propriedades fisiomecânicas associadas à eficiência de intumescimento, porosidade, grau de anisotropia e proliferação e viabilidade celular (*in vitro*) sugerem que o *scaffold* composto de COL-CH-SF, obtido por compressão plástica, apresenta potencial como material biomimético para engenharia reversa do tecido miocárdico.

O Capítulo III aborda a influência da utilização de agentes reticulantes na composição do *scaffolds* lamelares denso. Um agente de reticulação pode ser de origem sintética ou biológica com capacidade de ligar os grupos funcionais da cadeia

polimérica a outro, por meio de ligações covalentes ou interações supramoleculares, tais como ligação iônica ou ligação de hidrogênio. Esta reticulação pode afetar algumas propriedades físico-químicas, incluindo propriedades mecânicas, interações célula-matriz, resistência a temperaturas mais elevadas, resistência à degradação enzimática e química, e redução de permeação. Os agentes reticulantes utilizados neste estudo foram a proantocianidina (PA) e glutaraldeído (GA). O efeito dos agentes de reticulação modificou as propriedades fisiomecânicas, mas não modificou as propriedades de mucoadesão. *PA-scaffold* tem a capacidade de ligar a molécula da água e reduzir o espaço entre as cadeias poliméricas. *PA-scaffold* e *GA-scaffold* apresentaram, respectivamente, 44% e 17% de atividade antioxidante. Ambos os agentes de reticulação não influenciaram a viabilidade e proliferação de células H9c2. Considerando a estrutura anisotrópica, as propriedades fisiomecânicas, a compatibilidade celular e a ação protetora contra espécies reativas de oxigênio, este estudo pode fornecer uma maneira de melhorar a remodelação inversa do tecido cardíaco, após o infarto agudo do miocárdio.

O Capítulo IV aborda a incorporação de polianilina (PANi) em *scaffolds* lamelares densos obtidos por compressão plástica (Capítulo II). Para o tecido cardíaco, a matriz extracelular (MEC) serve como um suporte estrutural (*scaffold*) anisotrópico para guiar a migração e organização celular de forma alinhada. A MEC acomoda a contração e o relaxamento dos cardiomiócitos e facilita a transdução de força, a condutância elétrica, a comunicação intracelular e a troca metabólica no ambiente miocárdico. A PANi apresenta potencial uso na engenharia tecidual cardíaca, devido à sua fácil obtenção, estabilidade, condutividade e comprovadamente desempenha um importante papel na estimulação da proliferação, adesão ou diferenciação de vários tipos de células. Neste estudo, o objetivo é desenvolver *scaffold* lamelar denso com capacidade condutora de impulsos elétricos, utilizando PANi, e PA como agente reticulante. Os *scaffolds* lamelares densos contendo PANi foram fabricados via compressão plástica seguida de liofilização. Os *scaffolds* continham poros abertos e interconectados, com tamanho de poro variando entre 100-150 μm . PANi-*scaffold* apresentou módulo de Young de $1,77 \pm 0,11$ MPa. A condutividade do *scaffold* foi na ordem de $2 \cdot 10^{-6} \text{ S} \cdot \text{cm}^{-1}$ para o PANi-*scaffold* seco e $6 \cdot 10^{-4} \text{ S} \cdot \text{cm}^{-1}$ para o hidratado. Desta forma, PANi-*scaffold* possui propriedades fisiomecânicas e físico-químicas que auxiliam na viabilidade e proliferação dos cardiomiócitos.

Resumo gráfico



2 OBJETIVO

2.1 Geral

Projetar, desenvolver e avaliar *scaffold* lamelar denso baseado em biopolímeros, para engenharia reversa do tecido cardíaco.

2.2 Específico

- Projetar, com base em estudos de pré-formulação, a composição dos *scaffolds* lamelares densos baseados em hidrogéis;
- Preparar formulações dos *scaffolds* baseados em hidrogéis;
- Caracterizar as propriedades fisiomecânicas dos *scaffolds* lamelares densos baseados em hidrogéis;
- Caracterizar as propriedades físicas e físico-químicas dos *scaffolds* lamelares denso;
- Avaliar a capacidade antioxidante das amostras selecionadas;
- Avaliar, *in vivo*, a biocompatibilidade, citotoxicidade e viabilidade, das amostras selecionadas, dos *scaffolds* para aplicação em tratamentos cardíacos.

CAPÍTULO I

1 REVISÃO BIBLIOGRÁFICA

1.1 Infarto agudo do miocárdio

Em 2017, a Organização Mundial da Saúde (OMS) estimou que as doenças cardiovasculares levam 17,9 milhões de pessoas ao óbito todos os anos, o que significa 31% dos óbitos no âmbito mundial. As doenças cardiovasculares incluem uma ampla faixa de condições patológicas do coração e da vasculatura cardíaca como isquemia, malformação estrutural e vascular, cardiomiopatia, doença microvascular e falha cardíaca congestiva (TAYLOR; SAMPAIO; GOBIN, 2014a).

O tecido cardíaco é basicamente formado por miócitos cardíacos (elementos contráteis), células musculares lisas, fibroblastos, vasos sanguíneos, nervos e componentes da matriz extracelular (interstício cardíaco e colágeno) organizados de maneira muito particular. Os miócitos formam fibras musculares com mudança de orientação ao longo da parede ventricular até 180°. Ao mesmo tempo, as fibras musculares são organizadas em lâminas miocárdicas, 4-6 miócitos espessamente separados das lâminas vizinhas por colágeno extracelular. A organização dos miócitos ventriculares influencia a função mecânica e elétrica do coração, sendo que pequenas alterações podem levar a severas mudanças nestas funções (ARNAL-PASTOR et al., 2013). No entanto, o miocárdio adulto é incapaz de regenerar espontaneamente seus cardiomiócitos, em caso de morte celular (COSTA, 2016).

O termo infarto agudo do miocárdio (IAM) pode ser definido como a morte de cardiomiócitos causada por isquemia prolongada em uma região do músculo cardíaco. Em geral, essa isquemia é causada por trombose e/ou vasoespasmos sobre uma placa aterosclerótica. Essa oclusão deixa uma região do coração sem suprimento de sangue, ou seja, com a falta de oxigênio, nutrientes e metabólitos para a região afetada. Como consequência, o metabolismo aeróbico muda para glicólise anaeróbica, levando a uma diminuição do pH e redução da função contrátil (ARNAL-PASTOR et al., 2013; CHAUD et al., 2017; ZORNOFF; SPADARO, 1997). A perda de miócitos gerada por apoptose aumenta a carga sobre os miócitos restantes, que tenderão a sofrer necrose ou apoptose, criando um ciclo que piora a disfunção ventricular. Assim, a apoptose é considerado um contribuinte importante para a evolução do remodelamento e da insuficiência cardíaca (RICARDO et al., 2004).

Após o IAM, ocorrem alterações complexas na arquitetura ventricular, envolvendo tanto a região infartada como a não infartada. Após a obstrução coronariana, o processo inflamatório se instala na região infartada que, nas horas iniciais, é caracterizado pelo acúmulo de células inflamatórias e edema, em seguida ocorre a fase de proliferação de fibroblastos com a deposição de colágeno, sendo o tecido necrótico substituído por tecido fibroso, de cicatrização. O excesso de cicatrizes pode causar aumento da rigidez dos tecidos, atrofia dos cardiomiócitos, arritmia e hipóxia. Neste contexto, o tecido cicatricial tem sua contratilidade reduzida ou ausente em comparação com o tecido do miocárdio saudável, o que leva a uma redução na função cardíaca em geral (ARNAL-PASTOR et al., 2013; CHAUD et al., 2017; RICARDO et al., 2004; SUTTON; SHARPE, 2000; ZORNOFF; SPADARO, 1997).

Além disso, espécies reativas de oxigênio (EROs) podem ser produzidas por diferentes fontes no coração, incluindo sistema NADPH oxidase, atividade das enzimas ciclooxigenase, citocromo P450, glicose oxidase, xantina oxidase, lipoxigenase, bem como pela degradação de catecolaminas. Em condições fisiológicas, existe um equilíbrio entre a produção de EROs e defesa antioxidante. O estresse oxidativo ocorre quando são geradas EROs em excesso, as quais não podem ser neutralizadas pelos sistemas antioxidantes. As EROs têm efeito significativo sobre a matriz extracelular, estimulando a proliferação de fibroblastos cardíacos e ativando as metaloproteinases de matriz, efeitos centrais para a fibrose e a remodelação da matriz. Portanto, o remodelamento cardíaco pode estar diretamente relacionado ao estresse oxidativo, resultante do aumento da produção de espécies reativas e diminuição da defesa antioxidante (TAKIMOTO et al., 2014).

Nenhuma terapia eficaz, disponível atualmente, tem a capacidade de inibir que a fibrose cardíaca progrida no coração infartado, afim de preservar a função cardíaca e prevenir insuficiência cardíaca (CHAUD et al., 2017). Os métodos comumente utilizados incluem terapia medicamentosa (inibidores da enzima conversora da angiotensina, bloqueadores dos receptores da angiotensina, antagonistas dos receptores da aldosterona, bloqueadores dos receptores β , e nitratos); terapia trombolítica (recanalização da artéria coronária ocluída e restauração da perfusão); intervenção coronária percutânea e cirurgia de revascularização miocárdica (HASHIMOTO et al., 2018; RICARDO et al., 2004; ZORNOFF; SPADARO, 1997).

Considerando as inúmeras desvantagens do transplante cardíaco, tratamento farmacológico ineficientes, bem como a capacidade regenerativa restrita dos

cardiomiócitos para a recuperação da região infartada após IAM, vários estudos têm sido realizados em medicina regenerativa, criando alternativas para a regeneração miocárdica por meio da engenharia de tecidos (HASHIMOTO et al., 2018).

1.2 Regeneração de tecidos

A medicina regenerativa ou regeneração de tecidos, é o processo de substituir ou regenerar células, tecidos ou órgãos afim de restaurar suas funções normais. Este processo tem mostrado resultados promissores para a regeneração e substituição de uma variedade de tecidos e órgãos, incluindo pele, coração, rim e fígado, e o potencial para corrigir algumas falhas congênitas (DZOBO et al., 2018; MAO; MOONEY, 2015).

Para que esta estratégia seja bem-sucedida, os polímeros utilizados, fatores de crescimento e células-tronco, devem ser capazes de mimetizar o tecido danificado e ter as propriedades semelhantes e/ou estimular a regeneração do tecido original. As células utilizadas na regeneração de tecidos podem ser originárias do próprio paciente (autólogo) ou de outro indivíduo (alogenico). Além disso, células xenogênicas, como as de animais, também podem ser adotadas em estratégias da medicina regenerativa (DZOBO et al., 2018).

O potencial terapêutico de um transplante cardíaco é limitado devido o pequeno número de doadores de corações disponíveis, quando comparado a necessidade e compatibilidade dos indivíduos. O coração possui capacidade regenerativa limitada, o que é atribuída as pequenas populações de células tronco. Assim, há um interesse crescente no desenvolvimento de novas abordagens para tratar IAM. A engenharia de tecido cardiovascular é atualmente considerada uma promissora terapia alternativa, afim de restaurar a estrutura e função do miocárdio adulto infartado, via aplicação de um dispositivo biológico na região do tecido isquêmico (CHAUD et al., 2017; SHAPIRA; FEINER; DVIR, 2015).

O uso de fatores de crescimento despertou interesse na medicina cardiovascular devido às ações diretas dos fatores sobre diversas funções celulares como adesão, proliferação e migração. Apesar dos mecanismos de regeneração tecidual induzidos por fatores de crescimento, o potencial terapêutico dessas proteínas é limitado pela sua curta meia-vida biológica, baixa estabilidade em plasma e pouca especificidade aos órgãos-alvo. Nesse contexto, a terapia celular e a engenharia tecidual podem representar uma alternativa para estimular a regeneração

do tecido infartado, evitando a remodelação e a formação de cicatriz (BOFFITO; SARTORI; CIARDELLI, 2014; REBOUÇAS; SANTOS-MAGALHÃES; FORMIGA, 2016).

O intervalo de tempo entre a ocorrência do IAM e a aplicação de uma terapia regenerativa, influencia diretamente na reposta do paciente. A terapia celular estimula o processo reparativo, mantém a contratilidade da zona limítrofe e reduz a formação e remodelação da cicatriz, porém se realizada em poucos dias. O uso da terapia celular é mais adequado no caso de pequenas e localizadas lesões. Em contrapartida, os *scaffolds* tridimensionais fornecem algumas vantagens sobre a injeção celular: (i) os *scaffolds* substituem temporariamente o tecido lesionado, fornecendo um substrato para a colonização, migração e proliferação celular, e um suporte mecânico para o processo regenerativo e (ii) terapia celular requer a injeção de bilhões de células, e cerca de 90% das células injetadas morrem no prazo de uma semana (BOFFITO; SARTORI; CIARDELLI, 2014). O engenheiramento e fabricação de *scaffolds* são as principais áreas de pesquisa em biomateriais, e também na engenharia de tecidos e medicina regenerativa.

1.3 *Scaffolds*

Scaffolds são matrizes ou suportes tridimensionais porosos, temporários, biodegradáveis utilizados na engenharia de tecidos. A principal função dos *scaffolds* é servir como um suporte celular, mimetizando a função da MEC, que não apenas fornece um ambiente mecânico adequado para as células, mas também estimulam respostas celulares específicas em nível molecular capazes de promover a adesão, proliferação, diferenciação e metabolismo celular (LEE; CUDDIHY; KOTOV, 2008; MARTÍNEZ et al., 2015; O'BRIEN, 2011).

Um aspecto importante no engenheiramento de *scaffolds* é considerar o objetivo da aplicação do mesmo. No entanto, há alguns critérios comuns que devem ser considerados: (i) biocompatibilidade, (ii) biodegradabilidade, (iii) propriedades fisiomecânicas, (iv) um ambiente que favoreça a migração e integração celular, proliferação e diferenciação para o efeito terapêutico desejado (v) uma construção permeável que permite eficiente transferência de nutrientes e resíduos, (vi) injetabilidade (no caso de hidrogéis), (vii) espessura e, finalmente, (viii) tempo de

aplicação pós-IAM (DOMENECH et al., 2016; REIS et al., 2016; SERPOOSHAN et al., 2013).

O *scaffold* cardíaco, implantado sobre o tecido infartado e região adjacente, tem como objetivo melhorar a retenção de células reparadoras, limitar a remodelação do ventrículo esquerdo, prevenir dilatação e diminuição da espessura da parede do ventrículo esquerdo, melhorar as propriedades mecânicas do ventrículo e reduzir a apoptose de cardiomiócitos. Além disso, também estimular a angiogênese, liberação de citocinas e perfusão miocárdica. Todas essas propriedades dependem da escolha dos materiais para compor o *scaffold* (DOMENECH et al., 2016).

O miocárdio humano apresenta uma rigidez que varia de 20kPa (final da diástole) a 500kPa (final da sístole), enquanto o miocárdio de ratos varia de 0,1 a 140kPa. Um material concebido para aumentar a espessura artificialmente a parede do ventrículo, e manter a geometria ventricular durante o remodelamento deve ter uma rigidez igual ou superior ao do ventrículo nativo. Enquanto que um material concebido para ser injetado, para atuar como uma matriz temporária para células transplantadas e / ou para recrutar células endógenas pode ter uma baixa rigidez, mas suficiente para suportar a contração / dilatação do coração (REIS et al., 2016).

A técnica de fabricação dos *scaffolds* na engenharia de tecidos depende das propriedades de volume/densidade, formato, e da função proposta para o *scaffold*. A maioria das técnicas envolve a aplicação de calor e / ou pressão ao polímero, ou sua dissolução em solvente orgânico, afim de moldar o material na sua forma desejada. Embora cada método apresente vantagens e desvantagens distintas, a técnica apropriada deve ser selecionada para atender aos requisitos de acordo com o tecido. Além disso, a escolha do (s) biomaterial (ais) a partir do qual o *scaffold* deve ser fabricado, é um fator chave para se obter as características ideais para sua finalidade (DHANDAYUTHAPANI et al., 2011).

1.4 Biomateriais

A MEC é composta por proteínas fibrosas (colágeno tipo I e elastina), água, glicoproteínas (fibronectina e laminina), proteoglicanas e outras moléculas solúveis. A quantidade, estrutura e composição da MEC são específicas do tecido e estão em constante mudança por meio de modificações enzimáticas e não enzimáticas. O

colágeno é o principal componente proteico da MEC cardíaca (SHAPIRA; FEINER; DVIR, 2015).

Os biomateriais poliméricos utilizados na fabricação de dispositivos utilizados na engenharia de tecidos podem ser de origem sintética, natural ou semi-sintética. Em alguns casos, materiais inorgânicos como a hidroxiapatita, também podem ser utilizados (HERNANDEZ et al., 2016; SHAPIRA; FEINER; DVIR, 2015; SILVESTRI et al., 2013).

Biopolímeros de origem sintética tem sido amplamente utilizados na engenharia de tecidos, pois são facilmente obtidos, baixo custo, propriedades fisiomecânicas e químicas conhecidas, não tóxicos, não imunogênicos e pode ser engenheirados para um tempo de biodegradação desejado. Já os biopolímeros de origem natural são considerados mais biomiméticos a MEC, o que os tornam um maior atrativo para a migração e proliferação celular. No entanto, a baixa disponibilidade, preços relativamente mais altos, maior variabilidade de lote para lote, menor estabilidade física e química, propriedades mecânicas inadequadas e maior risco de imunogenicidade estão entre os fatores que restringem seu uso como componentes isolados na fabricação de dispositivos na engenharia de tecidos. Para alcançar ou se modular as necessidades específicas a cada tecido, além de combinações químicas, a mistura de dois ou mais polímeros permite o desenvolvimento de novos biomateriais que exibem combinações de propriedades que não poderiam ser obtidas com polímeros utilizados individualmente (HERNANDEZ et al., 2016; SHAPIRA; FEINER; DVIR, 2015).

1.4.1 Polímeros Naturais

O colágeno é um biopolímero composto por monômeros de tropocolágeno com massa molecular de 300 kDa, e pode ser encontrado em diversas formas (I – IV), de acordo com a origem do tecido e a composição de aminoácidos (MAXIMO; CUNHA, 2010). O colágeno tipo I compõe cerca de 80% da matriz de colágeno no tecido cardíaco, tornando este biopolímero um atrativo para a fabricação de *scaffolds* para tecido cardíaco. Suas principais características incluem biocompatibilidade, biodegradabilidade, estrutura contrátil fibrosa, fixação e crescimento celular, o que facilita a integração da célula hospedeira. No entanto, o colágeno fornece ao *scaffold* um baixo módulo de elasticidade, o que pode limitar sua integração mecânica ao

tecido cardíaco (DOMENECH et al., 2016). Serpooshan et al. (2013), otimizaram o módulo elástico do gel de colágeno tipo I afim de melhorar a contratilidade miocárdica no coração lesionado. O colágeno tipo I foi fabricado utilizando técnica de compressão plástica para gerar *scaffolds* densos com maior módulo elástico.

O colágeno em combinação com outros biomateriais como a quitosana mostraram um aumento do módulo elástico, o que o torna mais adequado para a estabilização da parede ventricular (ARPORNMAEKLONG; PRIPATNANONT; SUWATWIROTE, 2008; DENG et al., 2010; KIM et al., 2001; MARTÍNEZ et al., 2015). Rosellini et al. (2018), produziu *scaffolds* por liofilização e subsequente reticulação iônica e química, baseados nas misturas de colágeno ou gelatina com alginato. Os *scaffolds* de alginato/gelatina apresentam propriedades mecânicas superiores para a aplicação desejada, com melhor aderência, crescimento e diferenciação de mioblastos.

O colágeno pode ser reticulado, *in vitro*, utilizando luz UV, agentes reticulantes químicos (glutaraldeído e carbodiimida) ou natural (proantocianidinas ou genipin) e exposição a altas temperaturas. O processo de reticulação é usado extensivamente para diminuir a taxa de degradação, *in vivo*, e aumentar as propriedades fisiomecânicas de dispositivos compostos por colágeno (KAISER; COULOMBE, 2015; LEE; SABATINI, 2017; SHAVANDI et al., 2018; YANG; RITCHIE; EVERITT, 2017).

A quitosana (Qt) é um polímero natural, composto de glucosamina e N-acetilglucosamina. Tem sido amplamente utilizada nos campos farmacêutico e de engenharia de tecidos devido sua biocompatibilidade, biodegradabilidade e propriedades antimicrobianas (DOMENECH et al., 2016; SIONKOWSKA; PŁANECKA, 2013). Lu et al. (2009), projetaram um hidrogel de quitosana, o qual melhorou a sobrevivência de células-tronco embrionárias e a diferenciação de cardiomiócitos, em um modelo de infarto em rato. Embora o objetivo fosse a regeneração de cardiomiócitos, o *scaffold* projetado também melhorou a densidade do vaso sanguíneo e promoveu uma rápida angiogênese nos tecidos da córnea e da pele.

A fibroína de seda (FS) é polímero natural com aplicações biomédicas devido suas características de permeabilidade ao oxigênio e água, adesão e crescimento celular, baixa trombogenicidade e resposta inflamatória, e alta resistência à tração com flexibilidade. A FS é composta por duas proteínas de origem animal, fibroína e sericina, onde a fibroína é incorporada no interior da sericina. Além da organização

primária, a estrutura secundária e a organização hierárquica da fibroína de seda determinam muitas de suas propriedades biomateriais. Silk I proporciona uma boa solubilidade em água, uma vez que as sedas I são formados alternativamente por α -hélice e folha β . Silk II é rica em folha β , proporcionando boa resistência à solubilidade em água. Silk II é a principal configuração estrutural da FS. Devido a seda II, a SF exibe alta propriedade mecânica e propriedades físico-químicas. Silk III é uma estrutura cristalina helicoidal tripla e de baixa solubilidade. A estrutura de *random coil* normalmente está presente nas soluções do SF (GOBIN; FROUDE; MATHUR, 2005; KUNDU et al., 2013; LI et al., 2013; QI et al., 2017).

O ácido hialurônico (AH) é um polissacarídeo natural que juntamente com o colágeno, é um dos componentes mais abundantes da MEC. Como o AH é rico em grupos carboxila e hidroxila é capaz formar um hidrogel sob modificação química, reticulação ou foto-reticulação. Dispositivos contendo AH oferecem propriedades vantajosas como a biorresorbabilidade, inibição da formação de cicatriz e a promoção da angiogênese (BONAFÈ et al., 2014; COLLINS; BIRKINSHAW, 2013; ZHU et al., 2017). Durante a cicatrização cardíaca após IAM, ocorre um aumento precoce de AH, o qual pode ser detectado no tecido lesionado. Apesar dessas alterações servirem para reduzir o risco de ruptura da parede lesionada, elas geralmente predis põem à remodelação do ventrículo esquerdo (VE) e à insuficiência cardíaca (BONAFÈ et al., 2014).

O alginato é um polissacarídeo derivado de algas, com característica aniônica. É considerado um biomaterial biocompatível, de baixo custo, não trombogênico e semelhante estruturalmente com a MEC. Os hidrogéis de alginato podem ser utilizados na bioengenharia de enxertos cardíacos, liberação de células-tronco, em forma injetável acelular para suporte e reconstrução de tecidos, e como *scaffold* para liberação controlada de fatores de crescimento. O alginato é um copolímero linear formado por dois monômeros de base, β -D-manuronila e α -L-guluronila, conectados entre si por ligações glicosídicas entre seus carbonos 1 e 4. Na presença de cátions divalentes, ocorre uma interação dos blocos de monômeros G para formação de ligações iônicas, gelificação ionotrópica (LEE; MOONEY, 2012; RUVINOV; COHEN, 2016).

1.4.2 Polímeros Sintéticos

Poliésteres biodegradáveis são os polímeros sintéticos mais comumente empregados na regeneração do tecido cardíaco. Eles são sintetizados principalmente a partir do lactídeo (poliácido láctico), glicolídeo, lactona (ϵ -caprolactona) e copolímeros (poli [D, L-lactídeo-co-glicolídeo]). Dependendo do monômero, as propriedades mecânicas, físicas e de degradação podem variar, e são basicamente hidrofóbicos, o que desfavorece uma boa adesão celular. Além disso, os produtos de biodegradação ácida podem induzir elevada resposta inflamatória, e afetar a viabilidade das células circundantes (SILVESTRI et al., 2013).

Poliuretano (PU) é um grupo de biopolímeros amplamente utilizado no campo biomédico e industrial. O PU pode ser usado como biomaterial devido as suas propriedades mecânicas e químicas, por possuir boa taxa de degradação e bioestabilidade, biocompatibilidade e hemocompatibilidade. Degradação hidrolítica, enzimática ou oxidante são os principais mecanismos de degradação de PU. Os fatores de velocidade de degradação podem ser influenciados pela força intramolecular, cristalinidade, hidrofobicidade, peso molar, composição, grau de intumescimento e condições do ambiente (como o pH) (GANJI et al., 2014; SILVESTRI et al., 2013; TSAI et al., 2015).

1.4.3 Polímeros condutores

A condutividade elétrica é um fator chave na estruturação de biomateriais terapêuticos para o reparo cardíaco. *Scaffolds* contendo polímeros condutores podem ser utilizados para originar uma estrutura que mimetize o ambiente cardíaco, sendo capaz de ancorar células cardíacas funcionais, integrar eletromecânica, e / ou promover a integridade elétrica do coração, agindo diretamente sobre os cardiomiócitos nativos (YE; QIU, 2017).

Os polímeros condutores são capazes de exibir propriedades elétricas semelhantes às dos metais e semicondutores, podendo manter a flexibilidade e facilidade de processamento. As propriedades elétricas destes materiais podem ser moduladas, alterando seus processos de obtenção, incluindo a adição de diferentes agentes químicos (BIDEZ et al., 2005). Entre os diversos polímeros condutores/semicondutores, a polianilina (PANi) tem sido utilizada devido sua propriedade redox reversível, reação ácido/base simples e caráter de

dopagem/desdopagem, estabilidade ambiental, propriedades elétricas, e baixo custo de obtenção (BHADRA et al., 2009; BHOWMICK et al., 2013; MONTEIRO et al., 2017).

Alguns autores exploraram, *in vitro*, a capacidade de *scaffolds* à base de PANi, afim de verificar sua biocompatibilidade com cardiomiócitos (BAHEIRAEI et al., 2015; HSIAO et al., 2013). Baheiraei e colaboradores (2015) estudaram as propriedades de *scaffolds* compostos de policaprolactona e poliuretano contendo pentâmeros de anilina. Os *scaffolds* condutores promoveram adesão, crescimento e maior expressão de genes de cardiomiócito neonatal, envolvidos na contração e no alinhamento do citoesqueleto.

Mihic *et al.* (2015), abordaram o efeito de hidrogel injetável composto de quitosana e PANi, sobre a função cardíaca e propagação do potencial de ação em modelo de IAM em rato. O hidrogel foi administrado na região infartada do ventrículo esquerdo, após 1 semana da indução do IAM. Oito semanas após a administração, o grupo tratado com hidrogel contendo PANi/quitosana apresentou melhora da função ventricular esquerda e a duração do intervalo das ondas QRS (despolarização dos ventrículos) foi semelhante ao dos animais saudáveis. Além disso, o mapeamento óptico, *ex vivo*, mostrou que a velocidade de condução do impulso elétrico, na região da cicatriz, foi aumentada nos corações injetados com PANi/quitosana.

No entanto, existem algumas limitações no seu uso, como a baixa solubilidade, hidrofobicidade e baixa biodegradabilidade. A introdução de outros materiais compatíveis e degradáveis ou oligoanilinas de baixo peso molecular, durante a síntese podem aumentar as propriedades de solubilidade e biodegradação da PANi (BIDEZ et al., 2005; CHATTOPADHYAY; MANDAL, 1996; LUO et al., 2007; SHAO et al., 2011; ZEGHIOUD et al., 2015).

1.4.4 Agentes reticulantes

A reticulação é o processo responsável pela interligação de cadeias poliméricas por meio da reação das mesmas com uma substância denominada agente reticulante, o qual é capaz de gerar uma rede tridimensional polimérica mais rígida, com menor mobilidade das cadeias, por meio de ligações covalentes com o polímero. Um agente reticulante ideal deve ser não citotóxico para o tecido cardíaco e apresentar um baixo custo. Existem diversos agentes reticulantes utilizados para a fabricação de *scaffolds*, que podem ser classificados como agentes reticulantes químicos (carbodiimida,

compostos epóxi e glutaraldeído) e agentes reticulantes naturais (genipina, ácido tânico e procianidinas). Os agentes de reticulantes naturais apresentam superioridade em muitos aspectos em relação os agentes reticulantes químicos, devido a sua baixa citotoxicidade e atividade anticalcificante (HAN et al., 2003; SHAVANDI et al., 2018). Como resultado, a reticulação de cadeias poliméricas pode afetar as propriedades físico-químicas, incluindo propriedades mecânicas como resistência à tração, rigidez e tensão, interações célula-matriz, melhor desempenho em altas temperaturas, resistência à degradação enzimática e química, redução de permeação de gás e manter a forma original dos produtos (ORYAN et al., 2018).

A proantocianidina (PA) é um polifenol encontrado em frutas e vegetais, com potencial em gerar estruturas de ligações de hidrogênio com o colágeno gerando matrizes estáveis. PA é capaz de aumentar a síntese de colágeno e converter o colágeno solúvel em colágeno insolúvel. Da mesma forma, PAs podem inibir o catabolismo do colágeno solúvel, estimular a proliferação de fibroblastos normais da pele e aumentar a síntese de matriz extracelular, incluindo colágeno e fibronectina (HAN et al., 2003; YANG; RITCHIE; EVERITT, 2017).

O processo de reticulação e a estabilização do colágeno com PA pode aumentar significativamente as propriedades mecânicas do *scaffold*. Alguns autores observaram que a máxima resistência à tração do colágeno aumentou em aproximadamente 70% após o tratamento com 0,5% (m/m) de solução de PA. Além disso, a PA é amplamente utilizada como agente antioxidante natural, antimicrobiano, anti-inflamatório, antialérgico, inibidor de enzimas (fosfolipase A2, lipoxigenase e ciclooxigenase), cardioprotetora, e como suplementos dietéticos (BAGCHI et al., 2003; HAN et al., 2003; SHAVANDI et al., 2018).

O glutaraldeído (GA) reage com os grupos funcionais amina ou hidroxila de proteínas e polímeros, respectivamente através de uma reação de base de Schiff ligando as cadeias biopoliméricas via interações intra ou intermoleculares. Portanto, todos os grupos de aminas livres disponíveis presentes na estrutura química de moléculas de proteínas, como a gelatina, reagem com GA, formando uma rede mais fortemente reticulada (OLDE DAMINK et al., 1995; ORYAN et al., 2018). O GA é facilmente disponível, barato e suas soluções aquosas podem reticular efetivamente o colágeno em um curto período de tempo. A biocompatibilidade dos dispositivos baseados em colágeno reticulados com GA pode ser melhorada com a diminuição da concentração de soluções de GA (BIGI et al., 2001).

2 Perspectivas Futuras

A medicina regenerativa cardíaca tem realizado progressos significativos nos últimos anos. O engenheiramento de *scaffolds* está levando o campo da engenharia de tecidos e medicina regenerativa a maiores níveis de complexidade, com características do dispositivo mais biomiméticas ao tecido nativo.

No entanto, muito trabalho ainda precisa ser feito para melhor entender e resolver os desafios experimentais e das tecnologias existentes, melhorando as técnicas atuais e desenvolvendo novas técnicas, protocolos e métodos. Entre eles, um dos principais desafios na engenharia de tecidos e pesquisa de células-tronco tem sido imitar o micro e macro ambiente de tecidos humanos, controlando as características dos tecidos manipulados.

Estudos demonstraram a integração dos *scaffolds* cardíacos ao coração com capacidade de melhorar a função contrátil. Dispositivos acelulares, como MEC descelularizado ou *scaffolds* produzidos utilizando apenas biomateriais tem sido um crescente campo na engenharia de tecidos. Este estudo deverá contribuir para o avanço da ciência nesta nova abordagem de terapia clínica para reparação tecidual acelular, formação de mão de obra atualizada com visão de futuro, técnica e cientificamente capacitada e ajustada para demandas científicas atuais.

3 Referências

- ARNAL-PASTOR, M. et al. Biomaterials for Cardiac Tissue Engineering. **Intechopen**, p. 275–323, 2013.
- ARPORNMAEKLONG, P.; PRIPATNANONT, P.; SUWATWIROTE, N. Properties of chitosan-collagen sponges and osteogenic differentiation of rat-bone-marrow stromal cells. **International Journal of Oral and Maxillofacial Surgery**, v. 37, n. 4, p. 357–366, 2008.
- BAGCHI, D. et al. Molecular mechanisms of cardioprotection by a novel grape seed proanthocyanidin extract. **Mutation Research - Fundamental and Molecular Mechanisms of Mutagenesis**, v. 523–524, p. 87–97, 2003.
- BAHEIRAEI, N. et al. Preparation of a porous conductive scaffold from aniline pentamer-modified polyurethane/PCL blend for cardiac tissue engineering. **Journal of Biomedical Materials Research - Part A**, v. 103, n. 10, p. 3179–3187, 2015.
- BHADRA, S. et al. Progress in preparation, processing and applications of polyaniline. **Progress in Polymer Science (Oxford)**, v. 34, n. 8, p. 783–810, 2009.
- BHOWMICK, B. et al. In situ fabrication of polyaniline-silver nanocomposites using soft template of sodium alginate. **Journal of Applied Polymer Science**, v. 129, n. 6, p. 3551–3557, 2013.
- BIDEZ, P. R. et al. Polyaniline, an electroactive polymer, supports adhesion and proliferation of cardiac myoblasts. **Journal of Biomaterials Science**, v. 17, n. 1, p. 199–212, 2005.
- BIGI, A. et al. Mechanical and thermal properties of gelatin films at different degrees of glutaraldehyde crosslinking. **Biomaterials**, v. 22, n. 8, p. 763–768, 2001.
- BOFFITO, M.; SARTORI, S.; CIARDELLI, G. Polymeric scaffolds for cardiac tissue engineering: Requirements and fabrication technologies. **Polymer International**, v. 63, n. 1, p. 2–11, 2014.
- BONAFÈ, F. et al. Hyaluronan and cardiac regeneration. v. 1, p. 1–13, 2014.
- CHATTOPADHYAY, D.; MANDAL, B. M. Methyl Cellulose Stabilized Polyaniline Dispersions. **Langmuir**, v. 12, n. 6, p. 1585–1588, 1996.
- CHAUD, M. V et al. Three-Dimensional and Biomimetic Technology in Cardiac Injury After Myocardial Infarction: Effect of Acellular Devices on Ventricular Function and Cardiac Remodelling. In: **Scaffolds in Tissue Engineering - Materials, Technologies and Clinical Applications**. 2017. p. 227–251.
- COSTA, K. D. Decellularized scaffold hydrogel materials for mi treatment could “the matrix” really be the future? **Journal of the American College of Cardiology**, v. 67, n. 9, p. 1087–1090, 2016.
- DENG, C. et al. A Collagen–Chitosan Hydrogel for Endothelial Differentiation and Angiogenesis. **Tissue Engineering Part A**, v. 16, n. 10, 2010.

DHANDAYUTHAPANI, B. et al. Polymeric scaffolds in tissue engineering application: A review. **International Journal of Polymer Science**, v. 2011, n. ii, 2011.

DOMENECH, M. et al. Tissue Engineering Strategies for Myocardial Regeneration: Acellular Versus Cellular Scaffolds? **Tissue Engineering Part B: Reviews**, v. 22, n. 6, p. 438–458, 2016.

DZOBO, K. et al. Advances in Regenerative Medicine and Tissue Engineering : Innovation and Transformation of Medicine. **Stem Cells International**, v. 2018, 2018.

GANJI, Y. et al. Synthesis and characterization of gold nanotube / nanowire – polyurethane composite based on castor oil and polyethylene glycol. **Materials Science & Engineering C**, v. 42, p. 341–349, 2014.

GOBIN, A. S.; FROUDE, V. E.; MATHUR, A. B. Structural and mechanical characteristics of silk fibroin and chitosan blend scaffolds for tissue regeneration. **Journal of Biomedical Materials Research - Part A**, v. 74, n. 3, p. 465–473, 2005.

HAN, B. et al. Proanthocyanidin: A natural crosslinking reagent for stabilizing collagen matrices. **Journal of Biomedical Materials Research - Part A**, v. 65, n. 1, p. 118–124, 2003.

HASHIMOTO, H. et al. Therapeutic approaches for cardiac regeneration and repair. **Nature Review Cardiology**, v. 15, n. 10, p. 585–600, 2018.

HERNANDEZ, E. et al. An Overview of Mechanical Tests for Polymeric Biomaterial Scaffolds Used in Tissue Engineering. **Journal of Research Updates in Polymer Science**, v. 4, n. 4, p. 168–178, 2016.

HSIAO, C. et al. Biomaterials Electrical coupling of isolated cardiomyocyte clusters grown on aligned conductive nanofibrous meshes for their synchronized beating. **Biomaterials**, v. 34, n. 4, p. 1063–1072, 2013.

KAISER, N. J.; COULOMBE, K. L. K. Physiologically inspired cardiac scaffolds for tailored in vivo function and heart regeneration. **Biomedical materials** (Bristol, England), v. 10, n. 3, p. 034003, 2015.

KIM, S. E. et al. Three-dimensional porous collagen/chitosan complex sponge for tissue engineering. **Fibers and Polymers**, v. 2, n. 2, p. 64–70, 2001.

KUNDU, B. et al. Silk fibroin biomaterials for tissue regenerations. **Advanced Drug Delivery Reviews**, v. 65, n. 4, p. 457–470, 2013.

LEE, J.; CUDDIHY, M. J.; KOTOV, N. A. Three-Dimensional Cell Culture Matrices : State of the Art. **Tissue Eng Part B Rev**, v. 14, n. 1, 2008.

LEE, J.; SABATINI, C. Glutaraldehyde collagen cross-linking stabilizes resin–dentin interfaces and reduces bond degradation. **European Journal of Oral Sciences**, v. 125, n. 1, p. 63–71, 2017.

LEE, K. Y.; MOONEY, D. J. Alginate: Properties and biomedical applications. **Progress in Polymer Science (Oxford)**, v. 37, n. 1, p. 106–126, 2012.

LI, Z. H. et al. Silk fibroin-based scaffolds for tissue engineering. **Frontiers of Materials Science**, v. 7, n. 3, p. 237–247, 2013.

LU, W.-N. et al. Functional Improvement of Infarcted Heart by Co-Injection of Embryonic Stem Cells with Temperature-Responsive Chitosan Hydrogel. **Tissue Engineering Part A**, p. 1437-1447, 2009.

LUO, J. et al. Stable aqueous dispersion of conducting polyaniline with high electrical-conductivity. **Macromolecules**, v. 40, n. 23, p. 8132–8135, 2007.

MAO, A. S.; MOONEY, D. J. Regenerative medicine: Current therapies and future directions. **Proceedings of the National Academy of Sciences**, v. 112, n. 47, p. 14452–14459, 2015.

MARTÍNEZ, A. et al. Tailoring chitosan/collagen scaffolds for tissue engineering: Effect of composition and different crosslinking agents on scaffold properties. **Carbohydrate Polymers**, v. 132, p. 606–619, 2015.

MAXIMO, G. J.; CUNHA, R. L. Mechanical Properties of Collagen Fiber and Powder Gels. **Journal of Texture Studies**, v. 41, p. 842–862, 2010.

MIHIC, A. et al. A Conductive Polymer Hydrogel Supports Cell Electrical Signaling and Improves Cardiac Function After Implantation into Myocardial Infarct. **Circulation**, p. 772- 784, 2015.

MONTEIRO, L. M. et al. Restoring heart function and electrical integrity: closing the circuit. **Regenerative Medicine**, v. 2, n. 1, p. 9, 2017.

O'BRIEN, F. J. Biomaterials & scaffolds for tissue engineering. **Materials Today**, v. 14, n. 3, p. 88–95, 2011.

OLDE DAMINK, L. H. H. et al. Glutaraldehyde as a crosslinking agent for collagen-based biomaterials. **Journal of Materials Science: Materials in Medicine**, v. 6, n. 8, p. 460–472, 1995.

ORYAN, A. et al. Chemical crosslinking of biopolymeric scaffolds: Current knowledge and future directions of crosslinked engineered bone scaffolds. **International Journal of Biological Macromolecules**, v. 107, n. PartA, p. 678–688, 2018.

QI, Y. et al. A review of structure construction of silk fibroin biomaterials from single structures to multi-level structures. **International Journal of Molecular Sciences**, v. 18, n. 3, 2017.

REBOUÇAS, J. DE S.; SANTOS-MAGALHÃES, N. S.; FORMIGA, F. R. Cardiac Regeneration using Growth Factors: **Advances and Challenges. Arquivos Brasileiros de Cardiologia**, p. 271–275, 2016.

REIS, L. A. et al. Biomaterials in myocardial tissue engineering. **Jornaul of Tissue Engeneering and Regenerative Medicine**, v. 10, n. 1, p. 11–28, 2016.

RICARDO, M. et al. Remodelamento Ventricular : dos Mecanismos Moleculares e Celulares ao Tratamento. **Revista da Sociedade de Cardiologia do Rio Grande do Sul**, p. 1–7, 2004.

ROSELLINI, E. et al. Protein/Polysaccharide-based Scaffolds Mimicking Native Extracellular Matrix for Cardiac Tissue Engineering Applications. **Journal of Biomedical Materials Research - Part A**, p. 1–38, 2018.

RUVINOV, E.; COHEN, S. Alginate biomaterial for the treatment of myocardial infarction: Progress, translational strategies, and clinical outlook. From ocean algae to patient bedside. **Advanced Drug Delivery Reviews**, v. 96, p. 54–76, 2016.

SERPOOSHAN, V. et al. The effect of bioengineered acellular collagen patch on cardiac remodeling and ventricular function post myocardial infarction. **Biomaterials**, v. 34, n. 36, p. 9048–9055, 2013.

SHAO, L. et al. Synthesis and characterization of water-soluble polyaniline films. **Synthetic Metals**, v. 161, n. 9–10, p. 806–811, 2011.

SHAPIRA, A.; FEINER, R.; DVIR, T. Composite biomaterial scaffolds for cardiac tissue engineering. **Journal International Materials Reviews**, v. 00, n. 0, p. 1–19, 2015.

SHAVANDI, A. et al. Polyphenol uses in biomaterials engineering. **Biomaterials**, v. 167, p. 91–106, 2018.

SILVESTRI, A. et al. Biomimetic materials and scaffolds for myocardial tissue regeneration. **Macromolecular Bioscience**, v. 13, n. 8, p. 984–1019, 2013.

SIONKOWSKA, A.; PŁANECKA, A. Preparation and characterization of silk fibroin/chitosan composite sponges for tissue engineering. **Journal of Molecular Liquids**, v. 178, p. 5–14, 2013.

SUTTON, M. G. S. J.; SHARPE, N. Left Ventricular Remodeling After Myocardial Infarction : Pathophysiology and Therapy. **Circulation**, v. 101, n. 25, p. 2981–2988, 2000.

TAKIMOTO, E. et al. Role of Oxidative Stress in Cardiac Hypertrophy and Remodeling. **Hypertension**, p. 241–248, 2014.

TAYLOR, D. A.; SAMPAIO, L. C.; GOBIN, A. Building new hearts: A review of trends in cardiac tissue engineering. **American Journal of Transplantation**, v. 14, n. 11, p. 2448–2459, 2014.

TSAI, M. et al. Colloids and Surfaces B : Biointerfaces Evaluation of biodegradable elastic scaffolds made of anionic polyurethane for cartilage tissue engineering. **Colloids and Surfaces B: Biointerfaces**, v. 125, p. 34–44, 2015.

YANG, Y.; RITCHIE, A. C.; EVERITT, N. M. Comparison of glutaraldehyde and procyanidin cross-linked scaffolds for soft tissue engineering. **Materials Science and Engineering C**, v. 80, p. 263–273, 2017.

YE, G.; QIU, X. Conductive biomaterials in cardiac tissue engineering. **Biotarget**, n. 5, p. 1–7, 2017.

ZEGHIOUD, H. et al. Chemical synthesis and characterization of highly soluble conducting polyaniline in the mixtures of common solvents. **Journal of the Serbian Chemical Society**, v. 80, n. 7, p. 917–931, 2015.

ZHU, Z. et al. Hyaluronic acid : a versatile biomaterial in tissue engineering. **Plast Aesthet Res**, p. 219–227, 2017.

ZORNOFF, L. A. M.; SPADARO, J. Remodelação Ventricular após Infarto Agudo do Miocárdio . Conceitos , Fisiopatologia e Abordagem Terapêutica. **Arquivos Brasileiros de Cardiologia**, v. 68, n. no 6, p. 453–460, 1997.

CAPÍTULO II

1 Artigo 1 – “Dense lamellar scaffold as biomimetic materials for reverse engineering of myocardial tissue: preparation, characterization and physiomechanical”



Dense Lamellar Scaffold as Biomimetic Materials for Reverse Engineering of Myocardial Tissue: Preparation, Characterization and Physiomechanical Properties

Alves TFR¹, Souza JF¹, Severino P², Andréo Filho N³, Lima R¹, Aranha N^{4,5}, Silveira Filho LM⁶, Rai M⁷, Oliveira Junior JM⁸ and Chaud MV^{1*}

¹Laboratory of Biomaterials and Nanotechnology, University of Sorocaba, Sorocaba, ZC 18023-000, São Paulo, Brazil

²Laboratory of Nanotechnology and Nanomedicine, University of Tiradentes, Aracaju, ZC 49010-390, Sergipe, Brazil

³Laboratory of Pharmacology and Cosmetology, Federal University of São Paulo, ZC 09913-030, Diadema, São Paulo, Brazil

⁴Laboratory of Bioactivity Assessment and Toxicology of Nanomaterials, University of Sorocaba, Sorocaba, ZC 18023-000, São Paulo, Brazil

⁵Technological and Environmental Processes, University of Sorocaba, Sorocaba, ZC 18023-000, São Paulo, Brazil

⁶Medical Science College, State University of Campinas, Campinas, ZC 13083-887, São Paulo, Brazil

⁷Nanobiotechnology Laboratory, SGB Amravati University, ZC 444602, Maharashtra India

⁸Laboratory of the Nuclear Physical, University of Sorocaba, Sorocaba, ZC 18023-000, São Paulo, Brazil

1.1 Abstract

The aim of this study was to develop dense lamellar scaffold as a biomimetic material for myocardial tissue regeneration. To generate dense lamellar and porous structure with biomimetic polymers was used plastic compression method. The polymeric blends of collagen, chitosan and silk fibroin was used to obtain three-dimensional devices with interconnected porous, anisotropy, and anatomical similarity with the extracellular matrix. The texture profile analysis was employed to investigate the physiomechanical properties, including mucoadhesion and swelling efficiency. Fourier transform infrared spectroscopy, differential scanning calorimetry, computerized microtomography, scanning electron microscopy were employed to investigate the structural properties, surface morphology, porosity of the dense lamellar scaffold and, cell viability and image cytometer with H9c2 cells (cardiac myoblasts). The swelling efficiency of blends was evaluated using Enslin dispositive. The physiomechanical properties associated with swelling efficiency, porosity, anisotropy degree and, cell proliferation and viability (*in vitro*) suggest that the scaffold with COL-CH-SF obtained by plastic compression may be a potential biomimetic material for reverse engineering of myocardial tissue.

Keywords: Dense lamellar scaffold; reverse engineering; myocardial regeneration; collagen; plastic compression.

1.2 Introduction

Acute myocardial infarction (AMI) has been responsible for the reduction in life expectancy and large numbers of deaths worldwide. More than 17 million people die annually from cardiovascular disease, including heart attacks and strokes, according World Health Organization in 2015. The cardiovascular disease include a wide range of heart pathological condition and heart vasculature as ischemia, vascular malformation, cardiomyopathy structural, congestive heart failure and microvascular disease (TAYLOR; SAMPAIO; GOBIN, 2014b). When occurs an AMI, the coronary artery gets occluded thus resulting in areas of hypoxia on heart. As result of AMI an inflammatory process is initiated and occurs stimulating neighboring cells to increase matrix production ultimately leading to scar tissue formation. This tissue formed is unable to contract, losing the normal pumping action, thus causing an infarct area deformed over time, myocardial remodeling and reduced cardiac output (DOMENECH et al., 2016a).

The use of regenerative medicine to treat cardiovascular disease has arisen as a research topic in the last decades. Tissue engineering products can provide one way to overcome the actually therapy limitations for cardiovascular disease, replacing the damaged myocardium by AMI or inducing constructive forms of endogenous repair, which would significantly expand patient care options (SERPOOSHAN et al., 2013a). Thus, tissue regeneration can be facilitated by use of biomimetic material, as biopolymers that create a suitable microenvironment for cells recruitment, adhesion, proliferation and differentiation (O'BRIEN, 2011).

Biomaterial is broadly defined as a material that interacts with biological systems for biomedical purposes and must be biocompatible, biodegradable, reduce local microenvironment hostility and biopersistent to facilitate cell engraftment and integration with native tissue (CUI; YANG; LI, 2016; LAM; WU, 2012). The chemical composition, physiomechanical properties and 3D architecture of the scaffolds have been shown to play key roles in determining cell-microenvironment interactions and the fate of stem cells (SERPOOSHAN et al., 2013a).

Among various biomaterials to development of the scaffolds, collagen type I are increasingly being used as protein substrates in diverse biomedical applications, because it is predominant protein in mammalian extracellular matrix (GENERALI; DIJKMAN; HOERSTRUP, 2014; MAXIMO; CUNHA, 2010; SARGEANT et al., 2012;

VENKATESAN et al., 2015). Their main attributes include favorable fibrous structure, mechanical properties, biocompatibility, biodegradability and providing a biomimetic environment for cell growth.

Together with collagen, the chitosan and silk fibroin biomaterials have also been investigated as candidates for cardiac regeneration therapy. Was reported that mechanical strength and degradation resistance of collagen scaffold is enhanced by combining collagen with chitosan and/or silk fibroin matrixes. The addition of chitosan changed the collagen fiber cross linking and reinforced the structure and porosity of the composite sponge (ARPORNMAEKLONG; PRIPATNANONT; SUWATWIROTE, 2008; CUI; YANG; LI, 2016; KIM et al., 2001; SHE et al., 2008).

Chitosan, a natural linear polymer obtained by chitin deacetylation, can be used as a cell scaffold or carrier for controlled and localized drug delivery. This natural material displays high biocompatibility and biodegradability, has the capacity growth factor retention and strong cellular receptor adhesion due to its hydrophilicity. When mixed with natural materials, chitosan and/or silk fibroin scaffolds acquire other properties that favor cell maturation, adhesiveness, and scaffold coupling with the host myocardium (PEREA-GIL; PRAT-VIDAL; BAYES-GENIS, 2015; SHE et al., 2008).

However, collagen hydrogel shows a large volume and occupies a significant space to use in myocardium muscle. To reduce collagen hydrogel contraction without affecting its biocompatibility, Brown et al. (BROWN et al., 2005) and later others (BUSBY et al., 2013; BUXTON et al., 2008; HU et al., 2010; SERPOOSHAN et al., 2013b) developed a compressed collagen hydrogel technique (plastic compression) for tissue engineering through the rapid expulsion of fluid, producing scaffolds that are relatively dense and mechanically strong, with controllable mesoscale structures.

The plastic compression of collagen gels consists in transition of an initial state of a highly hydrated gel without structural competence to one of a relatively dense gel with the ability to support its own weight and provide resistance to fluid flow. During one-dimensional compression, the highly hydrated gel collapses against a rigid, porous support and forms a relatively dense gel layer (lamella) on top of this support, reminiscent of solute concentration polarization during ultrafiltration and gel formation. Therefore, at a microstructural level the highly hydrated gel transitions abruptly to a gel layer, resulting in a multi-layer model describing collagen gel compacted (SERPOOSHAN et al., 2011).

The present study aimed to develop and to evaluate with controllable mesoscale structures the dense lamellar scaffold as a biomimetic material for myocardial tissue regeneration. The different polymeric blends of collagen, chitosan and silk fibroin were used to obtain biomimetic three-dimensional devices, by plastic compression.

1.3 Materials and methods

1.3.1 Materials

The collagen powder, extracted from bovine hides, were supplied by NovaProm Food Ingredients Ltda. (São Paulo, Brazil). These samples were used without any chemical treatment. Chitosan of average molar mass, 75-85% deacetylate (Sigma-Aldrich Co, Saint Louis, USA), Dulbecco's Modified Eagle's Medium (DMEM) (Sigma-Aldrich Co, Saint Louis, USA) and cocoon of the *Bombyx mori*. The other reagents were of pharmaceutical grade.

1.3.2 Preparation of Fibroin Solution

Bombyx mori silk fibroin was prepared adapted from Komatsu et al. (2017) (KOMATSU et al., 2017). Briefly, silk sericin was extracted by treating silk cocoons in an aqueous solution of 0.5 wt % Na_2CO_3 (120°C) for 15 min using an autoclave. The silk fibroin was rinsed thoroughly with water to extract the sericin proteins. The degummed silk fibroin was dissolved in $\text{CaCl}_2 \cdot 2\text{H}_2\text{O}/\text{CH}_3\text{CH}_2\text{OH}/\text{H}_2\text{O}$ solution (mole ratio, 1:2:6) at 85°C. Then the fibroin solution (SF) was filtered and dialyzed against distilled water for 3 days to yield SF. The final fibroin concentration was about 2–3 wt %, which was determined by weighing the remaining solid after drying.

1.3.3 Preparation of chitosan hydrogel

The chitosan (CH) of average molar mass was used to prepare the hydrogel. Briefly, 3.0 g of the CH was added into 100 mL of the glacial acetic acid solution (1.5% v/v) and shaken until complete dissolution.

1.3.4 Preparation of collagen-chitosan hydrogel

The collagen dispersion was prepared by addition of 2 mL DMEM (Sigma, MO, US), 0.75g or 1g of collagen type I and, water enough to obtain 10 mL of dispersion.

The COL and CH hydrogels were mixed in the rate of 9:1 (m/m) and this hydrogel was used to prepare the COL-CH scaffold. The dispersions were placed into cylindrical containers (inner diameter = 21 mm and height = 11 mm), and incubated at 10 °C for 24 h for polymerization.

1.3.5 Preparation of collagen-chitosan-fibroin hydrogel

The collagen dispersion was prepared by addition of 2 mL DMEM (Sigma, MO, US), 0.75g or 1g of collagen type I and, water enough to obtain 10 mL of dispersion. The COL, CH and SF hydrogels were mixed in the rate of 9:1:5 (m/m/v) and this hydrogel was used to prepare the COL-CH-SF scaffold. The dispersions were placed into cylindrical containers (inner diameter = 21 mm and height = 11 mm), and incubated at 10 °C for 24 h for polymerization.

1.3.6 Preparation of dense lamellar scaffolds

Dense lamellar scaffolds for AMI were produced by plastic compression (using hydrostatic press), adapted from Brown et al (2005). Briefly, cast highly hydrated hydrogels were transferred to a porous support comprising (bottom to top) absorbent paper blot layers, a steel mesh and two nylon meshes. Subsequently, a static compressive stress of 4KN was applied to the hydrated scaffolds for 10 min in order to remove water and produce a dense biomaterial with improved biological and mechanical properties. Finally, the matrices were freeze-dried, resulting in cross-linked collagen-chitosan scaffolds.

1.3.7 Physiomechanical and Mucoadhesive Properties

Texture profile analysis (TPA) was used to measure the physiomechanical properties (elasticity, flexibility, drilling and resistance to traction) of scaffolds were performed using a Stable Micro Systems texture analyzer (Model TA-XT Plus) in texture profile analysis mode with load cell of 5 Kg. The samples (approximately 40 mm diameter) were hydrated for 1h or 7 days, excess of the water was removed, and after were fixed in suitable apparatus with hole. Test velocity was defined for rate of 2 mm.s⁻¹ for drilling and resistance to traction test and 0.5 mm. s⁻¹ for elasticity and flexibility test. Elastic (Young's) modulus was obtained by compressed until

densification occurred, at which point the tests were stopped (strain ranged approximately between 0 and 5%).

The mucoadhesive properties of scaffolds were evaluated using a Stable Micro Systems texture analyzer (Model TA-XT Plus). Mucin discs were prepared for compression (Lemaq, Mini Express LM-D8, Diadema, Brazil), using flat punches, cylindrical matrix with a diameter of 8mm and a compression load of 8 tons. The mucin discs showed diameter of 8 mm and thickness of 0.2 mm and, were previously hydrated and fixed to the lower end of the analytical probe. The samples (41 mm diameter) were fixed in suitable apparatus with hole. Mucin disc fixed in the probe was compressed on the surface of the scaffold with a force of 0.098 N, directed in the apical → basal. Contact time between mucin disc and sample was of 100 s, stipulated for an intimate contact of the mucin disc with the sample. The probe was removed of the scaffold surface with constant quickness of 10 mm.s⁻¹. The force required to detach the mucin disc from the surface of scaffold was determined from the time (s) x force (N) ratio.

1.3.8 Swelling efficiency

The swelling efficiency profile was obtained by Enslin dipositive (FAHR; VOIGT, 2000). Briefly, the samples were kept in touch with buffer solution pH 7.4 by 16 hours. To perform this study were used samples with 1 cm², and were put onto the sintering filter and the volume of media absorbed by the sample after predetermined times was measured with the graduated pipette of the device. The volume of liquid absorbed by the sample was noted and graphically plotted (volume of liquid absorbed x time).

1.3.9 Porosity, interconnectivity and pore size

The morphometric characteristic of the porosity, interconnectivity and pore size of scaffolds were evaluated by computerized microtomography (μ CT). The scaffolds pictures were captured by X-Ray microtomograph (Brucker-micro CT - SkyScan 1174, Kontich, Belgium) with high resolution scanner (28mM pixel and integration time at 1.7 s). The source of the X-rays was 34 keV of energy and 790 mA of current. The projections were acquired in a range of 180° with an angular step of 1° of rotation. 3D virtual models representative of various regions of scaffolds were created and the data were mathematically treated by CT Analyzer v. 1.13.5.

1.3.10 Scanning electron microscopy (SEM)

SEM photographs scaffolds were obtained using a scanning electron microscope (LEO Electron Microscopy/Oxford, Leo 440i, Cambridge, England) with a 10 kV accelerating voltage. All samples were affixed to a brass specimen holder using double-sided adhesive tape, and the powders were made electrically conductive by coating with gold using a sputter-coater for 4 min at 15 mA.

1.3.11 Differential scanning calorimetry (DSC)

DSC was performed on a Shimadzu, TA-60, Kyoto, Japan, calibrated using indium as the reference material. A sample of 2 mg was packed in a hermetically crimped aluminum pan, and heated under dry nitrogen purged at 30 mL.min⁻¹. The samples were heated from 25 to 340 °C at a rate of 5 °C min⁻¹.

1.3.12 Fourier transform infrared spectroscopy (FTIR)

FTIR analysis (Shimadzu, IRAffinity-1, Kyoto, Japan) was used to collect FT-IR spectra via Labsolutions Software v.2.10. The chemical functionalities of the samples were determined by an attenuated total reflectance (ATR) cell on the FTIR spectrophotometer over the range between 4000 and 600 cm⁻¹ at 4 cm⁻¹ resolutions, averaging 128 scans.

1.3.13 Cell viability

The cellular analyses were evaluated just for COL-CH-SF scaffolds, based on the best results presented in the other analyses. In order to evaluate cell viability, the material was initially extracted and kept in the culture medium for 24 hours. The extract was made using a 1cm² fragment in 2.5mL culture medium. This concentration of material is equivalent to exposing 1.6 m of material to a 70 kg individual.

Approximately 5x10⁵ cells/well (H9c2 cells - cardiac myoblasts) were plated in 96-well plates, after 24h period and total cell adhesion treatments were performed using the extracts at 100, 50 and 25% dilutions, and were maintained for a period of 24h. After the treatment, the culture medium was removed and 100µl of MTT solution (3- (4,5-dimethylthiazolyl-2) -2,5-diphenyltetrazolium bromide) at 5mg/ml was added to each well. After 3 hours in the oven at 37 °C, the MTT solution was withdrawn and

100 μ l of DMSO per well was added for cell attachment. The reading was performed using ELISA microplate reader at 570nm.

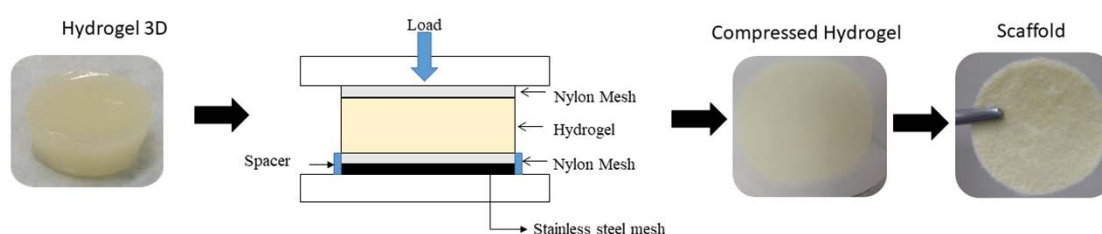
1.3.14 Image cytometer

Initially (Time 0h) 1×10^5 cells / well (H9c2 cells - cardiac myoblasts) were plated in a 24 well plate, which was incubated at 37 ° C - 5% CO₂ using Minimum Essential Alpha medium with ribonucleosides, deoxyribonucleosides, 2mM L-glutamine and 1mM sodium pyruvate, without ascorbic acid plus fetal bovine serum to a final concentration of 10%. After 24 hours and total adhesion of the cells, they were placed in contact with the material for 48 and 72 hours. After the treatment period, the samples were removed from the cultures and the cells were washed with PBS, trypsinized and counted using the Image Cytometry technique.

1.4 Results

The mesoscale analysis of the scaffold obtained by plastic compression showed stable and uniform physical structure and absence of the furrow, indicating that the process used was capable of getting the scaffold (Figure 1). Thus, the crosslinking has been confirmed to play an important role related to the scaffold with porous structure distribution and with the ability of water containing (WANG et al., 2013). The plastic compression was an efficient technique to get the dense lamellar scaffold, based on collagen, with potential use for cardiac regeneration by reverse engineering.

Figure 1. Dense lamellar scaffold obtained by plastic compression.

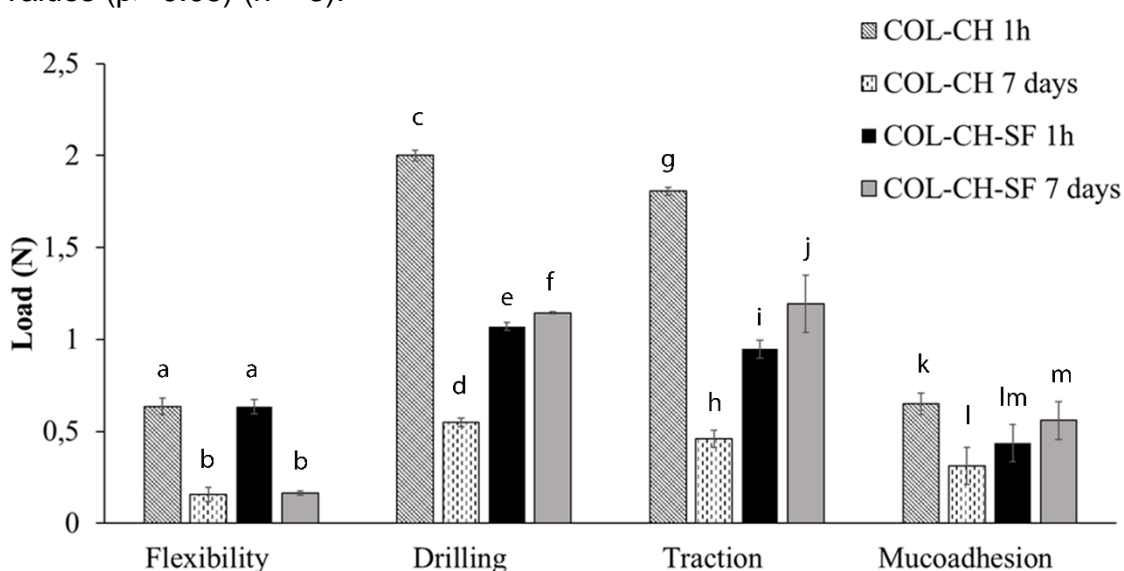


1.4.1 Physiomechanical and Mucoadhesive Properties

Figure 2 shows the mechanical resistance results of the scaffold obtained by plastic compression after 1 hour and after 7 days. When the scaffolds were hydrated for 1 hour the drilling, tensile strength and mucoadhesion properties of the scaffolds

containing COL and CH showed better results than scaffold with SF ($p < 0.05$), however the elasticity (Table 1) and flexibility properties (Figure 2) were the same for both formulations with and without SF (COL-CH and COL-CH-SF). After 7 days of the hydration the COL-CH scaffolds showed decrease for all mechanical properties studied ($p < 0.05$), this fact can be assigned to relaxation of the polymer's chains and the kind of crosslinking formed.

Figure 2. Physiomechanical properties of dense lamellar scaffolds. Equal letters (for the same analysis) indicate that there is no significant difference between the mean values ($p > 0.05$) ($n = 3$).



After 7 days the scaffolds containing SF (COL-CH-SF), showed decrease for flexibility properties and increase for tensile strength ($p < 0.05$). Although, the drilling and mucoadhesion properties were kept ($p > 0.05$). The results obtained with Young's modulus (Table 1) revealed that the introduction of SF to COL-CH significantly increases the values of this parameter for COL-CH-SF ($2,022.034 \pm 144.019$ kPa) scaffolds compared with COL-CH ($1,697.746 \pm 87.416$ kPa).

Table 1. Mechanical properties of Young's modulus of scaffolds (after 1 hour and 7 days in aqueous medium).

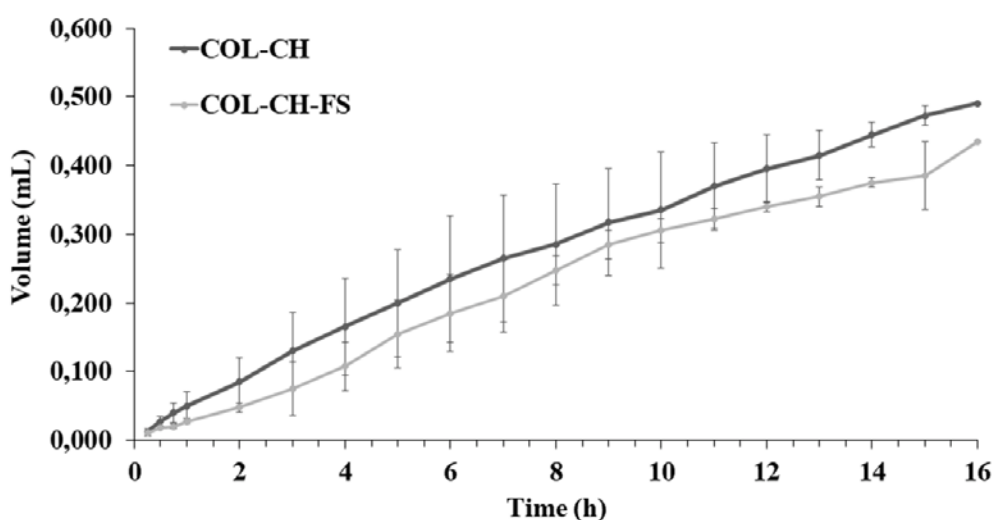
	1 hour	7 days
	Elasticity (KPa)	Elasticity (KPa)
COL-CH	0.726 ± 0.089^a	$1,697.746 \pm 87.416^b$
COL-CH-SF	0.784 ± 0.058^a	$2,022.034 \pm 144.019^c$

Thus, our results showed that SF increases significantly the Young's modulus of COL-CH scaffolds after 1 hour ($1,697.746 \pm 87.416$ KPa) and 7 days ($2,022.034 \pm 144.019$ KPa) of water immersion.

1.4.2 Swelling efficiency

Figure 3 shows the volume of buffer absorbed (mL) by the sample in function of time (h). The results show that hydrophilic equilibrium of the scaffolds COL-CH and COL-CH-SF after 16 hours was not yet reached, since the curve profile is upward. Until 12 hours the profiles were similar and statically equals ($p > 0.05$), after than the COL-CH scaffold showed a volume of liquid absorbed greater than the absorbed by COL-CH-SF ($p < 0.05$). The end of scaffold of COL-CH profile indicates that the hydrophilic equilibrium will be reached because a baseline is starting after 15 hours. However, after 15 hours was observed that COL-CH-SF scaffold shows the upward profile.

Figure 3. Swelling efficiency profile of dense lamellar scaffolds.



For both scaffolds were observed anomalous transport, when the n values were 0.79 and 0.88, respectively to COL-CH and COL-CH-SF.

1.4.3 Porosity, interconnectivity and pore size

The morphological and morphometric characteristic of dense lamellar scaffolds are showed in Table 2 and Figure 4-5. The COL-CH and COL-CH-SF scaffolds had the regular interconnected structure with large porosity (Table 2). The pores

interconnectivity of the COL-CH and COL-CH-SF scaffolds were 71.68% and 79.01%, respectively. The pores were oriented with rounded shape in both formulations (Figure 4-5). The values obtained to degrees of anisotropy of the COL-CH and COL-CH-SF scaffolds were 0.426 and 0.4, respectively.

Table 2. Morphological characteristics of scaffolds.

	COL-CH	COL-CH-SF
Pore interconnectivity (%)	71.68	79.01
Volume of open pores (mm⁻³)	2.66	2.14
Closed porosity (%)	0.15	0.2
Degree of anisotropy	0.426	0.400

Figure 4. Morphometric characteristic of dense lamellar scaffolds evaluated by computerized microtomography.

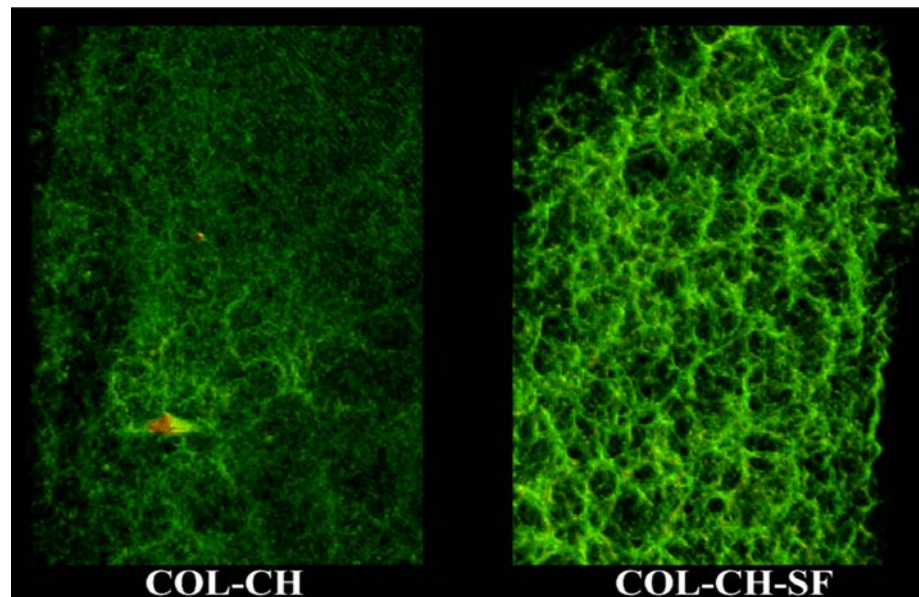
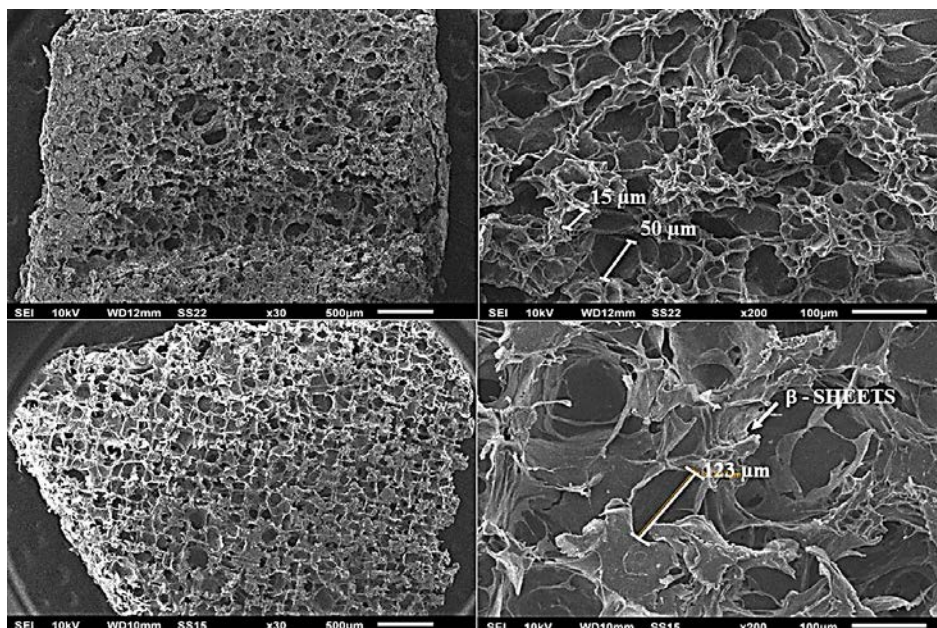


Figure 5 shows SEM images of compacted and freeze-dried scaffolds prepared from collagen/chitosan and collagen/chitosan/fibroin blend. The pores size for COL-CH-SF scaffold were 10x bigger than COL-CH scaffold.

Figure 5. Scanning electron microscopy of dense lamellar scaffolds.

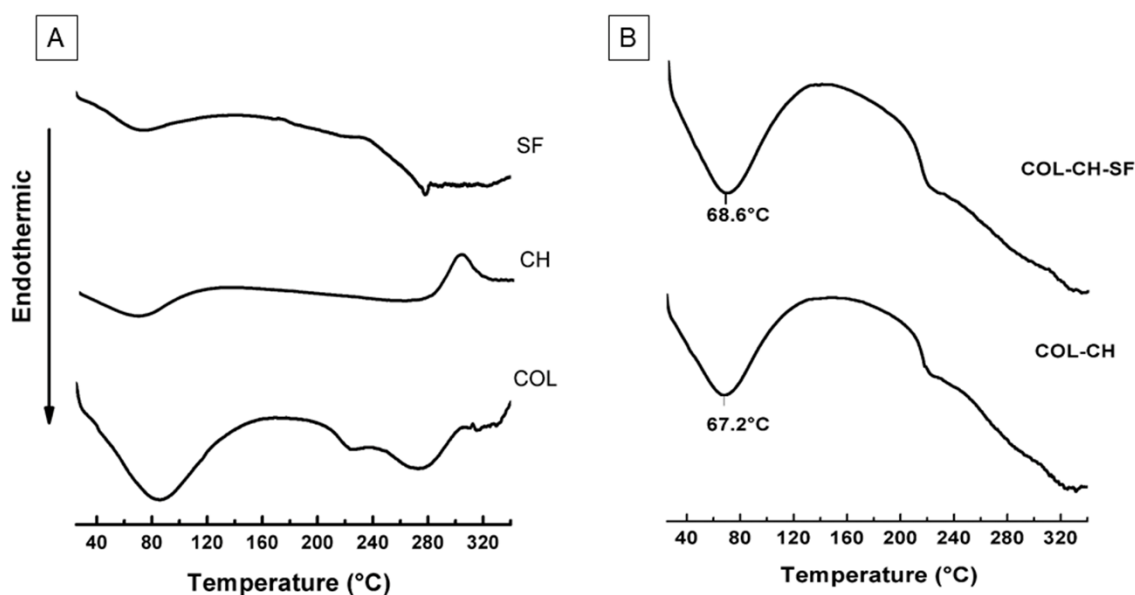


1.4.4 Differential scanning calorimetry (DSC)

Figure 6 (A-B) show the thermogram of polymers and scaffold COL-CH, and COL-CH-SF. The first thermic events between 45 and 110°C (Figure 6) are associated with lose of the water from the excipients and scaffolds formulations. In the Figure 6 (panel A-SF) the endothermic peak at 281°C is related as a thermal degradation of SF. To CH thermogram Figure 6 (panel A) the thermal event at 302 °C is an exothermic peak it may be related to the decomposition of amine (GlcN) units (GUINESI; CAVALHEIRO, 2006).

A denaturation temperature (T_d) of COL-CH scaffold was recorded at 67.2°C whereas COL-CH-FS exhibited T_d peak at 68.6°C (LAKRA et al., 2014). A single glass-transition temperatures (T_g 's) occurred at 220°C to COL-CH and COL-CH-SF scaffolds, the same was observed for COL in the natural form.

Figure 6. Differential scanning calorimetry of COL, CH, SF (panel A), and scaffolds samples (panel B).



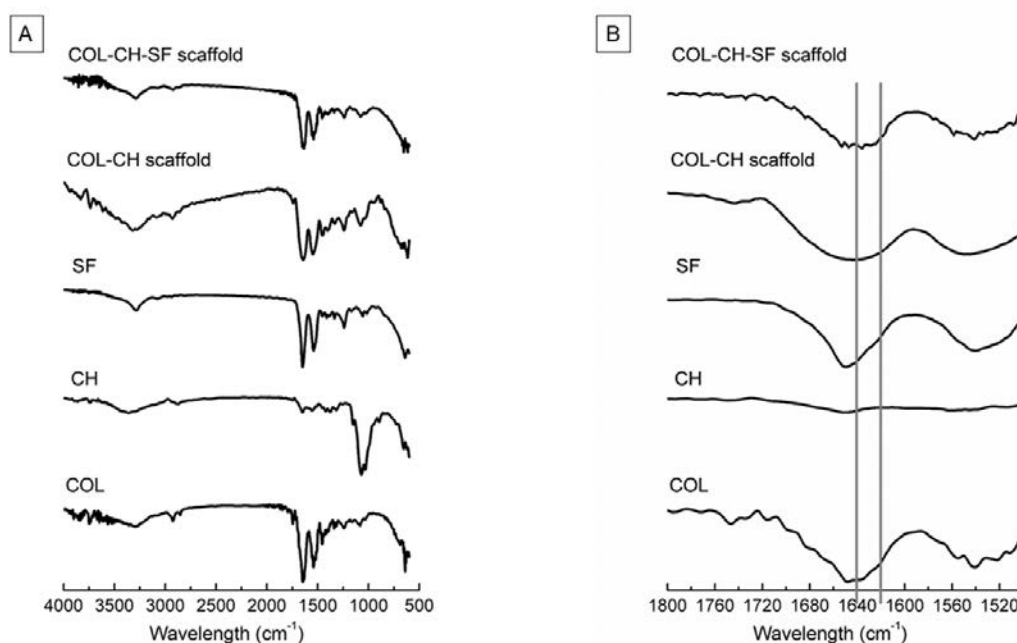
1.4.5 Fourier transform infrared spectroscopy (FTIR)

Infrared spectra show stretches characteristic of COL, CH, SF (Figure 7A) and scaffolds samples (Figure 7B). The spectrum of collagen depicts characteristic absorption bands in 1645 cm^{-1} corresponding to amide I absorption arises predominantly from protein amide C=O stretching vibrations and 1546 cm^{-1} corresponding to amide II is made up of amide N-H bending vibrations and C-N stretching vibrations. The 1240 cm^{-1} corresponding to amide III band is complex, consisting of components from C-N stretching and N-H in plane bending from amide linkages. The peaks identified at 1454 cm^{-1} and in the region between 1417 cm^{-1} and 1360 cm^{-1} correspond to the stereochemistry of the pyrrolidine rings of proline and hydroxyproline. Additionally, bands at 3450 , 2850 and 1450 cm^{-1} were observed, which represent the stretching of -OH, -CH₃ and pyrrolidine rings, respectively.

The spectrum of chitosan depicts characteristic absorption bands at 3352 , 2878 cm^{-1} , attributed to the -OH and -CH₃ groups. Furthermore, bands were identified at 1560 and 1404 cm^{-1} typical of the N-H group bending vibration and vibrations of -OH group of the primary alcoholic group, respectively. The bands at 1320 and 1077 cm^{-1} correspond to the stretching of C-O-N and C-O groups. The bands at 1154 and 897 cm^{-1} are attributed to the glycosidic bonds. The shoulder at 1650 cm^{-1} represents the stretching of C=O.

Pure SF shows absorption bands at 1645 cm^{-1} (amide I) and 1546 cm^{-1} (amide II), corresponding to the SF silk II structural conformation (β -sheet). Other absorption bands were observed at 1530 cm^{-1} (amide II) and 1236 cm^{-1} (amide III), which are characteristic of the silk I conformation (random coil and α -helix) these results were compatible with literature.

Figure 7. Infrared spectra of COL, CH, SF (panel A) and scaffolds samples (panel B).

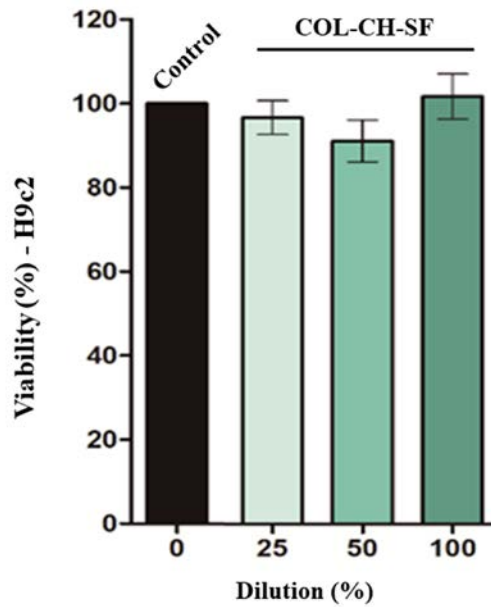


The FTIR spectra of the COL-CH and COL-CH-SF scaffolds show the characteristic bands of the parent molecules, indicating that did not have chemical interaction between the polymers used in the formulation.

1.4.6 Cell viability

The results are showed in Figure 8 and show the cellular viability after 24 hours of scaffold exposure. According to our results, no significant differences between control group and COL-CH-SF scaffolds. The viability for scaffold was greater than 90%. It is not possible in these concentrations to determine the IC₅₀.

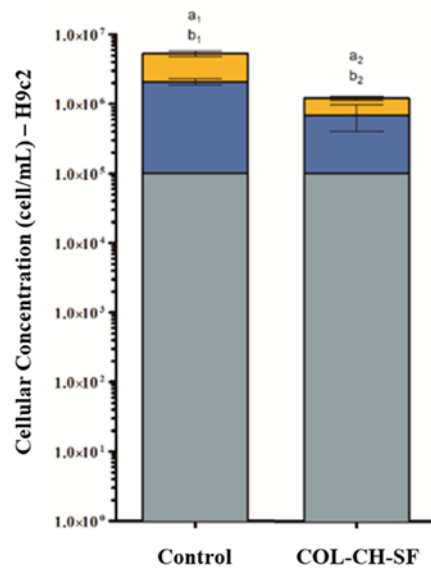
Figure 8. Results of MTT analyses, exposure to control and COL-CH-SF scaffold in H9c2 cells for 24h.



1.4.7 Image cytometer

The results show that COL-CH-SF scaffold presents a significant difference during growth with respect to the control, after 48 and 72 hours, presenting a decrease of cellular multiplication (Figure 9).

Figure 9. Results regarding cell growth (H9c2) after exposure to COL-CH-SF.



1.5 Discussion

To construct a scaffold in heart tissue engineering with biomimetics characteristics, it is needing to consider the critical factors as thickness, pore size range, mechanical strength, biodegradability, swelling capacity and biopersistence. Cell adhesion is a fundamental process directly involved in cell growth, cell migration, and cell differentiation. The surface hydrophilicity, the presence of ionic charges parameters and chemical composition influence these interactions (KIM et al., 2001).

The gel formation with the blend of polymers (COL, CH and SF) was induced by pH correction, this factor was important to improve the crosslinking and to provide a 3D formation (MAXIMO; CUNHA, 2010). However, the collagen gels show a poor mechanical property when pre-compressed due to the excess of the fluid present in untreated collagen. The development of the plastic compression (PC) technique can rapidly produce dense, mechanically strong collagen scaffolds with controllable microscale features and biomimetic function (CHEEMA; BROWN, 2013; MI et al., 2010). Dense collagen scaffolds mimicking the ECM fibrillar density and microstructure which have great potential for tissue engineering applications, such as skin grafts, cornea epithelial reconstructs, myocardium and bone regeneration (XIA; VILLA; WEI, 2015).

The myocardium is a muscle highly elastic, and elastic relaxation during diastole is essential for proper heart function. The elastic modulus of the scaffold and elastic deformation is a critical characteristic to the myocardium. Myocardial tissue has the stiffness of the left ventricle ranges from 10–20 kPa during diastole and 200–500 kPa during systole (KAISER; COULOMBE, 2015; RADISIC; CHRISTMAN, 2013). Therefore, the scaffolds should be able to maintain its shape and be mechanically robust to withstand the contraction and relaxation straight. The microstructure and stiffness properties affect the bioactivity, migration and adhesion of cells into the scaffolds. Thus, the characterization of the stiffness of the 3D tissue-engineered scaffold can allow the effect of this parameter on cell activity in a more realistic situation (CHAUD et al., 2017; DAVIDENKO et al., 2010; SARGEANT et al., 2012).

The mechanical properties of 3D scaffold are elasticity, flexibility, drilling and tensile. The elastic modulus or Young's modulus of the material (i.e. stiffness) is the ability of the scaffold to return to its original form after deformation, which is a critical characteristic of the myocardium tissue. Young's modulus is commonly used to try and

quantify an intrinsic elastic property of soft, viscoelastic biomaterials (KAISER; COULOMBE, 2015). The flexibility of scaffolds is related with the capacity of material to suffer a maximum external deformation without to fracture the crosslinking of the polymers. The drilling of scaffolds is the force at the maximum distance of a compression cycle or the maximum force reached prior to a fracture. The tensile strength is the measure of the force or stress required to stretch the scaffold (resistance to lengthwise stress) to the point where it breaks or before permanent result of deformation.

Mucoadhesion can be defined as the bond produced by contact between the scaffold and the mucin that recovers the membrane surface. The mucus is an external layer of gel-like material secreted by goblet cells, compound of the water, inorganic salts, lipids, and mucins, highly glycosylated glycoproteins with many cysteine residues on their backbone structure (ESHEL-GREEN et al., 2016).

The dense lamellar scaffolds obtained by our group have not used crosslinking agent as glutaraldehyde, carbodiimide, epoxy compounds, acyl azide or any natural crosslinking agent. After 7 days of the hydration the COL-CH scaffolds showed decrease for all mechanical properties studied ($p < 0.05$), this fact can be assigned to relaxation of the polymers chains and the kind of crosslinking formed. In collagen, the $-OH$ groups of hydroxyproline are involved in hydrogen bonds between chains, while interactions between other side groups are thought to be important in the formation of fibrils. These side groups are capable of forming hydrogen bonds with $-OH$ and $-NH_2$ groups in chitosan. Moreover, the end group $-COOH$ and $-NH_2$ in collagen-may also form hydrogen bonds with $-OH$ and $-NH_2$ groups from chitosan, as chitosan possesses large numbers of $-OH$ groups. Additionally, COL-CH may be bonded ionically. These molecules are capable of forming complexes with oppositely charged ionic polymers, particularly the cationic polysaccharide chitosan and anionic $-COOH$ group in collagen (SIONKOWSKA, 2004).

The results obtained with Young's modulus (Table 1) revealed that the introduction of SF to COL-CH significantly increases the values of this parameter for scaffolds compared with COL-CH. Cheema and Brown (2013), and Hadjipanayi et al. (2009) produced the collagen scaffolds by the same technique of plastic compression. The results obtained by themselves in Young's modulus test were similar to our found (CHEEMA; BROWN, 2013; HADJIPANAYI; MUDERA; BROWN, 2009). Serpooshan et al. (2013), produced collagen scaffolds by plastic compression technique using

different compression load. They obtained scaffolds with Young's modulus (stiffness) between 0.34 and 1.4 KPa (SERPOOSHAN et al., 2013a).

These studies have been performed to check the relation between stiffness of material and the cell proliferation. The results demonstrated the preferential accumulation of cells towards the stiffer regions of the gradient (GANGARAJU VAMSI K. LIN HAIFAN, 2009; HADJIPANAYI; MUDERA; BROWN, 2009; HADJIZADEH; DOILLON, 2010). If we compare our results with those obtained by Serpooshan et al. (2013a), we can assert based on Young's modulus, that the COL-CH-SF scaffolds have an environment more favorable to cell proliferation than those obtained by them.

Silk fibroin is composed by silks I and silks II. The silks I provides a good water solubility since is formed by α -helix and β -sheet. The silks II is the main structural configuration of the SF and is rich in β -sheet, it provides a poor water solubility. The high resistance to water permeation decrease the scaffold dissolution time. SF has reactive carboxyl groups and amino groups in its side chains, it can react with other functional groups being able to keep or to improve the mechanical properties of scaffolds, even after 7 days immersed in aqueous environment (LI et al., 2013b). Gobin et al. (2005) assigns this behavior is due to increased regions of β -sheets, which increase the amount of crystalline domains and increase tensile strength and stiffness. Sun et al. (2016), produced COL-SF scaffolds and observed that after 14 days immersed of culture medium, the thickness and Young's modulus of the scaffolds increased.

Water molecules from the environment migrate to the microscopic pores or voids in the compound to achieve concentration equilibrium. The moisture mass obtained by a polymer occurs in two states, mobile or bound. The first state is sometimes called physical absorption by polymers based on Fick's laws. The second state is when the water molecules become chemically bonded to the polymer chain' hydroxyl groups. This chemical absorption process can be irreversible and causes non-Fickian behavior (PLACETTE; FAN; EDWARDS, 2011).

By determining the diffusional exponent, n , one can gain information about the physical mechanism controlling solute uptake by or drug release from a particular device. For a film, $n = 0.5$ indicates Fickian diffusion, $n > 0.5$ indicates anomalous transport and $n = 1$ implies case II (relaxation-controlled) transport (GANJI; VASHEGHANI-FARAHANI; VASHEGHANI-FARAHANI, 2010). Since most polymers swell when they are in contact with certain solvents, one can use Fick's laws with

modified boundary conditions and/or a generalized diffusion coefficient to address the non-Fickian behavior (ROSSI; MAZICH, 1993).

The swelling efficiency test (Figure 3) indicated that the water-binding ability of the COL-CH or COL-CH-SF scaffolds could be attributed to both of their hydrophilicity and the maintenance of their three-dimensional structure. In general, the swelling ratio is decreased with the increases crosslinking degree due the decrease of the free hydrophilic groups. For both scaffolds were observed anomalous transport, when the n values were 0.79 and 0.88, respectively to COL-CH and COL-CH-SF. The anomalous transport is observed when the diffusion and relaxation rates are comparable and govern the moisture absorption.

The scaffolds properties to cardiac regeneration should have an interconnected porous structure, high porosity, and appropriate pore dimensions to favor cell homing and migration, cellular anchorage, vascularization, and oxygen, nutrient, metabolite diffusion. These factors must be considered and balanced with the understanding of the well-known effect of stiffness on cellular differentiation. A three-dimensional scaffolds wich were prepared by plastic compression and lyophilization had porous structure confirmed by μ CT (Figure 4) and SEM (Figure 5).

The major limitation of the conventionally fabricated cardiac scaffolds is their isotropic nature. The tissue that is formed into the pores of an isotropic scaffold is a negative or mirror image of the scaffold itself, and since most tissue has anisotropic arranged extracellular matrix components and concomitant mechanical properties, the tissue formed has no structural and mechanical relationship with the native tissue. Anisotropic scaffolds with a porous, tubular or other structure, that enable direct differentiation into the native tissue conFiguretion might be extremely helpful to realize this goal. The anisotropy is associated with lamellar characteristic on scaffolds. The use of μ CT allows to obtain the degrees of anisotropy of the scaffolds (Table 2), that can range from 0 (structure is completely isotropic) to 1 (structure is completely anisotropic) (DE MULDER; BUMA; HANNINK, 2009; SILVA et al., 2014). The values obtained to degrees of anisotropy of the COL-CH and COL-CH-SF scaffolds were 0.426 and 0.4, respectively. Thus, the scaffolds produced are partially lamellar (anisotropic). The result of degree anisotropy added up to mechanical (Figure 2 and Table 1) and structural (Table 2 and Figure 4-5) properties are suitable to stimulate the cell growth, the tissue formation and to withstand the stiffness of the left ventricle (10–

20 kPa during diastole and 200–500 kPa during systole) (KAISER; COULOMBE, 2015).

The SEM images are according to LV et al. 2005 (LV et al., 2005), it is common the sheets formation in structure surface of the scaffold when the same is added of fibroin. This information corroborates with our SEM results (Figure 5 C-D) obtained for COL-CH-SF scaffold. The analyze of results presented in Figure 2 show that the drilling and traction properties increased with hydration time.

Thermal degradation peaks of SF films at temperatures in the 290 °C region are characteristic of amorphous SF (silk I) and are present when SF films are not submitted to any kind of physical or chemical treatment to induce its conformation to a more stable structure (silk II) (FREDDI G.; PESSINA G.; TSUKADA M., 1999). Thermal decomposition peaks of collagen observed between 220 - 350 °C also were observed by Shanmugasundaram et al. (2001). León-Mancilla et al. (2016) related that endothermic peak at 325°C could be due the loss of hydrogen bonds, so this phenomenon of protein denaturation, could be initiated in this interval of temperature which the tertiary structure is lost. Although, this phenomenon is reversible if the protein is newly hydrated.

Triple helix of collagen are held together by hydrogen bonds and crosslinking stabilizes the triple helical structure of collagen by forming intramolecular and intermolecular network The DSC thermogram of COL-CH and COL-CH-FS are shown in Figure 6 (panel A-B). DSC is used to measure the denaturation temperature (T_d) which is a measure of crosslinking density. It gives a better understanding of unfolding of protein under the influence of temperature. The DSC plots gives an endothermic peak associated with helix to coil transition which indicates the extent of intermolecular crosslinking.

In general, the miscibility of the polymers blend depends on the self-association and inter-association of hydrogen-bonding donor polymers. This miscibility can be analyzed with DSC to determine when has a single glass-transition temperatures (T_g 's) (KUO; HUANG; CHANG, 2001). The T_g 's at 220°C to COL-CH and COL-CH-SF scaffolds can be also observed for COL in the natural form, indicating that COL, CH and SF form a miscible blend.

FTIR is commonly used to investigate the conformation of SF and blend of COL-CH-SF. The FTIR spectra represents typical absorption bands sensitive to the molecular conformation of SF. The FTIR in the range of 1800-1500 cm^{-1} (Figure 7B)

was analyzed to investigate the β -sheet formation ($1640\text{-}1620\text{ cm}^{-1}$) (SIONKOWSKA; PLANECKA, 2013) in the COL-CH-SF scaffolds. The analyze of spectra showed that was displacement of the band related to random coil conformation ($1650\text{-}1640\text{ cm}^{-1}$) for conformation β -sheet ($1640\text{-}1620\text{ cm}^{-1}$). This fact indicates that the scaffold manufacturing process and/or blend of polymers are able to convert random coil to β -sheet conformation. The FTIR spectra of scaffold shows that did not have chemical interaction between the polymers used in the formulation.

Cell viability and proliferation was widely assayed by the MTT, which was a quantitative colorimetric assay. The purple crystals can be formed by metabolically active cells and was detected by spectrophotometry at 520 nm. So, growth and proliferation of active cells can be tested indirectly using this method (SUN et al., 2014). To confirm the cell viability and proliferation was made the image cytometer. In general, it is possible to observe that the material leads to an initial imbalance in the cells tested, but these seem to return to normal after a period of 72h, as observed in Figure 9, where there are differences of the exposed material in relation to the control (without exposure). As no significant cell death was observed on exposure, it is concluded that the material does not lead to cell death but an initial decrease in multiplication that is restored after the 72 h period.

1.6 Conclusion

The plastic compression is an efficient technique to produce the dense lamellar scaffold with biomechanical properties to be evaluated in reverse engineering of myocardial tissue. The characterization by FTIR shows the transition of random coil to β -sheet conformation, which positively influence the biomechanical properties and swelling efficiency of dense lamellar scaffold, composed of collagen, chitosan and silk fibroin. The images captured by μ CT and SEM show that scaffold has the regular interconnected structure with large porous and high anisotropy degree. So, the COL-CH-SF scaffold may be an ideal biomimetic template for reverse myocardial tissue engineering. Considering the obtained result in this study, we observed that the selection of the biomaterial as scaffold does not influence cell proliferation and viability significantly *in vitro* condition.

1.7 References

- ARPORNMAEKLONG, P.; PRIPATNANONT, P.; SUWATWIROTE, N. Properties of chitosan-collagen sponges and osteogenic differentiation of rat-bone-marrow stromal cells. **International Journal of Oral and Maxillofacial Surgery**, v. 37, n. 4, p. 357–366, 2008.
- BROWN, R. A. et al. Ultrarapid engineering of biomimetic materials and tissues: Fabrication of nano- and microstructures by plastic compression. **Advanced Functional Materials**, v. 15, n. 11, p. 1762–1770, 2005.
- BUSBY, G. A. et al. Confined compression of collagen hydrogels. **Journal of Biomechanics**, v. 46, n. 4, p. 837–840, 2013.
- BUXTON, P. G. et al. Dense collagen matrix accelerates osteogenic differentiation and rescues the apoptotic response to MMP inhibition. **Bone**, v. 43, n. 2, p. 377–385, 2008.
- CHAUD, M. V et al. Three-Dimensional and Biomimetic Technology in Cardiac Injury After Myocardial Infarction: Effect of Acellular Devices on Ventricular Function and Cardiac Remodelling. In **Scaffolds in Tissue Engineering - Materials, Technologies and Clinical Applications**. [s.l: s.n.]. p. 227–251.
- CHEEMA, U.; BROWN, R. A. Rapid Fabrication of Living Tissue Models by Collagen Plastic Compression: Understanding Three-Dimensional Cell Matrix Repair In Vitro. **Advances in Wound Care**, v. 2, n. 4, p. 176–184, 2013.
- CUI, Z.; YANG, B.; LI, R.-K. Application of Biomaterials in Cardiac Repair and Regeneration. **Engineering**, v. 2, n. 1, p. 141–148, 2016.
- DAVIDENKO, N. et al. Collagen-hyaluronic acid scaffolds for adipose tissue engineering. **Acta Biomaterialia**, v. 6, n. 10, p. 3957–3968, 2010.
- DE MULDER, E. L. W.; BUMA, P.; HANNINK, G. Anisotropic porous biodegradable scaffolds for musculoskeletal tissue engineering. **Materials**, v. 2, n. 4, p. 1674–1696, 2009.
- DOMENECH, M. et al. Tissue Engineering Strategies for Myocardial Regeneration: Acellular Versus Cellular Scaffolds? **Tissue Engineering Part B: Reviews**, v. 22, n. 6, p. 438–458, 2016.
- ESHEL-GREEN, T. et al. PEGDA hydrogels as a replacement for animal tissues in mucoadhesion testing. **International Journal of Pharmaceutics**, v. 506, n. 1–2, p. 25–34, 2016.
- FAHR, A.; VOIGT, R. Pharmazeutische technologie: für Studium und Beruf. 9. ed. **Stuttgart**: [s.n.].
- FREDDI G.; PESSINA G.; TSUKADA M. Swelling and dissolution of silk fibroin (Bombyx mori) in N-methylmorpholine N-oxide. **International Journal of Biological Macromolecules**, v. 24, p. 251, 1999.

- GANGARAJU VAMSI K. LIN HAIFAN. Cell adaptation to a physiologically relevant ECM mimic with different viscoelastic properties. **Nat Rev Mol Cell Biol.**, v. 10 (2), n. 1, p. 116–125, 2009.
- GANJI, F.; VASHEGHANI-FARAHANI, S.; VASHEGHANI-FARAHANI, E. Theoretical Description of Hydrogel Swelling: A Review. **Iranian Polymer Journal**, v. 19, n. 5, p. 375–398, 2010.
- GENERALI, M.; DIJKMAN, P. E.; HOERSTRUP, S. P. Bioresorbable Scaffolds for Cardiovascular Tissue Engineering. **EMJ Interventional Cardiology**, v. 1, n. July, p. 91–99, 2014.
- GUINESI, L. S.; CAVALHEIRO, É. T. G. The use of DSC curves to determine the acetylation degree of chitin/chitosan samples. **Thermochimica Acta**, v. 444, n. 2, p. 128–133, 2006.
- HADJIPANAYI, E.; MUDERA, V.; BROWN, R. A. Guiding cell migration in 3D: A collagen matrix with graded directional stiffness. **Cell Motility and the Cytoskeleton**, v. 66, n. 3, p. 121–128, 2009.
- HADJIZADEH, A.; DOILLON, C. J. Close dependence of fibroblast proliferation on collagen scaffold matrix stiffness. **Journal of tissue engineering and regenerative medicine**, v. 4, n. 7, p. 524–531, 2010.
- HU, K. et al. Compressed collagen gel as the scaffold for skin engineering. **Biomedical Microdevices**, v. 12, n. 4, p. 627–635, 2010.
- KAISER, N. J.; COULOMBE, K. L. K. Physiologically inspired cardiac scaffolds for tailored in vivo function and heart regeneration. **Biomedical materials** (Bristol, England), v. 10, n. 3, p. 034003, 2015.
- KIM, S. E. et al. Three-dimensional porous collagen/chitosan complex sponge for tissue engineering. **Fibers and Polymers**, v. 2, n. 2, p. 64–70, 2001.
- KOMATSU, D. et al. Characterization of Membrane of Poly (L,co-D,L-lactic acid-co-trimethylene carbonate) (PLDLA-co-TMC) (50/50) loaded with Silk Fibroin. **SDRP Journal of Biomedical Engineering**, v. 2, n. 1, p. 1–11, 2017.
- KUO, S. W. E. I.; HUANG, C. F.; CHANG, F. C. Study of Hydrogen-Bonding Strength in Poly (ϵ -caprolactone) Blends by DSC and FTIR. **Journal of Polymer Science:Part B**, n. p. 1348–1359, 2001.
- LAKRA, R. et al. Enhanced stabilization of collagen by furfural. **International Journal of Biological Macromolecules**, v. 65, p. 252–257, 2014.
- LAM, M. T.; WU, J. C. Biomaterial applications in cardiovascular tissue repair and regeneration. **Expert review of cardiovascular therapy**, v. 10, n. 8, p. 1039–49, 2012.
- LEÓN-MANCILLA, B. H. et al. Physico-chemical characterization of collagen scaffolds for tissue engineering. **Journal of Applied Research and Technology**, v. 14, n. 1, p. 77–85, 2016.

LI, Z. H. et al. Silk fibroin-based scaffolds for tissue engineering. **Frontiers of Materials Science** v. 7, n. 3, p. 237–247, 2013.

LV, Q. et al. Three-dimensional fibroin/collagen scaffolds derived from aqueous solution and the use for HepG2 culture. **Polymer**, v. 46, n. 26, p. 12662–12669, 2005.

MAXIMO, G. J.; CUNHA, R. L. MECHANICAL PROPERTIES OF COLLAGEN FIBER AND POWDER GELS. **Journal of Texture Studies**, v. 41, p. 842–862, 2010.

MI, S. et al. Plastic compression of a collagen gel forms a much improved scaffold for ocular surface tissue engineering over conventional collagen gels. **Journal of Biomedical Materials Research - Part A**, v. 95 A, n. 2, p. 447–453, 2010.

O'BRIEN, F. J. Biomaterials & scaffolds for tissue engineering. **Materials Today**, v. 14, n. 3, p. 88–95, 2011.

PEREA-GIL, I.; PRAT-VIDAL, C.; BAYES-GENIS, A. In vivo experience with natural scaffolds for myocardial infarction: the times they are a-changin'. **Stem Cell Research & Therapy**, v. 6, n. 1, p. 248, 2015.

PLACETTE, M. D.; FAN, X.; EDWARDS, D. A dual stage model of anomalous moisture diffusion and desorption in epoxy mold compounds. 2011 12th Intl. **Conf. on Thermal, Mechanical & Multi-Physics Simulation and Experiments in Microelectronics and Microsystems**, p. 1/8-8/8, 2011.

RADISIC, M.; CHRISTMAN, K. L. Materials science and tissue engineering: Repairing the heart. **Mayo Clinic Proceedings**, v. 88, n. 8, p. 884–898, 2013.

ROSSI, G.; MAZICH, K. A. Macroscopic description of the kinetics of swelling for a cross-linked elastomer or a gel. **Physical Review E**, v. 48, n. 2, p. 1182–1191, 1993.

SARGEANT, T. D. et al. An in situ forming collagen-PEG hydrogel for tissue regeneration. **Acta Biomaterialia**, v. 8, n. 1, p. 124–132, 2012.

SERPOOSHAN, V. et al. Characterization and modelling of a dense lamella formed during self-compression of fibrillar collagen gels: implications for biomimetic scaffolds. **Soft Matter**, v. 7, n. 6, p. 2918, 2011.

SERPOOSHAN, V. et al. The effect of bioengineered acellular collagen patch on cardiac remodeling and ventricular function post myocardial infarction. **Biomaterials**, v. 34, n. 36, p. 9048–9055, 2013a.

SERPOOSHAN, V. et al. Hydraulic permeability of multilayered collagen gel scaffolds under plastic compression-induced unidirectional fluid flow. **Acta Biomaterialia**, v. 9, n. 1, p. 4673–4680, 2013b.

SHANMUGASUNDARAM, N. et al. Collagen- chitosan polymeric scaffolds for the in vitro culture of human epidermoid carcinoma cells. **Biomaterials**, v. 22, p. 1943–1951, 2001.

SHE, Z. et al. Preparation and in vitro degradation of porous three-dimensional silk fibroin/chitosan scaffold. **Polymer Degradation and Stability**, v. 93, n. 7, p. 1316–1322, 2008.

SILVA, A. M. H. DA et al. 193 Two and three-dimensional morphometric analysis of trabecular bone using X-ray microtomography (μ CT). **Revista Brasileira de Engenharia Biomédica**, v. 30, n. 2, p. 93–101, 2014.

SIONKOWSKA, A. Molecular interactions in collagen and chitosan blends. **Biomaterials**, v. 25, n. 5, p. 795–801, 2004.

SIONKOWSKA, A.; PŁANECKA, A. Preparation and characterization of silk fibroin/chitosan composite sponges for tissue engineering. **Journal of Molecular Liquids**, v. 178, p. 5–14, 2013.

SUN, K. et al. Silk fibroin/collagen and silk fibroin/chitosan blended three-dimensional scaffolds for tissue engineering. **European Journal of Orthopaedic Surgery and Traumatology**, v. 25, n. 2, p. 243–249, 2014.

SUN, K. et al. Comparison of three-dimensional printing and vacuum freeze-dried techniques for fabricating composite scaffolds. **Biochemical and Biophysical Research Communications**, v. 477, n. 4, p. 1085–1091, 2016.

TAYLOR, D. A.; SAMPAIO, L. C.; GOBIN, A. Building new hearts: A review of trends in cardiac tissue engineering. **American Journal of Transplantation**, 2014.

VENKATESAN, J. et al. Development of Alginate-Chitosan-Collagen Based Hydrogels for Tissue Engineering. **Journal of Biomaterials and Tissue Engineering**, v. 5, n. SEPTEMBER, p. 458–464, 2015.

WANG, H. M. et al. Novel Biodegradable Porous Scaffold Applied to Skin Regeneration. **PLoS ONE**, v. 8, n. 6, p. 2–12, 2013.

XIA, Z.; VILLA, M. M.; WEI, M. A Biomimetic Collagen-Apatite Scaffold with a Multi-Level Lamellar Structure for Bone Tissue Engineering. **Journal of Materials Chemistry B. Materials for biology and medicine.**, v. 14, n. 2, p. 1998–2007, 2015.

CAPÍTULO III

1 **Artigo 2 – “Design and evaluating of biomimetically inspired dense lamellar scaffold obtained by plastic compression: Development, physiomechanical characterization, and in vitro cellular activities”**
(Submitted)

Manuscript Details

Manuscript number	MSEC_2019_1562
Title	Design and evaluating of biomimetically inspired dense lamellar scaffold for cardiac tissue regeneration; Development, physiomechanical characterization, and in vitro cellular activities.
Article type	Research Paper
Abstract	<p>The regenerative medicine is an emerging field that aim is healing damaged tissue. The choice of crosslinking agent is one of the most important require for the development of 3D scaffolds devices. This study aimed to investigate the effects of proanthocyanidins (PA) and glutaraldehyde (GA) associated with plastic compression method on the properties of the dense lamellar scaffold with a stiffness above of the range of the heart muscle. The physiomechanical and physical-chemical properties of the scaffolds were evaluated. The antioxidant activity was investigated by DPPH method; viability and proliferation cellular were evaluated by MTT and imaging cytometer (H9c2 cells). The effect of the crosslinking agents modified the physiomechanical properties, but did not modify the mucoadhesion properties. PA-scaffold has the ability to bind water's molecule and to reduce the space between polymeric chains. PA-scaffold and GA-scaffold showed, respectively, 44% and 17% of antioxidant activity. Both crosslinking agents did not influence the viability and proliferation of H9c2 cells. Considering the anisotropic structure, the physiomechanical properties, cellular compatibility, and protective action against reactive oxygen species, this study may provide a way to improve the inverse remodulation of heart tissue, after infarct acute of the myocardium.</p>
Keywords	regenerative medicine; cardiac scaffold; dense lamellar scaffold; proanthocyanidin; glutaraldehyde; plastic compression.
Corresponding Author	Marco Chaud
Corresponding Author's Institution	Sorocaba University
Order of Authors	Thais Alves, Juliana Souza, Venancio Amaral, Alessandra Rios, Tais Costa, Renata Lima, Lindemberg Silveira Filho, Denise Grotto, Kessi Crescencio, Fernando Batain, Norberto Aranha, Jose Oliveira Filho, Patricia Severino, Marco Chaud
Suggested reviewers	Peter Frey, Tengfei Pan, Mahendra Rai, Bruce Bunnell, Eliane Souto

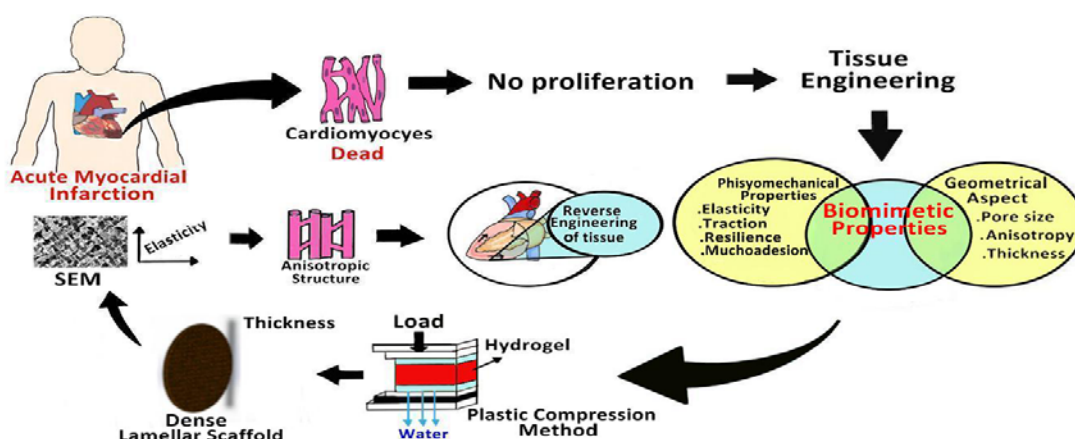
1.1 Abstract

The regenerative medicine is an emerging field that aim is healing damaged tissue. The choice of crosslinking agent is one of the most important require for the development of 3D scaffolds devices. This study aimed to investigate the effects of proanthocyanidins (PA) and glutaraldehyde (GA) associated with plastic compression method on the properties of the dense lamellar scaffold with a stiffness above of the range of the heart muscle. The physiomechanical and physical-chemical properties of the scaffolds were evaluated. The antioxidant activity was investigated by DPPH method; viability and proliferation cellular were evaluated by MTT and imaging cytometer (H9c2 cells). The effect of the crosslinking agents modified the

physiomechanical properties but did not modify the mucoadhesion properties. PA-scaffold has the ability to bind water's molecule and to reduce the space between polymeric chains. PA-scaffold and GA-scaffold showed, respectively, 44% and 17% of antioxidant activity. Both crosslinking agents did not influence the viability and proliferation of H9c2 cells. Considering the anisotropic structure, the physiomechanical properties, cellular compatibility, and protective action against reactive oxygen species, this study may provide a way to improve the inverse remodulation of heart tissue, after infarct acute of the myocardium.

Keywords: regenerative medicine; cardiac scaffold; dense lamellar scaffold; proanthocyanidin; glutaraldehyde; plastic compression.

Graphical Abstract



Highlights

- Tissue engineering has emerged as a promising alternative for cardiac regeneration.
- Dense lamellar scaffolds were obtained by plastic compression method.
- Crosslinking agent was important to modulate the physicochemical properties.
- Biomimetic properties as anisotropy and elasticity were obtained.
- The study may provide a way to improve the inverse remodulation of heart tissue.

1.2 Introduction

Cardiovascular disease is one of the most severe health problems in the world, and it yields a high level of the mortalities every year. Normally, heart failure is the final common stage of most types of cardiovascular disease, that preceded by myocardial infarction (MI), hypertension, arrhythmia, and a variety of cardiomyopathies. Heart muscle cells lose their capacity to divide early after birth. The loss of a relevant fraction of myocytes (e.g. during myocardial infarction) leads to a permanent reduction in contractile function and eventually heart failure (ESCHENHAGEN et al., 2012; LI; ZHANG, 2017).

Regenerative medicine is an emerging field that aims is improving or repairing the performance of damaged tissue or organ. Numerous strategies, including the use of materials and cells, as well as various combinations thereof, to take the place of missing tissue, effectively replacing it both structurally and functionally, or to contribute to tissue healing (MAO; MOONEY, 2015; MARTÍNEZ et al., 2015).

Scaffolds are tridimensional (3D) and porous structure that can be produced using biopolymers able to mimetic the extracellular matrix. The scaffolds should be able to mechanically support the native tissue during the necessary time of regeneration repair, and it also plays an important role in providing essential signals to cell activities. The choice of biomaterials and the selection of the experimental conditions for the design of these scaffolds are important parameters to assuring the appropriate setting for cell's growing and proliferation into the 3D matrices. (KARIKKINETH; ZIMMERMANN, 2013; NAVEED et al., 2018; O'BRIEN, 2011). Based on this concept, cardiac tissue engineering has been introduced as a promising technique to benefit patients with cardiovascular disease (LI; ZHANG, 2017).

The stiffness of heart muscle is 10 – 20 kPa at the beginning of diastole, and 200 – 500 kPa at the end of diastole. Although the materials should be designed to be proportional to the fractional volume of the scaffolds, the use of stiffer materials can contribute to attenuate the stress in the cardiac wall (CHEN et al., 2008).

Proteins and polysaccharides are considered promising natural molecules for the design of 3D scaffolds with biomimetic characteristics of original tissue. Collagen gels as scaffolds have been used in the tissue engineering because of their excellent biocompatibility, low antigenicity, and high biodegradability. The major problem with collagen gel for myocardial infarction is its low density; thus it occupies a large volume

(HU et al., 2010). Brown et al. (BROWN et al., 2005) developed a compressed collagen gel technique for tissue engineering through the rapid expulsion of fluid from hydrogels, by the application of plastic compression (PC) able to produce the dense lamellar scaffolds.

Mi et. al (2011) and Rich et.al (2013), produced collagen scaffolds using plastic compression technique associated with photochemical crosslinking that has been previously shown to significantly increase mechanical stability (tensile and compression strength), reduce the swelling rate and increase longevity, *in vivo*, without disintegration (MI et al., 2010; RICH et al., 2014).

The crosslinking technology is one of the most important areas of research focusing on the development of new tissue engineered that use the proteins and polysaccharides as polymer (ORYAN et al., 2018). A crosslinking agent can be physical or chemical origin, and both are able to connect the functional groups of the polymer chain to another one through covalent bonding or supramolecular interactions such as ionic bonding or hydrogen bonding. This crosslink can affect some physicochemical properties including mechanical properties such as tensile strength, stiffness, and strain, cell-matrix interactions, performance at higher temperatures, resistance to enzymatic and chemical desintegration, gas permeation reduction, and shape memory retention of the products (ORYAN et al., 2018; YANG; RITCHIE; EVERITT, 2017).

An ideal crosslinking agent should be no cytotoxicity for myocardium and has a low cost. It could improve the mechanical performance of the materials and inhibit calcification. There are many crosslinking agents for scaffolds, which may be classified as chemical crosslinking agents (carbodiimide, epoxy compounds and glutaraldehyde) and natural crosslinking agents (genipin, nordihydroguaiaretic acid, tannic acid, and procyanidins). The natural substances as crosslinking agents show superiority in many aspects than the chemical crosslinking agents, especially in terms of cytotoxicity and anti-calcification ability (HAN et al., 2003; SHAVANDI et al., 2018). The plastic compression associated with a chemical crosslinking agent has not related by literature.

Proanthocyanidins (PA) are parts of a specific group of polyphenolic compounds and belong to the category known as condensed tannins. PA is a natural product with a polyphenolic structure that has the potential to gives rise to a stable hydrogen bonded

structures and generate non-biodegradable collagen matrices. Mechanisms for interaction between PA and proteins include covalent interactions, ionic interactions, hydrogen bonding interactions or hydrophobic interactions. The relatively large stability of these crosslinks compared with other polyphenols (such as tannins) suggest a structure specificity, which although encouraging hydrogen binding also create hydrophobic pockets. Proline is an amino acid with carbonyl oxygen adjacent to secondary amine nitrogen and is a very good hydrogen bond acceptor. Proline-rich proteins like collagen form especially strong hydrogen bonds and are an extremely high affinity for PA (ALONSO et al., 2018; HAN et al., 2003).

In addition, the PA possesses antibacterial, antiviral, anti-inflammatory, antiallergic and vasodilatory actions. Furthermore, has the capacity to inhibit lipid peroxidation, platelet aggregation, capillary permeability, and fragility. PA have been shown to modulate the activity of regulatory enzymes including cyclooxygenase, lipoxygenase, protein kinase C, angiotensin-converting enzyme, hyaluronidase and cytochrome P450 activities (BAGCHI et al., 2003; BAGCHI; BAGCHI; STOHS, 2002).

Glutaraldehyde (GA) has been extensively used as a chemical crosslinking agent to crosslink various types of biopolymeric for tissue scaffolds, hydrogels, and composites (HO; LIN; SHEU, 2001; LEE; SABATINI, 2017; LIKITAMPORN; MAGARAPHAN, 2014; LIU; MA; GAO, 2012; YAP; YANG, 2016). Glutaraldehyde reacts with the amine or hydroxyl functional groups of proteins and polymers, respectively through a Schiff-base reaction and connects the biopolymeric chains via intra- or intermolecular interactions. Therefore, all the available free amine groups which are present in the chemical structure of protein molecules such as gelatin, react with GA, forming a more strongly cross-linked network (OLDE DAMINK et al., 1995; ORYAN et al., 2018).

Although PA cross-linked collagen scaffold has been studied in a previous study (CHOI; KIM, 2016; ORYAN et al., 2018; WEI et al., 2018; YANG; RITCHIE; EVERITT, 2017), to date there are no other studies have been conducted using plastic compression in association to improve the mechanical properties as well as cellular behaviors on GA as a crosslinking agent for collagen 3D porous scaffolds.

This study aimed to investigate the effects of PA and GA associated with plastic compression on the properties of the dense lamellar scaffold with a differential of stiffness above a range of heart muscle. Moreover, the dense lamellar scaffolds should

have proper characteristics about biomechanical properties, swelling, anisotropic degree, disintegration, antioxidant activity, and cytotoxicity. The polymers used to modulate the properties of dense lamellar scaffolds were collagen, fibroin, chitosan, hyaluronic acid, Poloxamer 407 and polyethylene glycol 400.

1.3 Materials and methods

1.3.1 Materials

Collagen powder type I was supplied by NovaProm Food Ingredients Ltda. (Brazil). Deacetylate (75-85%) chitosan of average molar mass, glutaraldehyde, poloxamer 407 and DMEM were purchases of the Sigma-Aldrich Co, (USA). Proanthocyanidin was purchase of the GAMA Ltda, (Brazil). Hyaluronic acid was purchase of the Via Farma Ltda, (Brazil). Polyethyleneglycol 400 was purchase of the Dinâmica Ltda, (Brazil). The other reagents were of pharmaceutical grade. All samples were used without any chemical treatment.

1.3.2 Extraction of Fibroin

Bombyx mori silk fibroin was prepared adapted from Komatsu et al. (2017) (KOMATSU et al., 2017). The sericin extracted obtained by autoclaving (120°C / 15 min.) of silk cocoons in an aqueous solution of Na₂CO₃ 0.5 wt %. The silk fibroin was soaked methodically with water to extract the residual sericin. The degummed silk fibroin was dissolved in CaCl₂.2H₂O/CH₃CH₂OH/H₂O solution (mole ratio, 1:2:6) at 85°C. The solution was filtered, transferred to a dialyzer tubing with a molecular weight cut-off 14,000, and dialyzed against distilled water for 72 h to yield fibroin solution (FS). The fibroin concentration determined by weighing the remaining solid after drying was 2,7 wt %.

1.3.3 Preparation of hydrogel cross-linked with Proanthocyanidin or Glutaraldehyde

Formulations of the hydrogels for the manufacture of scaffolds cross-linked with PA or GA are shown in Table 1. The collagen dispersion was prepared with 2 mL of DMEM, 1 g of collagen type I (COL) and enough ultrapure water to obtain 10 mL of dispersion. In preparation of hydrogel formulation, the solution of fibroin (SF),

Polyethylene glycol 400 (PEG), Poloxamer 407 (P407), hydrogel chitosan (CH) previously prepared with CH of average molecular weight (Alves et al., 2018), and crosslinking agent (PA or GA) were added to the collagen dispersion following this order. The mixture of the compound was done by mechanical stirring until obtaining a uniform hydrogel. Thereafter, the pH of the formulation was adjusted to 10 using 2M NaOH and added hyaluronic acid (HA) to the polymer dispersion.

To complete the polymerization reaction, the colloidal dispersions were left at 10 ° C for 24 h into a cylindrical mold with capacity for 4.0 cm³, to become a thick solid-looking gel.

Table 1. Formulation of PA-scaffold and GA-scaffold

	PA-scaffold	GA-scaffold
Collagen	1.0 g	1.0 g
Chitosan hydrogel (3%)	1.0 g	1.0 g
Poloxamer 407	0.06 g	0.06 g
Proanthocyanidin	0.08 g	-
Glutaraldehyde (25% H ₂ O)	-	0.08 g
Hyaluronic Acid (1 %)	0.06 g	0.06 g
Fibroin Solution	4.0 mL	4.0 mL
Polyethylene glycol 400 (3%)	2.0 mL	2.0 mL
DMEM	4.0 mL	4.0 mL
H ₂ O ultrapure	8.0 mL	8.0 mL

1.3.4 Preparation of dense lamellar scaffolds

Dense lamellar scaffolds were produced by plastic compression (using a hydrostatic press), adapted from Brown et al (2005) (BROWN et al., 2005). Briefly, cast highly hydrated hydrogels were transferred to a porous support comprising (bottom to top) absorbent paper blot layers, a steel mesh, and two nylon meshes. Subsequently, a static compressive stress of 4 KN was applied to the hydrated scaffolds for 10 min in order to remove water and produce a dense biomaterial with improved biological and mechanical properties. Finally, the matrices were freeze-dried, resulting in cross-linked scaffolds.

1.3.5 Physiomechanical and Mucoadhesive Properties

Texture profile analysis (TPA) was used to measure the physiomechanical properties (elasticity, flexibility, drilling, and resistance to traction) of scaffolds. The tests were performed using a Stable Micro Systems Texture Analyzer (Model TA-XT Plus) in texture profile analysis mode with a load cell of 5 Kg. This process was previously described by Alves et al. Briefly, the samples scaffolds, with approximately 40 mm of diameter, were hydrated for 1h. The excess of the water of scaffolds was removed and fixed in suitable apparatus to each analyze. The speeds of the tests were previously defined for a rate of 2 mm.s⁻¹ and 0.5 mm. s⁻¹, respectively, for drilling and resistance to traction, and elasticity and flexibility. Elastic (Young's) modulus was obtained by compressed until densification of the sample. The Elastic modulus was calculated with a strain ranged between 0 and 5% (ALVES et al., 2018).

The mucoadhesive properties of scaffolds were evaluated using a Stable Micro Systems Texture Analyzer (Model TA-XT Plus) using mucin discs. The mucin discs were prepared for compression (Lemaq, Mini Express LM-D8, Brazil) with flat punches, and cylindrical matrix with diameter of 8mm, and a compaction load of 8 tons. This process was previously described by Alves et al. Briefly, the mucin discs with a thickness of 0.2 mm were previously hydrated and attached to the lower end of the analytical probe.

The scaffold samples with 40 mm of diameter were fixed in a suitable apparatus. Mucin disc attached in the probe was compressed on the surface of the scaffold with a force of 0.098 N, directed in the apical → basal way. Contact time between mucin disc and the sample was of 100 s, (this time was previously established in a pre-qualification study and been considered great to perform an intimate contact of the mucin disc with the sample.). The test was performed with a constant speed of 10 mm.s⁻¹. The force required to detach the mucin disc from the surface of the scaffold was determined from the time (s) x force (N) ratio (ALVES et al., 2018).

1.3.6 Swelling efficiency

The scaffolds were cut in the square shape (15 × 15 mm), weighed and then immersed in 3 mL PBS (Phosphate Buffer Saline, pH 7.4) at 37 °C for up to 14 days. As described by Alves et al., at different time points, the samples were removed, and different measurements to evaluate the capacity to retain PBS fluid were made. The

first measurement was aimed at assessing the ability of the scaffold structure as a whole (i.e, the material itself together with the pore system) to absorb the PBS. For this, at each time point, the samples were removed from fluid, shaken gently and then weighed without dripping (Wws). The second measurement was carried out after pressing and “drying” the same soaked samples between sheets of filter paper to remove the water retained in its porous structure (Wwm). In this way the swelling ability of scaffold material itself was determined. The scaffolds were then dried at 37 °C until constant weight was reached (Wd). The percentage of fluid uptake, in both cases, was calculated as shown (Equation 1):

$$\text{Fluid uptake of scaffolds (\%)} = \left(\frac{W_w - W_d}{W_d} \right) \times 100 \quad (1)$$

Where W_w represents W_{ws} or W_{wm} and W_d is dry scaffold. Each sample was measured in triplicate.

1.3.7 *In vitro* disintegration study

PA-scaffold and GA-scaffold were hydrated in PBS at 37°C to evaluate their degree of degradation. Scaffolds were cut to square shape (15 x 15 mm), weighed prior to the degradation study (W_d'), and then immersed in 3 ml PBS at 37°C for up to 14 days. At different time points, they were removed, washed in a large volume of deionized water to remove buffer salts, and dried at 37 °C until constant mass was reached. Finally, the samples were weighed (W_a) and the percentage weight loss was calculated as follows (Equation 2):

$$\text{Weight loss (\%)} = 100 \times \left(\frac{W_d' - W_a}{W_d'} \right) \quad (2)$$

The pH value of the PBS was measured at each time point using a pH-meter (Tecnal, TE-5, Piracicaba, Brazil). Each sample was measured in triplicate.

1.3.8 Porosity, interconnectivity and pore size

The morphometric characteristic of the porosity, interconnectivity and pore size of scaffolds were evaluated by computerized microtomography (μ CT). The scaffold pictures were captured by X-Ray microtomography (Brucker-micro CT - SkyScan 1174, Belgium) with -resolution scanner of the 28mM pixel and integration time at 1.7 s. The source of the X-rays was 35 keV and 800 μ A of current. The projections were acquired in a range of 180° with an angular step of 1° of rotation. Three-dimensional

virtual models' representative of various regions of scaffolds were created, and CT Analyzer (v. 1.13.5) mathematically treated the data (REBELO et al, 2016).

1.3.9 Permeability Measurement

Specific permeability was measured in the current work using a constant pressure gradient (GILMORE et al., 2018). across of the scaffold, which was defined by the hydrostatic water ($\Delta P = r.H.g$), where one face of scaffold was exposed to the atmosphere. The pressure was held constant across the scaffold (thickness scaffold = L) and the volumetric flow rate (Q) of distilled water across the scaffold was measured (from the mass of water passing through the scaffold in a given time). This mass was measured, using a balance with a precision of 1 mg, and converted to volumetric flow using the fluid density ($\rho = 0.998 \text{ Mg m}^{-3}$). From Q , the sectional area (A) and the pressure gradient, $\Delta P/L$, the specific permeability, k , was calculated using Darcy's Law (Equation 3):

$$k = \frac{Q \cdot L \cdot \mu}{A \cdot h} \quad (3)$$

in which h , the dynamic viscosity, has units of Pa s and k has units of m^2 . The viscosity of the water was taken as $8.9 \times 10^{-4} \text{ Pa.s}$. A total of 3 samples (1.5 cm diameter) were used. The water column (H) was 56 cm. Furthermore, a press fit mount was used to prevent scaffold deformation. The mount aperture was slightly larger than the scaffold diameter in the dry state. When hydrated, the scaffold expanded to fill the entire aperture.

1.3.10 Scanning electron microscopy (SEM)

SEM photographs scaffolds were obtained using a scanning electron microscope (LEO Electron Microscopy/Oxford, Leo 440i, England) with a 10 kV accelerating voltage. Scaffold samples was previously frozen with liquid nitrogen, cut out (dimension 30 x 30 mm) and mounted on pins stubs specimen using carbon double-sided adhesive tape. The samples were sputtered coated with gold for 4 min at 15 mA, using SC7640 Sputter-Coater.

1.3.11 Differential scanning calorimetry (DSC)

DSC was performed on a Shimadzu, TA-60, Kyoto, Japan, calibrated using indium as the reference material. A sample of 2 mg was packed in a hermetically crimped aluminum pan, and heated under dry nitrogen purged at 50 mL.min⁻¹. The samples were heated from 25 to 350 °C at a rate of 10 °C min⁻¹.

1.3.12 Fourier transform infrared spectroscopy (FTIR)

FTIR analysis (Shimadzu, IRAffinity-1, Japan) was used to collect FTIR spectra by Labsolutions Software v.2.10. The stretches of the chemical bonds of the main functional groups of each molecule making up the sample were determined by an attenuated total reflectance (ATR) over the range between 4000 and 600 cm⁻¹ at 4 cm⁻¹ resolutions, averaging 128 scans. The scaffold samples were carefully manipulated and put on the ATR-8200HA support before of each analyze.

1.3.13 *In vitro* antioxidant activity

The antioxidant activity, *in vitro*, of the PA-scaffolds and GA-scaffolds were determined using an ethanolic solution of 2,2-diphenyl-1-picrylhydrazyl (DPPH) 0.1 mM, as a free radical, and DPPH as radical sequestering. The absorbance was determined at a wavelength of 515 nm in a spectrophotometer (Lambda 35, PerkinElmer, USA) at 0, 15, 30 45 and 60 min. The tubes containing the samples were kept under the light. The ability of the radical sequestering sample (DPPH), expressed as *per cent* inhibition was calculated according to Equation 4 and plotted.

$$Inibição (\%) = \frac{Abs1 - Abs2}{Abs1} \times 100 \quad (4)$$

1.3.14 Cell viability

Initially, the extract of scaffold was made using a 1cm² scaffold fragment in 2.5ml culture medium for 24 hours. After this time, the total cell adhesion treatments were performed using the extracts at 100, 50 and 25% dilutions, and were maintained for 24h. Approximately 5x10⁵ cells/well (H9c2 cells - cardiac myoblasts) were plated in 96-well plates.

The culture medium was removed and 100µl of MTT solution (3- (4,5-dimethylthiazolyl-2) -2,5-diphenyltetrazolium bromide) at 5mg.ml⁻¹ was added to each

well and maintained in 37°C for 3 hours. After this, the MTT solution was withdrawn and 100µl of DMSO per well was added for cell attachment. The reading was performed using ELISA microplate reader at 570nm. The concentration of material in this method is equivalent to exposing 1.6 m of material to a 70 kg individual.

1.3.15 Image cytometer

Approximately, 1×10^5 cells / well (H9c2 cells - cardiac myoblasts) were plated in a 24 well plate, at time 0h, and was incubated at 37 ° C - 5% CO₂ using Minimum Essential Alpha medium with ribonucleosides, deoxyribonucleosides, L-glutamine (2mM) and sodium pyruvate (1mM) to a final concentration of 10%, without ascorbic acid added of the fetal bovine serum. After 24 hours and total adhesion of the cells, they were placed in contact with the material for 48 and 72 hours.

The samples were removed from the cultures and the cells were washed with PBS, trypsinized and counted using the Image Cytometry technique.

1.4 Results and Discussion

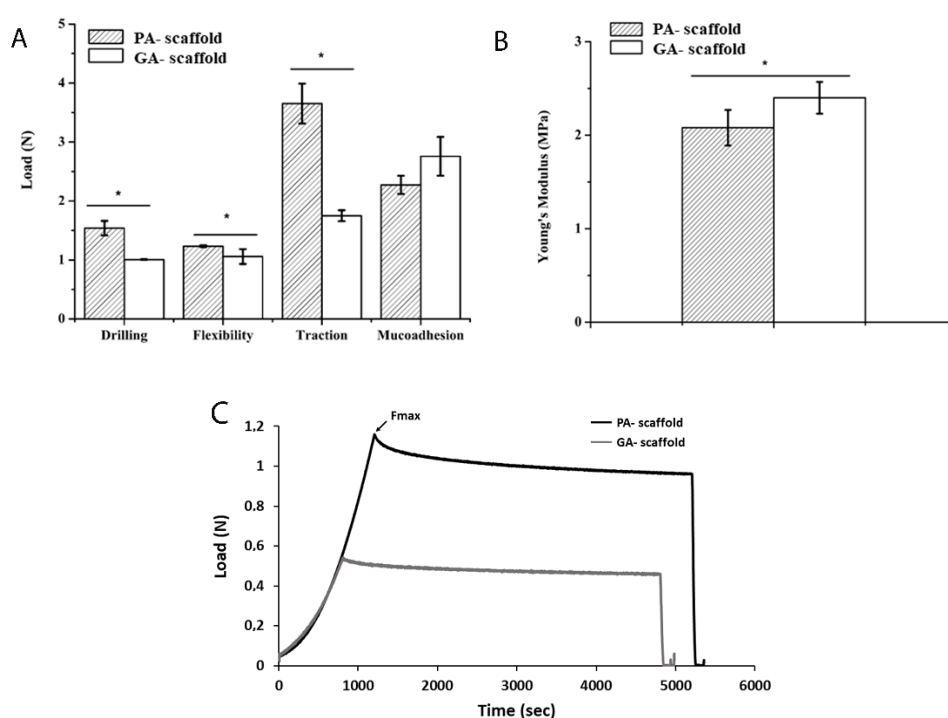
When suitable autologous tissue is injured or lacking, mostly the use of non-biodegradable synthetic material to maintain the 3D structure and to increase the time of biodegradation in scaffolds to restore, and repair the tissue is associated with several disadvantages, such as the significant risk of thromboembolism, fibrosis and calcification. In the order hand, the use of biodegradable material to assure structural and biomechanical features that mimetic of the cardiac extracellular matrix has the inconvenient of the fast disintegration, generally, lesser than eight weeks. Techniques to modulate the biomechanical and features properties of 3D porous scaffold based on biocompatible polymers, natural or synthetic, crosslinking agent or by compressing hydrogels. In this manuscript, we associated the biocompatible and biodegradable, natural and synthetic polymers, crosslinking agent, and plastic compression to obtain the dense lamellar scaffolds in such a way that new mechanical and biomechanical properties arise.

1.4.1 Biomechanical and Mucoadhesive Properties

The requirements of such a scaffold are: i) highly porous and 3D structures to allow cell and nutrient infiltration, ii) proper biomechanical properties, iii) the ability

to desintegrate to non-toxic products and iv) biocompatibility, allowing cells to attach and proliferate. The scaffolds were obtained with glutaraldehyde and proanthocyanidins as a crosslinking agent. Figure 1 (A-C) show the results of biomechanical properties of the scaffold obtained by plastic compression, 1 hour after hydration.

Figure 1. Biomechanical properties of PA-scaffold and GA-scaffold. Drilling, flexibility, traction, and mucoadhesion (1A). Young's Modulus test (1B). Relaxation stress test (1C). * Means that statistical differences were found between PA-scaffold and GA-scaffold ($p < 0.05$) ($n = 3$; bar charts represent standard deviation values).



The PA-scaffold showed better results ($p < 0.05$) for drilling, flexibility, and traction properties than GA-scaffold (Fig. 1-A). The mucoadhesion property was similar ($p > 0.05$) for both scaffolds (Fig. 1-A). The PA-scaffold exhibited a rigid structure due to a highly cross-linked polymer. The Young's modulus (Fig. 1-B) was 2.04 ± 0.12 MPa, traction strength of the 3.65 ± 0.33 N and drilling strength 1.54 ± 0.12 N (Fig. 1-A).

It is known that Young's modulus depends upon the relative density and porosity of the scaffold, and of a constant related to the pore geometry. The linear elastic (Young's) modulus calculated from stress-strain analysis gives precisely the measure of the resistance of the struts to bending and buckling under compression. Compressive properties are of greater interest when studying the impact of scaffold

mechanics on cellular activity, because cells, through their action, tend to bend and buckle individual struts within the scaffold (DAVIDENKO et al., 2015). The analyse of results depicted in the Figure I show that dense lamellar PA-scaffold could potentially be applied as heart patch materials in terms of stiffness.

The authors like as Chen et. al (2008), Ravichandran et. al (2013), and Kai et. al (2011) (CHEN et al., 2008; KAI et al., 2011; RAVICHANDRAN, 2013), obtained scaffolds to cardiac regeneration by electrospinning using poly(glycerol sebacate), poly(ϵ -caprolactone) associated with gelatin, and by mold using collagen with poly(glycerol sebacate), respectively. The Young's modulus results found by them were 1.2, 1.45, and 2.06 MPa, respectively. The Ravichandran et. al, describe that the scaffolds obtained by your group provide guidance for cardiac cells growth and mesenchymal stem cells differentiation into cardiac lineage with the potential to obtain structurally and functionally competent cardiac tissue constructs.

Engineered heart devices must develop systolic (contractive) force with suitable compliance, at the same time they must withstand diastolic (expansive) loads. Ideally, the compliance (defined as $1/E$, where E is stiffness) of the scaffold material should be that of the collagen matrix of the heart muscle. Most of these biomaterials, including collagen fibers, are much stiffer than myocardium. This explains why the current solid engineered, as scaffolds, do not a contractile function (CHEN et al., 2008). Thus, the plastic compression technique associated with a crosslinking agent can be considered the efficient to modulate the stiffness and proper biomechanical properties of the scaffold produced.

The mucoadhesion is the ability of a material to adhere to a biological substrate, mucosal tissue. The interaction between mucus and mucin is a result of physical entanglement and secondary bonding, mainly H bonding and van der Waals attraction, which according the many authors, are mainly related to the following polymer properties: capability to create strong H bonding, high molecular weight, sufficient chain flexibility, and surface load properties favoring spreading onto mucus (MACKIE et al., 2017). Therefore, non-covalently binding mucoadhesive polymers are commonly classified according to their molecular charge into anionic, cationic, nonionic and amphiphilic polymers.

Anionic polymers, carrying $-\text{COOH}$ groups, can form hydrogen bonds with the hydroxyl groups of the glycoprotein's oligosaccharide side chain. This group includes

polymers such as hyaluronic acid. Cationic polymers carry a positively charged amine group and can, therefore, adhere to mucous due to ionic attraction to the sialic acid groups on the oligosaccharide side chain as chitosan. The interaction of nonionic polymers is based on the interpenetration of the polymer chains followed by chain entanglement as P407 (DAVIDOVIK-PINHAS; BIANCO-PELED, 2010). Thus, the mechanism of scaffold's mucoadhesion can be explained due the hyaluronic acid, chitosan and P407 into both formulations. In this case, the PA and GA presence did not show the difference between the mucoadhesion studies ($p > 0.05$).

The stress relaxation demonstrates the transient mechanical behavior of gels through the relative ability of the gel network to withstand the targeted strain. The gel structure could be revealed through the amount of energy that the network absorbed or dissipated. For stress relaxation tests, the fracture does not occur and the energy intake during compression is not completely stored in the material but is partly dissipated. The gel strength and deformability depend on the number and the type of bonds within the gel network (ORTOLANI et al., 2015; TAN et al., 2014). The value of maximum force (F_{max}) represents the initial firmness of the gel at 10% of compression strain.

The results of relaxation stress are shown in Figure I-C. PA-scaffold showed the highest level of F_{max} . The high level of firmness in PA-scaffold might owe to the strong and stable network strand. While GA-scaffold exhibited the lower level of F_{max} and this could be attributed to the PA addition that became more flexible the network strands that were able to distribute force during compression.

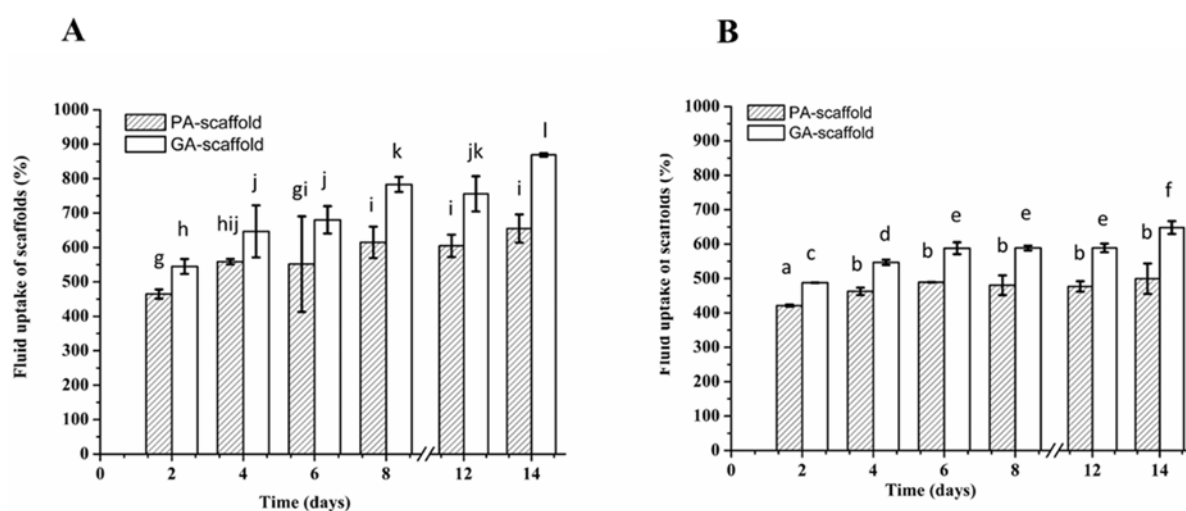
1.4.2 Swelling efficiency

The results of scaffold PBS-absorption ability are presented in Figure 2, where swelling characteristics related to fluid retained both by the whole scaffold structure (W_{wd}) in Figure 2A. Figure 2B displayed the scaffold without PBS excess (W_{we}). Both scaffolds (PA and GA) showed a high capacity for PBS uptake. However, differences in absorption were observed between the scaffolds with the PA or GA crosslinking agent. In both studies, the GA-scaffold showed, on average, a fluid retention 1.24 times bigger than PA-scaffold during fourteen days. For PA-scaffold the uptake saturation was achieved in four days. The comparasion between the results showed in Figures 2A and 2B suggest that PBS solution is more retained by matrix polymeric than by the

porous. This result can be explained by small difference of PBS removed of the porous (Fig. 2B). This suggests that PA treatment not only reduces the number of hydrophilic groups on the biopolymers of the formulation, which have the ability to bind water and to reduce the space between the chains (TRIFKOVIĆ et al., 2015; YANG; RITCHIE; EVERITT, 2017). As a result, the capability of water absorption decreases gradually as the concentration of cross-linker increases.

Crosslinking is considered to be a primary factor decreasing the water absorption and retention of scaffolds, and the results of this study are in accordance with similar results where gelatin and chitosan associated with glutaraldehyde, glyoxal or proanthocyanidin (BIGI et al., 2001; GUPTA; JABRAIL, 2006; YANG; RITCHIE; EVERITT, 2017). Our group found the PBS absorption of GA-scaffolds was bigger than PA-scaffolds.

Figure 2. Fluid uptake of scaffolds (%) fluid retained both by the whole scaffold structure (A), and by the scaffold material itself (B) in PBS at 37 °C according to crosslinking agent. Different letters mean that statistical differences were found between PA-scaffold and GA-scaffold ($p < 0.05$) ($n = 3$; bar charts represent standard deviation values).



1.4.3 *In vitro* disintegration study

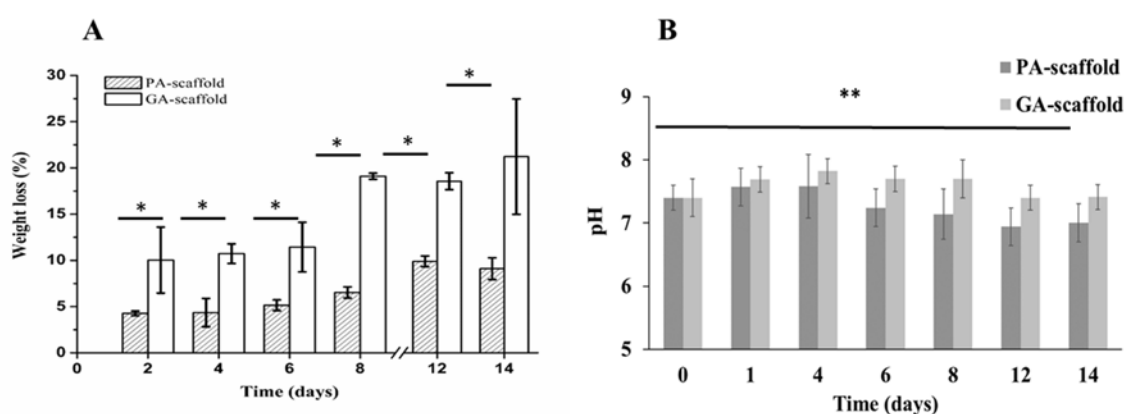
The resistance of scaffolds to disintegrate in the PBS presence, at 37 °C for 14 days was strongly dependent on the crosslinking agent, as shown in Figure 3A. For GA-scaffold (Figure 3) the percentage of mass loss was significantly higher (~2x) than

the PA-scaffolds. At the end of 14 days the mass loss was approximately 20 and 9 % for GA-scaffold and PA-scaffold, respectively.

The hydrolytic disintegration GA-scaffold and PA-scaffold did not cause a significant change in pH value, this being maintained in a range of 6.5 and 7.8 throughout fourteen days of experiments. The pH values during disintegration studies are critical because variations can induce the alteration or dead cellular.

The PA as crosslinking agent enhanced scaffold resistance to disintegration. Martínez et. al (2015) (MARTÍNEZ et al., 2015), produced collagen/chitosan scaffolds by freeze-drying and used carbodiimide and sodium tripolyphosphate as crosslinking agent. At the end of 14 days, the scaffolds showed weight loss in the range of 40- 50% in PBS medium. Thus, the PA as a natural polyphenolic component has the ability to crosslink proteins (collagen, rich in proline) through hydrogen bonding slowing down the biodisintegration of scaffolds.

Figure 3. (A) Weight loss (%) and (B) pH of scaffolds in PBS at 37 °C according to crosslinking agent. * Means that statistical differences were found between PA-scaffold and GA-scaffold ($p < 0.05$) ($n = 3$; bar charts represent standard deviation values).



1.4.4 Porosity, interconnectivity and pore size

Scaffolds must possess a highly porous structure, with open porous, and fully interconnected for providing a large surface area that will allow cell ingrowth, uniform cell distribution, and facilitate the neovascularization of the construct (DHANDAYUTHAPANI et al., 2011).

The morphological characteristics of PA-scaffold and GA-scaffold were obtained by μ CT, and are shown in Table 2. The pores interconnectivity of the PA-

scaffold and GA-scaffold were 75.23 % and 74.74 %, respectively. Cell behavior is directly affected by the scaffold architecture (e.g., porosity, pore size, interconnectivity, and diameter of fibers) since the extracellular matrix (ECM) provides cues that influence the specific integrin–ligand interactions between cells and the surrounding. The role of porosity and interconnectivity in scaffolds is to favor cell migration within the porous structure such that cell growth is enabled while overcrowding is avoided. Besides affecting the cell proliferation capability, the pore size of scaffolds can also influence the amount of ECM, that is the amount of glycosaminoglycan (GAG) secretion and the expression of collagen gene markers (LOH; CHOONG, 2013).

Most types of cells are able to sense orientation, texture and physical properties of scaffolds. In a material perspective of the scaffold, the topographic anisotropy of the constructs represents an important factor in cells motility, alignment and functions (DHANDAYUTHAPANI et al., 2011). The anisotropy is associated with lamellar characteristic on scaffolds. Thus, the scaffolds obtained by plastic compression technique (PA-scaffold and GA-scaffold) produced structures anisotropic, that is, dense lamellar scaffolds. The use of μ CT allows to obtain the degrees of anisotropy of the scaffolds (Table 2), that can range from 0 (the structure is completely isotropic) to 1 (structure is completely anisotropic) (DE MULDER; BUMA; HANNINK, 2009; SILVA et al., 2014). The values obtained to degrees of anisotropy of the PA-scaffold and GA-scaffold were 0.99 and 0.81, respectively. Thus, the scaffolds obtained by plastic compression technique produced structures anisotropic, that is, dense lamellar scaffolds.

Table 2. Morphological characteristics of scaffolds

	PA-scaffold	GA-scaffold
Total VOI volume (mm⁻³)	4,65	4,97
Pore interconnectivity (%)	75.23	74.74
Volume of open pores (%)	75.26	47.28
Closed porosity (%)	0.14	0.18
Degree of anisotropy	0.99	0.81

1.4.5 Permeability Measurement

The permeability coefficient can be used as quantitative tool to predict the barrier performance of porous media, and to estimate parameters as anisotropy or

isotropy of the porous. Likewise, it was possible to use the permeability of the dense lamellar scaffolds to evaluate the thickness required, and the plastic compression performance may be estimated from Equation 3. The permeability coefficient of PA-scaffold was 7.10^{-9} m^2 , and GA-scaffold was 2.10^{-10} m^2 . These results are coherent with degree of anisotropy showed in the Table 2.

The permeability of scaffolds is the combination of important parameters: (i) porosity, (ii) porous size and distribution, (iii) porous interconnectivity, and (iv) porous orientation (anisotropy). The permeability (k , units of m^2) of a scaffold is a property defining fluid flow through a porous material. Thus, as previously noted, the permeability of biological tissues and tissue-engineered scaffolds plays a significant role in the nutrient and waste transport. There are two mechanisms available for transport of metabolites to and waste products from cells in a scaffold: diffusion, and transport through capillary networks, formed throughout the scaffold via angiogenesis (VARLEY et al., 2016).

1.4.6 Scanning electron microscopy (SEM)

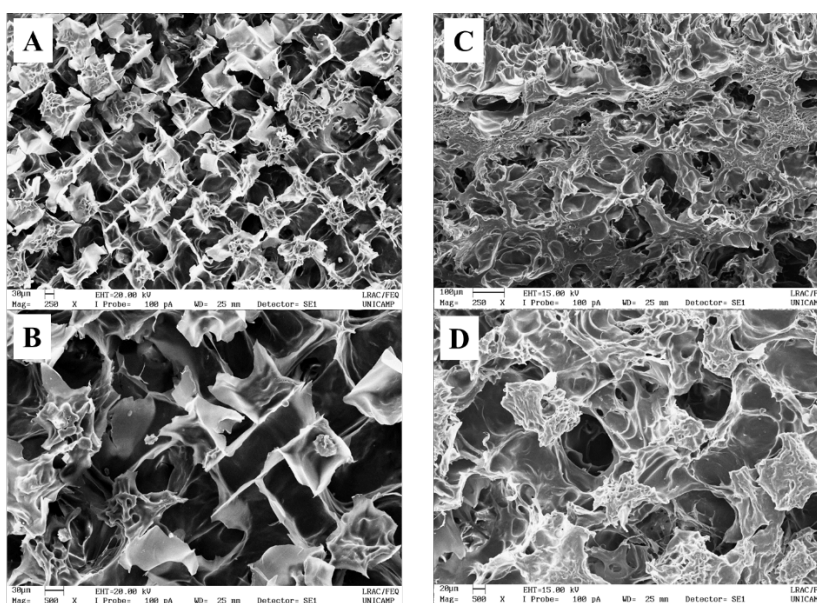
Surface properties include both chemical and topographical characteristics can control and affect cellular adhesion, proliferation, and is the primary site of interaction with surrounding cells and tissue. Furthermore, the pore size is also a very important issue because if the pores employed are too small, pore occlusion by the cells will happen, which will prevent cellular penetration, extracellular matrix production, and neovascularization of the inner areas of the scaffold (DHANDAYUTHAPANI et al., 2011).

Figure 4 compares the inner morphology of the PA-scaffold (A-B) and GA-scaffold (C-D). A continuous structure of interconnected pores with mainly uniform distribution was obtained in the PA-scaffold, and the same did not observe for GA-scaffold. The PA-scaffold showed the uniform rectangular shape in its surface (Figure 4 A-B), while the GA-scaffold showed irregular rounded shapes (Figure 4 C-D). The pore dimensions estimated from SEM microphotographs were mostly in the range of 100-150 μm for both scaffolds. The use of PA in formulation associated a plastic compression technique generated the sheets formation in structure surface of the scaffold (Figure 4 A- B) due to the presence of silk fibroin. Yang Yang et.al (2017)

(YANG; RITCHIE; EVERITT, 2017) related the opposite result, that structures of the PA and GA not significantly influenced the formation of internal porous.

The scaffold produced by our group using the PA as crosslinking agent showed appropriate morphology and size porous, this can favor the cellular adhesion and proliferation.

Figure 4. SEM of PA- scaffold (A-B) and GA-scaffold (C-D). Magnification of A-C images is 250x, and B-D images is 500x.

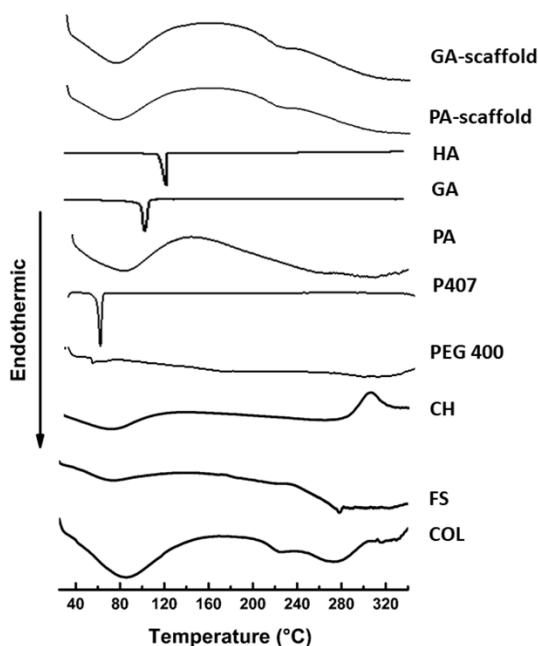


1.4.7 Differential scanning calorimetry (DSC)

The DSC thermogram of excipients, PA-scaffold, and GA-scaffold are shown in Figure 5 DSC is used to measure the denaturation temperature (T_d) which is a measure of crosslinking density. It gives a better understanding of the unfolding of protein under the influence of temperature. The DSC plots give an endothermic peak associated with helix to coil transition which indicates the extent of intermolecular crosslinking (LAKRA et al., 2014). The T_d of PA-scaffold and GA-scaffold were near 90 °C.

In general, the miscibility of the polymers blend depends on the self-association and inter-association of hydrogen-bonding donor polymers. This miscibility can be analyzed with DSC to determine when has a single glass-transition temperature (T_g 's) (KUO; HUANG; CHANG, 2001). The T_g 's at 220°C to PA-scaffold and GA-scaffold can be also observed for COL in the natural form, indicating that blend of polymers forms a miscible blend.

Figure 5. DSC thermogram of excipients, PA-scaffold, and GA-scaffold.



1.4.8 Fourier transform infrared spectroscopy (FTIR)

Representative FTIR spectra for excipients of formulation and scaffolds are presented in Figures 6. The spectra of COL depict characteristic absorption bands in 1645 cm^{-1} corresponding to amide I absorption arises predominantly from protein amide C=O stretching vibrations and 1545 cm^{-1} corresponding to amide II is made up of amide N-H bending vibrations and C-N stretching vibrations. The 1240 cm^{-1} corresponding to amide III band is complex, consisting of components from C-N stretching and N-H in-plane bending from amide linkages. The band at 1098 cm^{-1} corresponded to the stretching vibration of the C-O bond (HENDRADI; HARIYADI; ADRIANTO, 2018; NEMATOLLAHI et al., 2017; VIDAL et al., 2016).

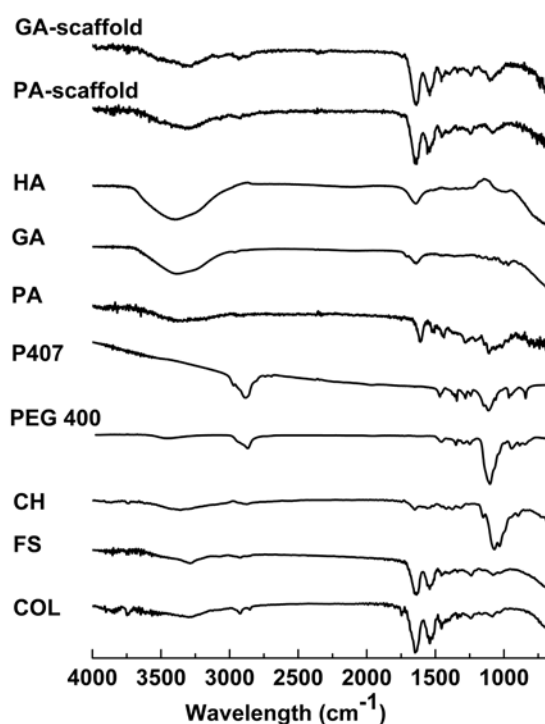
The spectra of PA-scaffold and GA-scaffold showed the crosslinking formation between COL and PA/GA.

The hydrogen bonding is the main mechanism of interaction between hydroxyl groups present in PA and amino and amide groups of COL. However, hydrophobic interactions were also proposed to explain the binding of polyphenols to proteins, which might occur through the association of their aromatic rings with proline residues (VIDAL et al., 2016). The spectra were scaled to equal absorption at 3302 cm^{-1} which is assigned to the -CH₂ chemical group. -CH₂ group remains unchanged during the crosslinking reaction of COL. It can be seen in the Figure 6 that crosslinking of COL

matrices by PA/GA has increased its intensity of transmittance at 1643 cm^{-1} comparing to the native COL matrix. It can be concluded from increasing the intensity of transmittance at 1643 cm^{-1} that carboxyl ($-\text{COOH}$) groups in COL matrix have been reduced due to the crosslinking reaction. Furthermore, it can be seen a decreased the intensity of transmittance at 1082 cm^{-1} after crosslinking of COL matrix. It can be concluded from decreasing the intensity of transmittance at 1082 cm^{-1} that crosslinking of COL makes more amide bonds between COL macro-molecules.

Crosslinking of COL with GA involves the reaction of the free amine groups of lysine or hydroxylysine amino acid residues of the polypeptide chains with the GA aldehyde groups. More specifically, the first step of the reaction involves the nucleophilic addition of the $\epsilon\text{-NH}_2$ groups to the carbonyl groups ($\text{C}=\text{O}$) of the aldehyde to form a tetrahedral unstable intermediate called carbinolamine. In a second step, protonation of the $-\text{OH}$ group followed by loss of a water molecule yields the conjugated Schiff bases (OLDE DAMINK et al., 1995). The transmittance at $\sim 1600\text{ cm}^{-1}$ is due to the amide II band, which originates from the N-H bending vibration and the C-N stretching vibration. One notes a shift in the amide II band of scaffold, indicating that the amide groups may be involved in the crosslinking reaction to form Schiff bases.

Figure 6. FTIR spectra of excipients, PA-scaffold, and GA-scaffold.



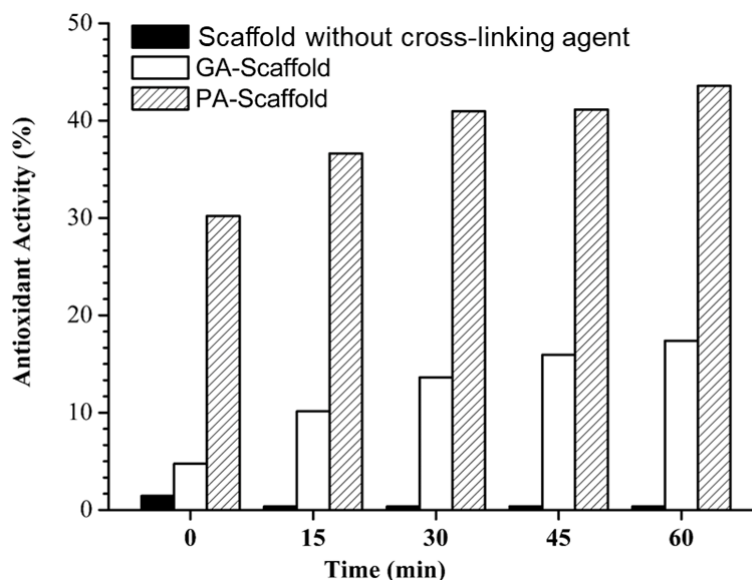
1.4.9 *In vitro* antioxidant activity

The evaluation of antioxidant activity of scaffold needs to be taken into account when considering these polymers and a crosslinking agent for biomedical applications. Figure 7 shows the antioxidant activity of the scaffold without a crosslinking agent, PA-scaffold, and GA scaffold. The analyze of the scaffold without a crosslinking agent was made as a control to know if the blend of polymer had antioxidant property. In of the end, PA-scaffold showed 44% antioxidant activity, this is 2.6 times more than GA-scaffold (17%), and 121 times more the scaffolds without the crosslinking agent (0.36%).

Proanthocyanidins are known to possess antibacterial, antiviral, anti-inflammatory, antiallergic and vasodilator actions. They have also been shown to inhibit lipid peroxidation, platelet aggregation, capillary permeability, and fragility. Proanthocyanidins have been shown to modulate the activity of regulatory enzymes including cyclooxygenase, lipoxygenase, protein kinase C, angiotensin-converting enzyme, hyaluronidase enzyme, and cytochrome P450 activities (BAGCHI et al., 2003; BAGCHI; BAGCHI; STOHS, 2002).

There is an increasing interest towards studying natural and synthetic antioxidants to prevent the uncontrolled oxidation of lipids, proteins, and DNA caused by the development of various diseases like cardiac and cerebral ischemia, infection and cardiovascular diseases (BAHEIRAEI et al., 2014). Our results confirm the ability of the PA to inhibit free radical moieties. Utilizing of PA in the scaffolds may have a striking effect on healing of tissues suffering from high oxidative stress especially due to infarction.

Figure 7. Antioxidant activity as a function of time of the scaffolds.

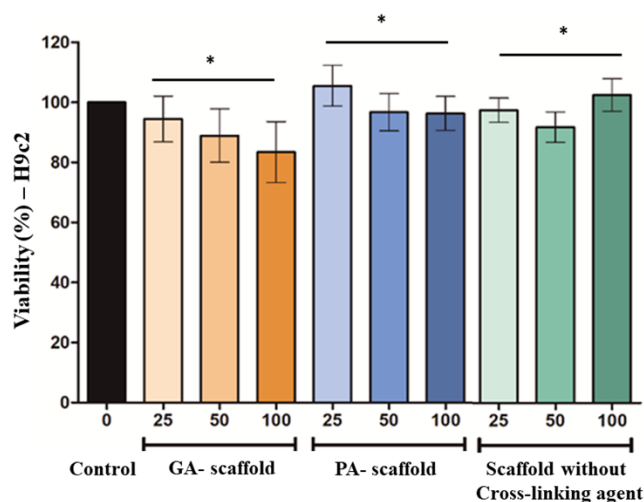


1.4.10 Cell viability

Chronic cytotoxicity is always of primary concern when designing biomedical devices using cross-linked collagen matrices. PA is widely used as a food supplement, and their lack of toxicity has been extensively demonstrated. In addition, PA has been reported to pose antibacterial, antiviral, anticarcinogenic, anti-inflammatory, and anti-allergic activities (HAN et al., 2003).

The results showed that after 24h the cellular viability of exposure to GA was the only one that presented a decrease, about 15% with respect to the control, however, it was not significant. Regarding the exposure to PA-scaffold and GA-scaffold, and scaffold without crosslinking agent, viabilities greater than 90% were observed. It being not possible at these concentrations to determine the IC_{50} (Figure 8).

Figure 8. Results of MTT analyses, exposure to GA-scaffold, PA-scaffold, and scaffold without crosslinking agent in H9c2 cells for 24h.



1.4.11 Cytometer Image

The results showed that PA-scaffold and GA-scaffold presented significant differences during the growth in relation to the control, after 48 and 72 hours, presenting a decrease of the cellular multiplication (Figure 9). The graph of Figure 10 shows the cell growth curve of the different scaffolds.

Figure 9. Results on cell growth (H9c2) after exposure to GA-scaffold, PA-scaffold, and scaffold without crosslinking agent at 48 and 72h.

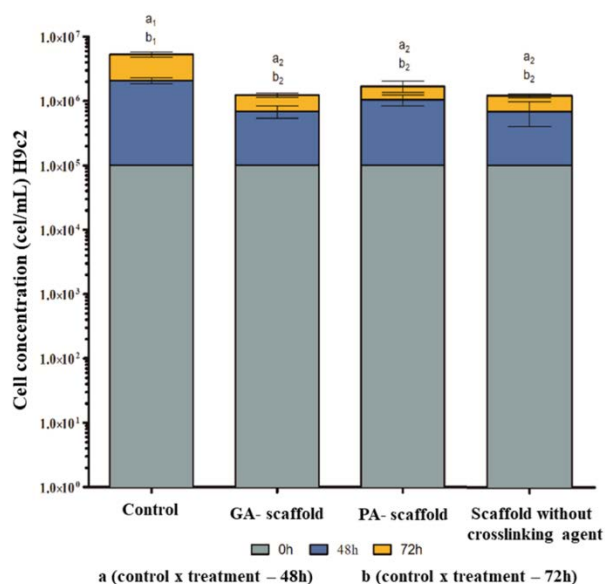
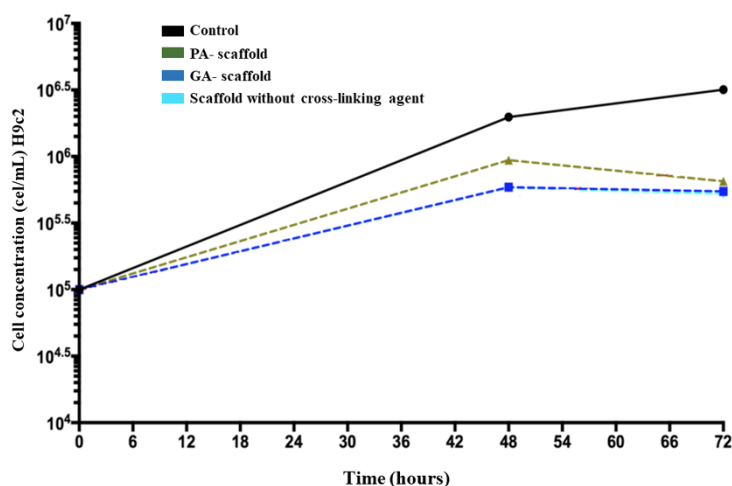


Figure 10. Cell growth curve (H9c2) after exposure to GA-scaffold, PA-scaffold, and scaffold without crosslinking agent at 48 and 72h.



In general, it is possible to observe that the material leads to an initial imbalance in the cells tested, but these seem to return to normal after a period of 72h, as observed in Figure 10, where there are differences of the exposed material in relation to the control (without exposure), but no significant difference between the different types of exposure is observed. As no significant cell death was observed on exposure, it is concluded that the material does not lead to cell death but an initial decrease in multiplication that is restored after the 72 h period.

According Yang et al. (2017), the PA cross-linked scaffold has the ability to promote cells attachment at the early stage after seeding. It is able to increase cell proliferation rate compared to the GA and uncross-linked scaffolds. What's more, it has been reported that PA related polyphenols could stimulate the proliferation of normal cells and increase the synthesis of ECM, and PA cross-linked collagenous materials could enhance the cell's ability to deposit collagen where collagen is widely known to play important role in cell adhesion and ECM formation (YANG; RITCHIE; EVERITT, 2017).

According Bo Han, *et al.* (2001) in a cytotoxicity assay using fibroblast cultures revealed that PA is ~120 times less toxic than GA, a currently used tissue stabilizer. *In vitro* degradation, a criterion often used to examine the degree of collagen crosslinking showed that fixed tissue was resistant to digestion by bacterial collagenase.

1.5 Conclusion

The choice of biomaterial and experimental condition for the design of these scaffolds were important parameters to assuring the biomimetic performance. The scaffolds obtained by plastic compression associated with crosslinking agent showed to be able to modulate the stiffness and suitable physiomechanical properties to support the reverse modulation of the myocardium. The effect of crosslinking agent modified the physiomechanical properties such as drilling, flexibility, traction and stress relaxation, but it did not modify the mucoadhesion property. The results of uptake saturation and weight loss suggest that PA-scaffold has a potential for mechanically support the native tissue during the necessary time for tissue regeneration. The antioxidant activity of PA-scaffold will have a more significant effect healthful to remodel native tissue that underwent oxidative stress. Both crosslinking agents did not influence in the H9c2 viability ($> 90\%$), the H9c2 multiplication presenting a discreet decrease after 48 and 72h. However, as no significant cell death was observed on exposure, it is concluded that the scaffold did not lead to cell death but a small decrease in multiplication that was restored after the 72 h period. Considering the anisotropic structure, the physiomechanical properties, cellular compatibility, and protective action against reactive oxygen species, this study may provide a way to improve the inverse remodulation of heart tissue, after infarct acute of the myocardium.

Author contributions

T. F. R.A developed the study, organization and discussion of results, and wrote the manuscript. J. F.S. and K.M.M.C. assisted in textural analyze and swelling test. D.G. performed and analyzed the antioxidant activity. R.L. performed and analyzed viability and multiplication cell. N.A., V.A.A and F.B. provided the silk cocoons of *Bombys mori*, and assisted in the extraction of silk fibroin. L. M.S. F. assisted with the cardiac discussion about biomimetic scaffolds. J. M.O.J. performed and analyzed the morphometric characteristic by computerized microtomography. P.S., A.C.R and C.T.B performed the physical-chemical analyzes. M.V.C. is head of LaBNUS, and was responsible for project administration and general supervision of works. All authors reviewed and commented on the manuscript.

Conflicts of interest

The authors have no competing interests to declare.

Acknowledgments

This work was supported by the National Council for Scientific and Technological Development [grant number 4252712016-1]; the São Paulo Research Foundation [grant number 2018/13432-0]; and the Postgraduate Support Program for Private Education Institution – Coordination for the Improvement of Higher Education Personnel (Prosup-Capes) with financial support for project and scholarship.

1.6 References

- ALONSO, J. R. L. et al. Effect of crosslinkers on bond strength stability of fiber posts to root canal dentin and in situ proteolytic activity. **Journal of Prosthetic Dentistry**, v. 119, n. 3, p. 494.e1-494.e9, 2018.
- ALVES, T. F. R. et al. Dense Lamellar Scaffold as Biomimetic Materials for Reverse Engineering of Myocardial Tissue: Preparation, Characterization and Physiomechanical Properties. **Journal of Material Science & Engineering**, v. 07, n. 05, 2018a.
- ALVES, T. F. R. et al. Formulation and evaluation of thermoresponsive polymeric blend as a vaginal controlled delivery system. **Journal of Sol-Gel Science and Technology**, p. 1–17, 2018b.
- ALVES, T. F. R. et al. Association of Silver Nanoparticles and Curcumin Solid Dispersion: Antimicrobial and Antioxidant Properties. **AAPS PharmSciTech**, v. 19, n. 1, 2018c.
- BAGCHI, D. et al. Molecular mechanisms of cardioprotection by a novel grape seed proanthocyanidin extract. **Mutation Research - Fundamental and Molecular Mechanisms of Mutagenesis**, v. 523–524, p. 87–97, 2003.
- BAGCHI, D.; BAGCHI, M.; STOHS, S. J. Cellular Protection with Proanthocyanidins. **Annals New York Academy of Sciences**, v. 270, p. 260–270, 2002.
- BAHEIRAEI, N. et al. Synthesis, characterization and antioxidant activity of a novel electroactive and biodegradable polyurethane for cardiac tissue engineering application. **Materials Science and Engineering C**, v. 44, p. 24–37, 2014.
- BIGI, A. et al. Mechanical and thermal properties of gelatin films at different degrees of glutaraldehyde crosslinking. **Biomaterials**, v. 22, n. 8, p. 763–768, 2001.
- BROWN, R. A. et al. Ultrarapid engineering of biomimetic materials and tissues: Fabrication of nano- and microstructures by plastic compression. **Advanced Functional Materials**, v. 15, n. 11, p. 1762–1770, 2005.

CHEN, Q. Z. et al. Characterisation of a soft elastomer poly(glycerol sebacate) designed to match the mechanical properties of myocardial tissue. **Biomaterials**, v. 29, n. 1, p. 47–57, 2008.

CHOI, Y.; KIM, J. Effects of proanthocyanidin , a crosslinking agent , on physical and biological properties of collagen hydrogel scaffold. **Restorative Dentistry e Endodontics**, v. 7658, p. 296–303, 2016.

DAVIDENKO, N. et al. Control of crosslinking for tailoring collagen-based scaffolds stability and mechanics. **Acta Biomaterialia**, v. 25, p. 131–142, 2015.

DAVIDOVIK-PINHAS, M.; BIANCO-PELED, H. Drug delivery systems based on mucoadhesive polymers. In: **ZILBERMAN, M.** (Ed.). Active implants and scaffolds for tissue regeneration. Springer ed. [s.l: s.n.]. p. 439–456.

DE MULDER, E. L. W.; BUMA, P.; HANNINK, G. Anisotropic porous biodegradable scaffolds for musculoskeletal tissue engineering. **Materials**, v. 2, n. 4, p. 1674–1696, 2009.

DHANDAYUTHAPANI, B. et al. Polymeric scaffolds in tissue engineering application: A review. **International Journal of Polymer Science**, v. 2011, n. ii, 2011.

ESCHENHAGEN, T. et al. Physiological aspects of cardiac tissue engineering. **AJP: Heart and Circulatory Physiology**, v. 303, n. 2, p. H133–H143, 2012.

GILMORE, J.; YIN, F.; BURG, K. J. L. Evaluation of permeability and fluid wicking in woven fiber bone scaffolds. **Society for Biomaterials**, n. December, 2018.

GUPTA, K. C.; JABRAIL, F. H. Glutaraldehyde and glyoxal cross-linked chitosan microspheres for controlled delivery of centchroman. **Carbohydrate Research**, v. 341, n. 6, p. 744–756, 2006.

HAN, B. et al. Proanthocyanidin: A natural crosslinking reagent for stabilizing collagen matrices. **Journal of Biomedical Materials Research - Part A**, v. 65, n. 1, p. 118–124, 2003.

HENDRADI, E.; HARIYADI, D. M.; ADRIANTO, M. F. The effect of two different crosslinkers on in vitro characteristics of ciprofloxacin-loaded chitosan implants. **Research in Pharmaceutical Sciences**, v. 13, n. 1, p. 38–46, 2018.

HO, H. O.; LIN, C. W.; SHEU, M. T. Diffusion characteristics of collagen film. **Journal of Controlled Release**, v. 77, n. 1–2, p. 97–105, 2001.

HU, K. et al. Compressed collagen gel as the scaffold for skin engineering. **Biomedical Microdevices**, v. 12, n. 4, p. 627–635, 2010.

KAI, D. et al. Guided orientation of cardiomyocytes on electrospun aligned nanofibers for cardiac tissue engineering. **Journal of Biomedical Materials Research - Part B Applied Biomaterials**, v. 98 B, n. 2, p. 379–386, 2011.

KARIKKINETH, B. C.; ZIMMERMANN, W.-H. Myocardial tissue engineering and heart muscle repair. **Current pharmaceutical biotechnology**, v. 14, n. 1, p. 4–11, 2013.

KOMATSU, D. et al. Characterization of Membrane of Poly (L,co-D,L-lactic acid-co-trimethylene carbonate) (PLDLA-co-TMC) (50/50) loaded with Silk Fibroin. **SDRP Journal of Biomedical Engineering**, v. 2, n. 1, p. 1–11, 2017.

KUO, S. W. E. I.; HUANG, C. F.; CHANG, F. C. Study of Hydrogen-Bonding Strength in Poly (ϵ -caprolactone) Blends by DSC and FTIR. n. February, p. 1348–1359, 2001.

LAKRA, R. et al. Enhanced stabilization of collagen by furfural. **International Journal of Biological Macromolecules**, v. 65, p. 252–257, 2014.

LEE, J.; SABATINI, C. Glutaraldehyde collagen cross-linking stabilizes resin–dentin interfaces and reduces bond degradation. **European Journal of Oral Sciences**, v. 125, n. 1, p. 63–71, 2017.

LI, Y.; ZHANG, D. Artificial Cardiac Muscle with or without the Use of Scaffolds. **BioMed Research International**, v. 2017, 2017.

LIKITAMPORN, S.; MAGARAPHAN, R. Mechanical and thermal properties of sericin/pva/bentonite scaffold: Comparison between uncrosslinked and crosslinked. **Macromolecular Symposia**, v. 337, n. 1, p. 102–108, 2014.

LIU, Y.; MA, L.; GAO, C. Facile fabrication of the glutaraldehyde cross-linked collagen/chitosan porous scaffold for skin tissue engineering. **Materials Science and Engineering C**, v. 32, n. 8, p. 2361–2366, 2012.

LOH, Q. L.; CHOONG, C. Three-Dimensional Scaffolds for Tissue Engineering Applications: Role of Porosity and Pore Size. **Tissue Engineering Part B: Reviews**, v. 19, n. 6, p. 485–502, 2013.

MACKIE, A. R. et al. Innovative Methods and Applications in Mucoadhesion Research. **Macromolecular Bioscience**, v. 17, n. 8, p. 1–32, 2017.

MAO, A. S.; MOONEY, D. J. Regenerative medicine: Current therapies and future directions. **Proceedings of the National Academy of Sciences**, v. 112, n. 47, p. 14452–14459, 2015.

MARTÍNEZ, A. et al. Tailoring chitosan/collagen scaffolds for tissue engineering: Effect of composition and different crosslinking agents on scaffold properties. **Carbohydrate Polymers**, v. 132, p. 606–619, 2015.

MI, S. et al. Plastic compression of a collagen gel forms a much improved scaffold for ocular surface tissue engineering over conventional collagen gels. **Journal of Biomedical Materials Research - Part A**, v. 95 A, n. 2, p. 447–453, 2010.

NAVEED, M. et al. Cardio-supportive devices (VRD & DCC device) and patches for advanced heart failure: A review, summary of state of the art and future directions. **Biomedicine & Pharmacotherapy**, v. 102, n. March, p. 41–54, 2018.

NEMATOLLAHI, Z. et al. Fabrication of chitosan silk-based tracheal scaffold using freeze-casting method. **Iranian Biomedical Journal**, v. 21, n. 4, p. 228–239, 2017.

O'BRIEN, F. J. et al. The effect of pore size on permeability and cell attachment in collagen scaffolds for tissue engineering. **Royal College of Surgeons in Ireland**, v. 15, n. 1, p. 3–17, 2007.

O'BRIEN, F. J. Biomaterials & scaffolds for tissue engineering. **Materials Today**, v. 14, n. 3, p. 88–95, 2011.

OLDE DAMINK, L. H. H. et al. Glutaraldehyde as a crosslinking agent for collagen-based biomaterials. **Journal of Materials Science: Materials in Medicine**, v. 6, n. 8, p. 460–472, 1995.

ORTOLANI, E. et al. Mechanical qualification of collagen membranes used in dentistry. **Ann Ist Super Sanità**, v. 51, n. 3, p. 229–235, 2015.

ORYAN, A. et al. Chemical crosslinking of biopolymeric scaffolds: Current knowledge and future directions of crosslinked engineered bone scaffolds. **International Journal of Biological Macromolecules**, v. 107, n. PartA, p. 678–688, 2018.

RAVICHANDRAN, R. Cardiogenic differentiation of mesenchymal stem cells on elastomeric poly (glycerol sebacate)/collagen core/shell fibers. **World Journal of Cardiology**, v. 5, n. 3, p. 28, 2013.

REBELO, M. A. et al. Chitosan-based scaffolds for tissue regeneration: preparation and microstructure characterization. **European Journal of Biomedical and Pharmaceutical Sciences**, v.3, n. 1, 2016.

RHEDER, D. T. et al. Synthesis of biogenic silver nanoparticles using *Althaea officinalis* as reducing agent: evaluation of toxicity and ecotoxicity. **Scientific Reports**, v. 8, n. 1, p. 1–11, 2018.

RICH, H. et al. Effects of photochemical riboflavin-mediated crosslinks on the physical properties of collagen constructs and fibrils. **Journal of Materials Science: Materials in Medicine**, v. 25, n. 1, p. 11–21, 2014.

SHAVANDI, A. et al. Polyphenol uses in biomaterials engineering. **Biomaterials**, v. 167, p. 91–106, 2018.

SILVA, A. M. H. DA et al. 193 Two and three-dimensional morphometric analysis of trabecular bone using X-ray microtomography (μ CT). **Revista Brasileira de Engenharia Biomédica**, v. 30, n. 2, p. 93–101, 2014.

TAN, T. C. et al. Comparative assessment of rheological properties of gelatin or gellan in maize starch - egg white composite gels. **Journal of King Saud University - Science**, v. 26, n. 4, p. 311–322, 2014.

TRIFKOVIĆ, K. et al. Chitosan crosslinked microparticles with encapsulated polyphenols: Water sorption and release properties. **Journal of Biomaterials Applications**, v. 30, n. 5, p. 618–631, 2015.

VARLEY, M. C. et al. Cell Structure , Stiffness and Permeability of Freeze-dried Collagen Scaffolds in Dry and Hydrated States. **Acta Materialia Inc.**, 2016.

VIDAL, C. M. P. et al. Collagen-collagen interactions mediated by plant-derived proanthocyanidins: A spectroscopic and atomic force microscopy study. **Acta Biomaterialia**, v. 41, p. 110–118, 2016.

WEI, Y. et al. Integrated Oxidized-Hyaluronic Acid/Collagen Hydrogel with β -TCP Using Proanthocyanidins as a Crosslinker for Drug Delivery. **Pharmaceutics**, v. 10, n. 2, p. 37, 2018.

YANG, Y.; RITCHIE, A. C.; EVERITT, N. M. Comparison of glutaraldehyde and procyanidin cross-linked scaffolds for soft tissue engineering. **Materials Science and Engineering C**, v. 80, p. 263–273, 2017.

YAP, L. S.; YANG, M. C. Evaluation of hydrogel composing of Pluronic F127 and carboxymethyl hexanoyl chitosan as injectable scaffold for tissue engineering applications. **Colloids and Surfaces B: Biointerfaces**, v. 146, p. 204–211, 2016.

CAPÍTULO IV

1 Artigo 3 – “Biomimetic dense lamellar scaffold based on a colloidal complex of the polyaniline (PANI) and biopolymers for electroactive and physiomechanical stimulation of the myocardial.”



Colloids and Surfaces A: Physicochemical and
Engineering Aspects

Available online 4 July 2019, 123650

In Press, Accepted Manuscript 



Biomimetic dense lamellar scaffold based on a colloidal complex of the polyaniline (PANI) and biopolymers for electroactive and physiomechanical stimulation of the myocardial

Thais Alves ^a, Juliana Souza ^a, Venancio Amaral ^a, Danilo Almeida ^b, Denise Grotto ^c, Renata Lima ^d, Norberto Aranha ^e, Lindemberg Silveira Filho ^f, Jose Oliveira Junior ^g, Cecilia Barros ^a, Patricia Severino ^h, Alexandro Souza ⁱ, Marco Chaud ^a  

[Show more](#)

<https://doi.org/10.1016/j.colsurfa.2019.123650> [Get rights and content](#)

1.1 Abstract

A novel biodegradable conductive scaffold containing water-soluble polyaniline (PANI) was manufactured. The conductive dense lamellar scaffolds were obtained by a mixture of collagen, fibroin solution, hyaluronic acid, and water-soluble polyaniline, using plastic compression method. Scaffolds held open and interconnected pores having a pore size ranging from several 100 to 150 μm . PANi-scaffolds had compression modulus and strength of 1.77 ± 0.11 MPa. The isoelectric point of the scaffold was observed by surface zeta potential in pH 7.7. The conductivity of the scaffold was measured as $2 \cdot 10^{-6}$ S.cm⁻¹ for dry PANi-scaffold and $6 \cdot 10^{-4}$ S.cm⁻¹ for hydrated. The PANi-scaffold has physiomechanical, and physico-chemical properties supported the viability and proliferation of cardiomyocytes. Our results highlight the potential of incorporation of PANi as an electroactive moiety for induction of cardiomyocyte proliferation and repair of damaged heart tissue.

Keyword: Electroactive scaffold; Dense lamellar scaffold; Polyaniline; Acellular myocardial regeneration.

1.2 Introduction

The World Health Organization (WHO) estimates that cardiovascular diseases (CVDs) take the lives of 17.9 million people per year (31% of all global deaths). Myocardial infarction leads to ventricular remodelling, fibrosis, necrosis, heart failure, among others, which may cause partial or total cardiac dysfunction. Tissue engineering is an approach to treat disease or damage in tissues and organs. The success of tissue engineering is related to hosts scaffold properties the cells and improves their survival, proliferation, and differentiation. Then the scaffold function as a biomimetic extracellular matrix (ECM) until new tissue could be formed by migration of the peripheral cells into the scaffold. The ECM is an elaborate meshwork in which most of the normal anchorage-dependent cells reside. To cardiac tissue, ECM serves as an anisotropic structural scaffold to guide aligned cellular distribution and organization. It accommodates contraction and relaxation of cardiomyocytes and facilitates force transduction, electrical conductance, intracellular communication, and metabolic exchange within the myocardial environment (RAI et al., 2018). Electromagnetic fields can affect of tissues as cardiac, muscle, nerve and skin. Moreover, it has an important role in a multitude of biological processes (e.g., angiogenesis, cell division, cell signalling, nerve sprouting, prenatal development, and wound healing) (FUNK; MONSEES, 2006).

Polyaniline (PANI) is one of the most promising due to its straightforward polymerization, environmental stability, relatively high conductivity, and it has been proved to play an essential role in stimulating proliferation, adhesion or differentiation of various cell types. Also, PANi has been validated for the ability to scavenge harmful free radicals from the environment, which makes it a right candidate in incidents where tissues experience high oxidative stress, especially post-infarction (BAHEIRAEI et al., 2014). However, conducting PANi is not generally processable due to its less solubility for almost of all solvents and poor melt property (BAHEIRAEI et al., 2014; SHAO et al., 2011).

In development cardiac scaffolds, important parameters as porosity, mechanical properties, and chemical components have to be taken into account in order to reach an optimum cell migration as well as oxygen and nutrition transfer [5]. So, after the manufacturing process of the scaffold is crucial that the existence of porous open and interconnected with each other. These concerns, in turn, have encouraged the use of

polymers that can be processed in aqueous media, mainly when PANi is used as a component of aqueous coatings (BAHEIRAEI et al., 2014; SHAO et al., 2011).

To mimic the extracellular matrix of tissue, the architecture of scaffolds the of is one of the most critical challenges in the field of tissue engineering. Polymeric scaffolds show potential with mechanical properties, high interconnectivity of porous (high anisotropy degree), and with a wide range of degradation, the qualities which are essential for a range of tissue engineering applications. Thus, the polymer scaffolds have all the perspective to provide a new means to control the physical and chemical environment of the biological system (DHANDAYUTHAPANI et al., 2011).

The join of the heart's physiopathology after a heart attack and the understanding of the multidisciplinary of the tissue engineering, we have proposed the design of an acellular cardiac patch that prevents myocardial wall remodelling and ultimately restores function to the heart. Among the potential approaches are to stimulate the cellular migration, anchorage of the migratory cells, and its multiplication, provide biological activity and biophysical support to the heart. The primary combination of cells and biomaterial scaffold composition increased biological activity and biophysical of this device. This work created more advanced engineered cardiac tissue and presented better screening tools to test bioengineered cardiac patches in vitro.

The novel conductive cardiac scaffold was fabricated by plastic compression followed by lyophilization. Further, we successfully showed that mechanical and biomechanical properties, biodegradability, morphologic, conductive capacity, antioxidant activity, and in vitro cellular proliferation.

1.3 Materials and Methods

1.3.1 Materials

The collagen powder type I (NovaProm Food Ingredients Ltda. São Paulo, Brazil). DMEM (Sigma-Aldrich Co, Saint Louis, USA), proanthocyanidin (GAMA, São Paulo, Brazil), hyaluronic acid (Via Farma, São Paulo, Brazil), polyethylene glycol 400 (Dinâmica, São Paulo, Brazil), HCl (Dinâmica, São Paulo, Brazil), aniline (Synth, São Paulo, Brazil), ammonium persulphate (Synth, São Paulo, Brazil), Polyvinylpyrrolidone K30 [MW 40,000 g.mol⁻¹ (Synth, São Paulo, Brazil)]. Cocoon of the Bombyx mori. MTT 3-(4,5-dimethylthiazol-2-yl)-2,5-diphenyltetrazolium bromide (MW = 414,), SDS

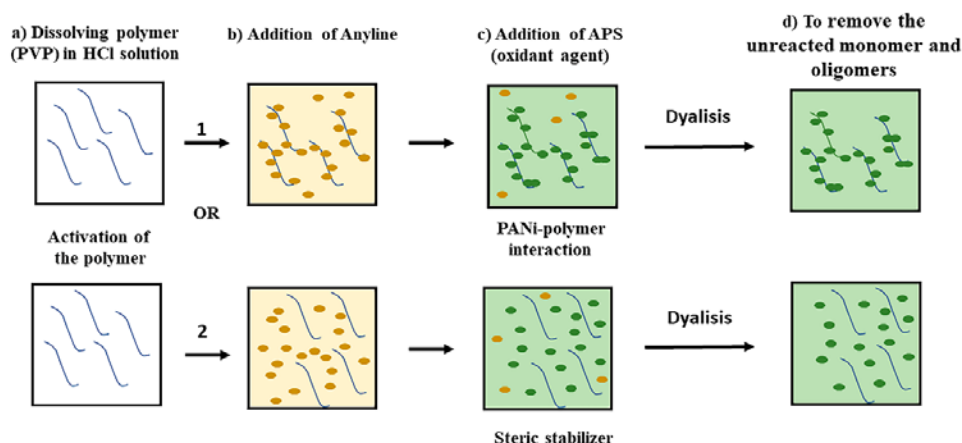
sodium dodecyl sulphate (MW = 288, Component B) was purchase of Thermo Fisher Scientific. The other reagents were of pharmaceutical grade. All materials were used without any previous treatment.

1.3.2 Preparation of PANi-PVP water-soluble

Water-soluble PANi was synthesized by chemical oxidation polymerization using aniline as a monomer, HCl (1M) as a dopant, and ammonium persulphate (APS) as an initiator. Polyvinylpyrrolidone (PVP) polymer was used as a solubilizing agent and steric stabilizer. The Figure 1 illustrates the water-soluble PANi synthesis. PVP (1g) was added in 20 ml of HCl 1M and stirred to dissolve at 25°C (Figure 1a). The solution was allowed to cool. Aniline (2 ml) was dropped wisely into PVP/HCl solution at 0-5 °C and stirred for 1 hours for activation of the polymer (Figure 1b). Then, 10 ml of APS (1M) aqueous solution was added slowly into aniline/PVP/HCl solution to initiate polymerization (Figure 1c). Polymerization was carried out at 0-5 °C for 3 hours. The polymer was purified with the help of dialysis tubing with HCl (1M) as dialysate for 13 hours, hourly, in order to remove the unreacted monomer and oligomers (Figure 1d).

The electrical conducting behaviour of PANi – polymers were analysed through UV- Vis (FEMTO, Model 800XI, São Paulo, Brazil) in the wavelength range of 220 – 300 nm for residual aniline and 350 - 900 nm for PANi characteristic peaks.

Figure 1. Illustration of water-soluble PANi-PVP. Route 1 depicts that the polymer in acid medium can be activated by breaking hydrogen bonds. Route 2 depicts that the increase of solubility occurs by steric stabilization.



1.3.3 Preparation of Fibroin Solution

Bombyx mori silk fibroin (SF) was prepared adapted from Komatsu et al. (2017). Briefly, silk sericin was extracted by treating silk cocoons in an aqueous solution of Na₂CO₃ (0.5 wt %), 120°C, for 15 min using an autoclave. The SF was rinsed thoroughly with water to extract the sericin proteins. The degummed silk fibroin was dissolved in a solution of the CaCl₂.2H₂O/CH₃CH₂OH/H₂O solution (mole ratio, 1:2:6) at 85°C. Then the SF was filtered and dialyzed against distilled water for three days to yield SF. The final fibroin concentration was about 2–3 wt %, which was determined by weighing the remaining solid after drying.

1.3.4 Preparation of hydrogel with PANi

Hydrogels formulations scaffolds were manufactured cross-linked with PANi (Table 1). Briefly, the collagen dispersion was prepared by the addition of 2 ml of DMEM, 1 g of collagen type I (COL) and enough ultrapure water to obtain 10 ml of dispersion. In preparation of hydrogel formulation, the solution PANi-PVP, solution fibroin (FS), Polyethylene glycol 400 (PEG), and crosslinking agent (PA) were added to the collagen dispersion in this order, followed by mechanical stirring until obtaining a uniform hydrogel. After that, the pH of the formulation was adjusted to 6.9 using 2M NaOH and added hyaluronic acid (HA) to the polymer dispersion. The gel dispersion was placed into cylindrical containers with a capacity for 3.8 cm³ and refrigerated at 10 °C for 24 h for polymerization.

Table 1. Formulation of PANi-scaffold

	PANi-scaffold
Collagen	1.0 g
Proanthocyanidin	0.08 g
PANi- PVP (solution)	1.0 mL
Hyaluronic Acid (1 %)	0.06 g
Fibroin Solution	4.0 mL
Polyethylene glycol 400 (50%)	2.0 mL
DMEM	4.0 mL
H ₂ O ultrapure	8.0 mL

1.3.5 Preparation of dense lamellar scaffolds

Dense lamellar scaffolds were produced by plastic compression (using a hydrostatic press), according to Alves et al. (2018). Briefly, the hydrogel moulded in the cylindrical form was transferred to porous support, formed (from bottom to top) of layers paper absorbent blot, a steel mesh, and two nylon meshes. The static compressive force of 4 KN was applied for 10 min to remove the water of the hydrogel and produce a dense biomaterial. Finally, the matrices were freeze-dried, resulting in cross-linked scaffolds.

1.3.6 Fourier transform infrared spectroscopy (FTIR)

The FTIR spectra were obtained by Labsolutions software IR s. v.2.10 (Shimadzu, IRAffinity-1, Kyoto, Japan). The stretches of the chemical bonds of the main functional groups of each molecule making up the sample were determined by an attenuated total reflectance (ATR) over the range between 4000 and 600 cm^{-1} at 4 cm^{-1} resolutions, averaging 128 scans (ALVES et al., 2018). The scaffold samples were carefully manipulated and put on the ATR-8200HA support before of each analyze.

1.3.7 Differential scanning calorimetry

The differential scanning calorimetry (DSC) was done on a Shimadzu, TA-60, Kyoto, Japan, calibrated using indium as the reference material. A sample of 2 mg was pressed in a hermetically crimped aluminum pan, and heated under dry nitrogen purged at 40 $\text{ml}\cdot\text{min}^{-1}$. The scaffold samples were heated from 25 to 350 ° C at a rate of 10 ° C min^{-1} .

1.3.8 Physiomechanical and mucoadhesive properties

The physiomechanical and mucoadhesive properties were measured, according to Alves et al. (2018). The physiomechanical properties evaluated in this work were (i) elastic modulus (Young's modulus)—measured strain in response to a given tensile or compressive stress along the force; (ii) flexural modulus (flexibility)—measured the relationship between a bending stress and the resulting strain in response to a given tensile or compressive stress perpendicular under load; (iii) tensile

strength (traction strength)—maximum stress that the material can withstand before it breaks; (iv) maximum strain (drilling strength)—ductility of a material or total strain exhibited prior to fracture (DHANDAYUTHAPANI et al., 2011).

A texturometer (Stable Micro Systems Texture Analyzer - TA-XT Plus) was used to measure the biomechanical properties such as compression and traction of dense lamellar scaffolds properties. The analyses were performed using a load cell of 5 Kg. The samples with 40 mm of diameter were hydrated for 1h, the excess of the PBS was removed with blot absorbent filter paper, and they were fixed in a suitable apparatus. The speed test was defined for the rate of 1 mm.s^{-1} for drilling and to traction test, and a speed test of 0.75 mm. s^{-1} for elasticity and flexibility test. The samples were stretched until failure, and the stress was measured by dividing the force generated during the extension by the cross-sectional area. The resulting stress-strain curves were used to calculate Young's modulus (E) and stress at 20% strain, and the failure strain for each of the different scaffold compositions.

The scaffolds mucoadhesive properties were evaluated using a Stable Micro Systems Texture Analyser (Model TA-XT Plus) in the compression mode. The discs of mucin were prepared for compaction using flat punches, a cylindrical matrix and a compression load of 8 tons (Lemaq, Mini Express LM-D8, Diadema, Brazil), The mucin discs with 8 mm of diameter and thickness of 0.2 mm, were previously moistened and fixed to the bottom of the analytical probe. The scaffold samples were fixed in a suitable apparatus. Mucin disc was compressed on the surface of the scaffold with a force of 0.098 N in the apical-basal direction. The contact time between the mucin disc and the scaffold sample surface was previously established in the study protocol and set to 100s. The probe was removed from the scaffold surface with a constant speed of 10 mm.s^{-1} . The force required to detach the mucin disc from the surface of the scaffold was determined from the time (s) vs. force (N) ratio (ALVES et al.,2018).

1.3.9 Swelling efficiency

The scaffolds were cut to approximate in a square shape ($15 \times 15 \text{ mm}$), weighed and then immersed in 3 ml PBS at $37 \text{ }^{\circ}\text{C}$ for up to 14 days. At different time points, they were removed, and two different measurements of their capacity to retain biological fluid were made. The first measurement was aimed at assessing the ability of the scaffold structure as a whole (the material itself together with the pore system)

to absorb PBS. For this, at each time point, the samples were removed from PBS, shaken gently, and then weighed without dripping (W_{wd}). The second measurement was carried out after pressing and “drying” the same soaked samples between sheets of filter paper to remove the water retained in its porous structure (W_{wp}). In this way, the swelling ability of scaffold material itself was determined. The scaffolds were then dried at 37 °C until a constant mass was reached (W_d). The percentage of fluid uptake, in both cases, was calculated as shown (Equation 1):

$$\text{Fluid uptake of scaffolds (\%)} = \left(\frac{W - W_d}{W_d} \right) \times 100 \quad (1)$$

Where W represents W_{wd} or W_{wp} . Each sample was measured in triplicate.

1.3.10 *In vitro* disintegration study

PA-scaffold and GA-scaffold were hydrated in PBS (Phosphate Buffer Saline, pH 7.4) at 37°C to evaluate their degree of degradation. Scaffolds were cut to an approximately square shape (15 x 15 mm), weighed before the degradation study ($W_{d'}$), and then immersed in 3 ml PBS at 37 °C for up to 14 days. At different time points, they were removed, washed in a large volume of deionized water to remove buffer salts, and dried at 37 °C until a constant mass was reached. Finally, the samples were weighed (W_a), and the percentage weight loss was calculated as follows (Equation 2):

$$\text{Weight loss (\%)} = 100 \times \left(\frac{W_{d'} - W_a}{W_{d'}} \right) \quad (2)$$

The pH value of the PBS was measured at each time point using a pH-meter (Tecnal, TE-5, Piracicaba, Brazil). Each sample was measured in triplicate.

1.3.11 Morphometric characteristics

The pore size, porosity (%), and the interconnectivity of the porous in the scaffolds were evaluated by microtomography (μ CT). The scaffolds pictures were captured by X-Ray microtomography (Brucker-micro CT - SkyScan 1174, Kontich, Belgium), scanner resolution of the 28 μ m pixel, and integration time at 1.7 s. The X-rays source was 35 keV and 795 mA. The projections were taken in a range of 180°

with an angular level of 1° of circumrotating. A 3D virtual models, representative of various sections of scaffolds were built, and the data was mathematically managed by CT Analyzer software, v. 1.13.5.2.2.8.

1.3.12 Permeability measurement

Specific permeability was measured in the current work using a constant pressure gradient method. The rig allows small pressure differences to be imposed across the scaffold, defined by the hydrostatic head of water ($\Delta P = r.H.g$) since the bottom of the scaffold is exposed to the atmosphere. The pressure was held constant across the scaffold (thickness L), and the volumetric flow rate (Q) of distilled water through the scaffold was measured (from the mass of water passing through the scaffold in a given time). This mass was measured, using a balance with a precision of 1 mg, and converted to volumetric flow using the fluid density ($\rho = 0.998 \text{ Mg m}^{-3}$). From Q , the sectional area (A) and the pressure gradient, $\Delta P/L$, the specific permeability, k , was calculated using Darcy's Law (Equation 3):

$$k = \eta \frac{Q}{A} \frac{L}{\Delta P} \quad (3)$$

When η , the dynamic viscosity, has units of Pa s and k has units of m^2 . The viscosity of the water was taken as $8.9 \times 10^{-4} \text{ Pa.s}$. A total of 2 samples (5 mm diameter, 3 mm height) were used, and three repeat measurements were made on each sample. The water column (H) was 9 cm. Furthermore, a press-fit mount was used to prevent scaffold deformation. The mounting aperture was slightly larger than the scaffold diameter in the dry state. When hydrated, the scaffold expanded to fill the entire aperture.

1.3.13 Surface zeta potential

The electrokinetic potential (zeta potential) and the isoelectric points of the scaffold were determined using the SurPASS 3 (Anton Paar). Samples were placed inside the adjustable gap cell. For each measurement, a pair of the samples in the form of a dense lamellar scaffold with the same top layer was fixed on two sample holders (cross-section $20 \times 10 \text{ mm}^2$). The zeta potential and/or isoelectric points were determined using the potential streaming method. The sample was measured in

contact with a 0.001 mol. L⁻¹ KCl electrolyte solution and the pH was adjusted with a 0.05 mol. L⁻¹ HCl solution and a 0.05 mol. L⁻¹ NaOH in the pH range from 8 to 4.

1.3.14 Scanning electron microscopy

Scanning electron microscopy (SEM) images of various scaffold structures scaffold were obtained using a Scanning Electron Microscope (LEO Electron Microscopy/Oxford, Leo 440i, Cambridge, England) with a 10 kV accelerating voltage. Scaffold samples were previously frozen with liquid nitrogen, cut out (dimension 30 x 30 mm) and mounted on pins stubs specimen using carbon double-sided adhesive tape. The samples were sputtered coated with gold for 4 min at 15 mA, using SC7640 Sputter-Coater.

1.3.15 Electrical conductivity

The electrical conductivity (σ , Siemens.cm⁻¹) of the dry and hydrated scaffolds (exposed to DMEM, at 37° C for 24 h) was measured at room temperature using the two-point probe technique. The corresponding electrical current was obtained after providing a voltage (144 V). The electrical conductivity of the samples was calculated by the Equation 4:

$$\sigma (S\ cm^{-1}) = \frac{1}{(R*S)/L} \quad (4)$$

where σ is the electrical conductivity of the material (Siemens.cm⁻¹), S is transverse area of the sample (cm²), L is the sample thickness (cm), R is the resistance of the material subjected to electrical tension (Ω), and ρ is resistivity ($\Omega\text{cm}^2.\text{cm}^{-1}$). The scaffold was maintained horizontally to perform the analysis.

1.3.16 *In vitro* antioxidant activity

The antioxidant activity of the PANi-scaffolds was determined using a solution 0.1mM of 2,2-diphenyl-1-picrylhydrazyl (DPPH) as free radical. After the addition of DPPH to the samples, absorbance was determined at a wavelength of 515 nm in a

spectrophotometer (Lambda 35, PerkinElmer, USA) at 0, 15, 30 45 and 60 min. The tubes containing the samples were kept under the light. The ability of the radical sequestering sample (DPPH), expressed as *per cent* inhibition was calculated according to Equation 5 and plotted.

$$Inibição (\%) = \frac{Abs1 - Abs2}{Abs1} \times 100 \quad (5)$$

1.3.17 Cell viability

Among several methods for cell viability, the MTT assay is still one of the most versatile and popular essays. The cellular viability by MTT assay was evaluated just for COL-CH-SF-Polyaniline scaffolds. Vybrant® MTT Cell Proliferation Assay Kit was used for determination of cell number using standard microplate absorbance readers. The reagent solutions were prepared as described by the manufacturer. For the test, the sample was extracted and kept in the culture medium for 24h. The extract was made with a sample of the 1cm², in 2.5 mL culture medium, corresponding to exposing 1.6 m of sample to the body mass of an individual of 70 kg. Approximately 5x10⁵ cells/well (H9c2 cells - cardiac myoblasts) were plated in 96-well plates with 1 ml complete culture medium at a density of 5.10³ cells per well. After 24h the total cell adhesion treatments were completed using the extracts at 100% and diluted at 25 and 50%, and then maintained for a further 24h (VAN MEERLOO; KASPERS; CLOOS, 2011). After the treatment, the culture medium was removed and 100µl of MTT solution at 5mg.ml⁻¹ was added to each well. After 3 hours in the oven at 37 °C, the MTT solution was withdrawn, and 100µl of DMSO per well was added for cell attachment. The reading was performed using ELISA microplate reader at 570nm.

1.3.18 Image cytometer

Initially (time 0h) 1x10⁵ cardiac myoblasts cells per well (H9c2 cells) were plated in a 24 well plate. Cells were grown at 37° C in 5% CO₂ using Minimum Essential Medium Eagle Alpha Modification (Alpha MEM) with ribonucleotides, deoxyribonucleosides, 2mM L-glutamine and 1mM of sodium pyruvate and fetal bovine serum to a final concentration of 10%. Subsequent total adhesion of the cells (24h), they were placed in contact with the scaffold sample for 48 and 72 h. After the

treatment period, the sample was removed from the culture's medium, and the cells were washed with PBS, enzymatically dissociated with trypsin, and counted using the Image Cytometry Technique (HAN; LO, 2015; KESSEL et al., 2017; KREDIET et al., 2015).

1.4 Results and Discussion

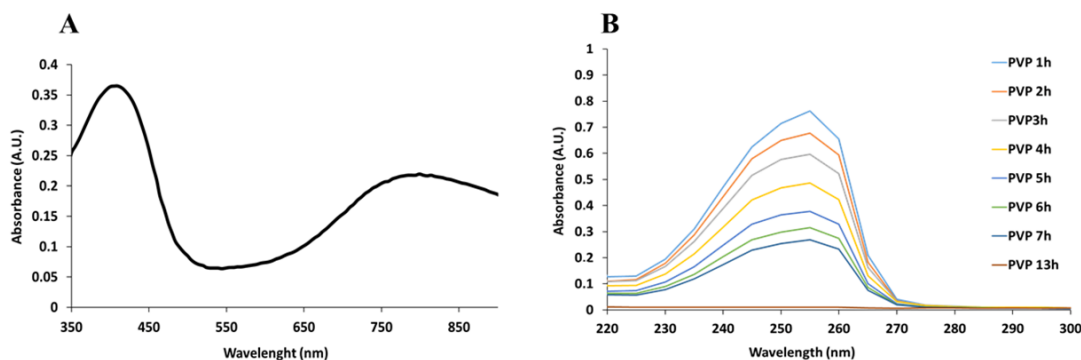
The limited regenerative potential of the heart after IAM causes scar formation in and around the infarction, leading to abnormal electric signal propagation and desynchronized cardiac contraction. Electrical conductivity is a key factor in structuring therapeutic devices for cardiac repair. The development of electrically conductive biomaterials, with featuring biomimetic properties to the cardiac tissue has received more attention. Conductive biomaterials can be incorporated into cardiac scaffolds for restoring the disorder electrophysiological function of the damaged heart (MIHIC et al., 2015; YE; QIU, 2017).

1.4.1 Preparation of PANi-PVP water-soluble

The main problem associated with the effective utilization of PANi, is associated with its poor solubility in all available solvents. However, the solubility can be improved through doping with a suitable dopant or the using of polymers as stabilizing agent, as PVP (CHATTOPADHYAY; MANDAL, 1996). The PVP was used to obtain a solid dispersion system (Figure 1).

Two characteristic adsorption bands for doped PANi at a wavelength of 350–450 nm and 650–850 nm are observed (Figure 2A). UV-Vis absorption spectra of PANi-PVP dispersion is shown in Figure 2B. The absorption bands at 350–450 nm is referred to the transition from the π band to the π^* band centred on the benzene rings associated with the extended π orbital on polymer backbone (bandgap excitation) and interaction between PANi chains and a water-soluble polymer. The absorption bands at 650–850 nm is related to the doping level and polaron-bipolaronic transition. The extent of dopant–polymer interaction is also reflected in the formation of bipolaronic levels (ZEGHIOUD et al., 2015). Meanwhile, the absorption below 255 nm disappeared (Figure 2B) due to the removal of unreacted aniline monomer or oligomer (HUSSIN et al., 2017).

Figure 2. UV–Visible spectra of water-soluble polyaniline in emeraldine salt form (A). Residual aniline over 13 hours (B).



1.4.2 Fourier transform infrared spectroscopy (FTIR)

Representative FTIR spectra for excipients of formulation and scaffold are presented in Figures 3. The possible interactions were evaluated between the polymers, and the influence of PANi-PVP in scaffold.

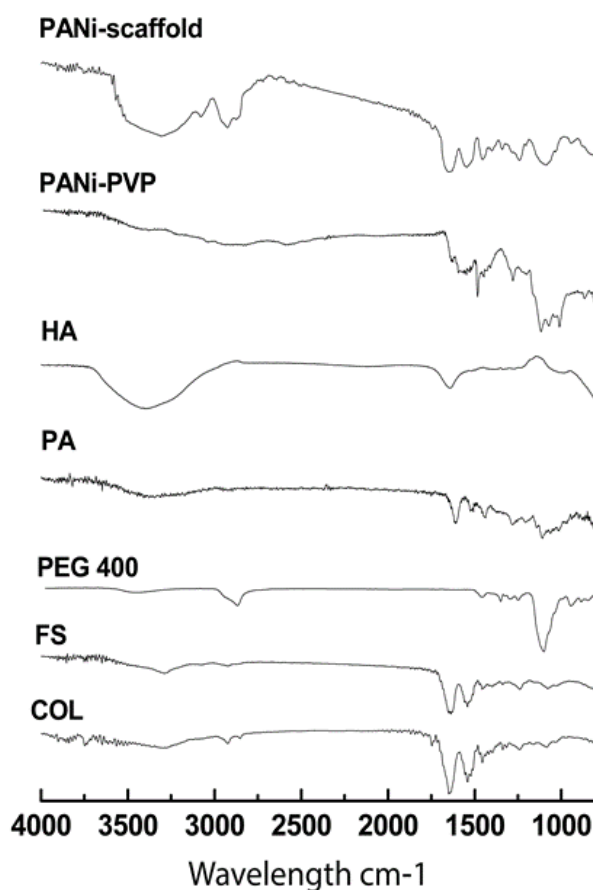
The spectra of collagen depict characteristic absorption of amide I in the wavenumbers at 1655 cm^{-1} , and 1645 cm^{-1} was found corresponding peptide secondary structure and hydrogen bonding between N - H stretch and C = O. The absorption correspondent at amide II band was observed at 1545 cm^{-1} . The wavenumber at 1240 cm^{-1} is corresponding to amide III and correspond at components from C - N, and C -H bending vibration in-plane bending form amide linkages. The band at 1098 cm^{-1} corresponded at C-OH stretching vibrations that could be attributed at carbohydrate group (RIAZ et al., 2018).

The typical feature of pure PANI is also well known in the literature (MO et al., 2009). The peaks around 1485 and 1570 cm^{-1} result from stretching vibration of N–A–N and N=B=N structures, respectively (where –A–, =B= stand for benzenoid and quinoid moieties in the PANI chains). The peaks at 1125 and 1294 cm^{-1} are respectively, a vibration of C–H in benzene ring and a stretching of C–N.

The most significant changes in these PANi-scaffold spectra are the stretching vibration of C–N near at 1200 cm^{-1} region, the stretching vibrations of aliphatic C–H at $2900\text{--}2800\text{ cm}^{-1}$ region, and the stretching vibration of hydroxyl group as a broad band centred at 3002 cm^{-1} . It is important to note that other bands of polymers were

overlapped with the sharp COL bands. Sarvari et al., 2016 observed the same stretching (SARVARI et al., 2016).

Figure 3. Fourier transform infrared spectroscopy (FTIR) spectra of the PANi-scaffold, polymers: collagen (COL); silk fibroin (SF); polyethylene glycol 400 (PEG 400); proanthocyanidin (PA); hyaluronic acid (HA) and PANi-PVP (copolymer polyaniline-polyvinylpyrrolidone).



1.4.3 Differential scanning calorimetry (DSC)

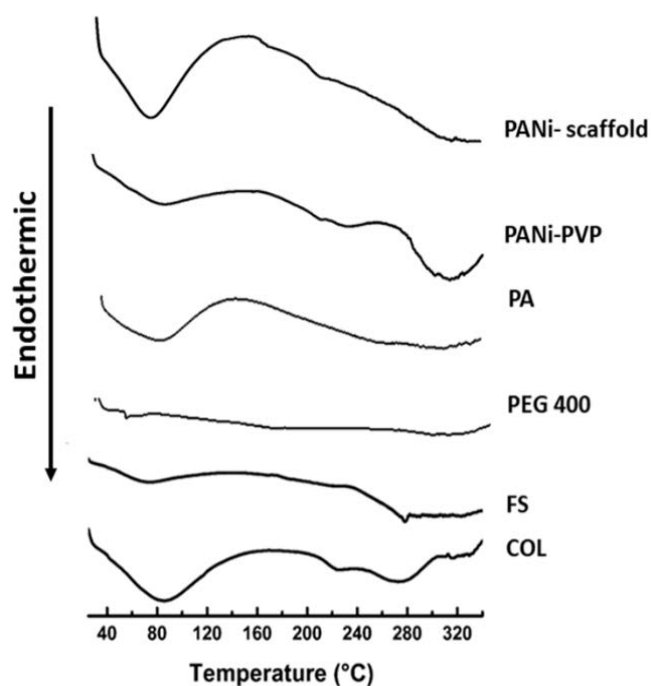
The thermodynamic properties of COL, SF, PEG 400, PA, PANi-PVP, and PANi-scaffold using DSC are shown in Figure 4.

The PANi-scaffold thermogram showed an endothermic peak (80°C) associated with the thermal transition of collagen molecule from triple helix conformation to a random coil conformation, and it involves the breakage of hydrogen bonds between the adjacent polypeptide chains of collagen (ZHANG; LI; SHI, 2006).

The endothermic events observed between 220-350o C also were observed by Shanmugasundaram et al. (2001), and they correlated with thermal decomposition of collagen (SHANMUGASUNDARAM et al., 2001). León-Mancilla et al. (2016) related that sharp endothermic transition at 320°C could be due to the loss of hydrogen bonds (LEÓN-MANCILLA et al., 2016)

The PANi can exist in three different forms: leucoemeraldine base (fully reduced form), emeraldine base (partially oxidized form), and base per-nigraniline (fully oxidized form). But, the emeraldine salt is the only one that presents electrical conductivity. However, the emeraldine base can be converted to emeraldine salt, and vice-versa, by protonation/ deprotonation with HCl and HCOOH (GOMES; OLIVEIRA, 2012). The thermogram of PANi-PVP displays an endothermic peak at 88 °C (Figure 4). This peak can be associated with water in the form of moisture absorbed by the polymer. Others two sharp endothermic peaks appear, respectively at 235 and 300 °C, both are, respectively, associated to evaporation of water linked to the polymer chain as a dopant, and dopant loss (GOMES; OLIVEIRA, 2012).

Figure 4. Differential Scanning Calorimetry (DSC) curves of spectra of the PANi-scaffold, polymers: collagen (COL); silk fibroin (SF); polyethylene glycol 400 (PEG 400); proanthocyanidin (PA); hyaluronic acid (HA) and PANi-PVP (copolymer polyaniline-polyvinylpyrrolidone).



The glass-transition temperatures (T_g) were observed at 220°C to PANi-scaffold but can also be observed for collagen in the natural form, indicating that blend of polymers, including of PANi is miscible.

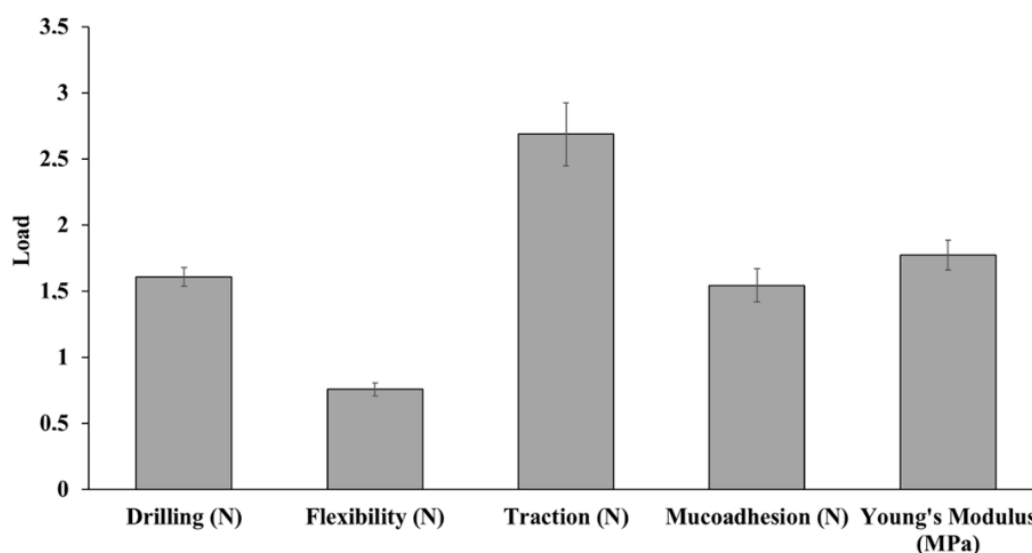
1.4.4 Physiomechanical and Mucoadhesive Properties

Figure 5 shows the results of physiomechanical properties of the PANi-scaffold obtained by plastic compression. The traction strength was 2.68 ± 0.23 N, drilling strength 1.60 ± 0.07 N, mucoadhesion strength of the 1.54 ± 0.12 N and flexibility of the 0.75 ± 0.05 N. The Young's modulus obtained for PANi-scaffold was 1.77 ± 0.11 MPa (Figure 5). Previously, our group obtained scaffolds without the PANi use into the formulation, and the physiomechanical properties were over than PANi-scaffolds.

The presence of PANi decreased the physiomechanical properties of scaffolds, except for drilling strength, that was equal. Compression drilling strength (or simply drilling strength) is a measure of material's related to the force per unit cross-sectional

area required for perforation. Drilling strength may be determined and related to scaffold mechanical properties and sometimes give indirect measurements of some elastic properties of the material. The drilling strength is proportional to Young's modulus (Figure 5). This approach has the advantage of provides a realistic estimate of scaffold strength and show the potential to promote myocardial repair and to improve the cardiac function.

Figure 5. Physiomechanical properties of PANi-scaffold. Drilling, flexibility, traction, mucoadhesion and Young's Modulus test (n = 3; the bars charts represent means and standard deviation values).



The human myocardium ranges in stiffness from 0.02 MPa (end of diastole) to 0.5 MPa (end of systole) (JAWAD et al., 2007; RADISIC; CHRISTMAN, 2013). The in vivo model to evaluate the stiffness of scaffold film or patches is Young's modulus. Qazi et al. produced poly(glycerol-sebacate) films with Young's modulus of 1.2 ± 0.3 MPa, and when the film was added at the PANi the Young' modulus increased to 6 ± 2 MPa (QAZI et al., 2014). Baheiraei et al., produced conductive scaffold from aniline pentamer-modified polyurethane/PCL blend, with Young's modulus of 4.1 MPa (BAHEIRAEI et al., 2015).

The results obtained by Qazi et al. to the stiffness was respectively, s6.0 times and 2.4 times higher than the average stiffness end of diastole, and end of systole. Baheiraei et al. obtained, respectively 300 times and 12 times higher than the average stiffness end of diastole, and end of systole. Our results reached respectively 20.5

times and 8.2 times higher than the average stiffness end of diastole, and end of systole.

The results found in PANi scaffold and in the papers cited above do not mimic the functionality of cardiac tissue. However, our opinion is that the stimulus on the damaged area of the heart should be higher than that of healthy tissue. Therefore, the scaffold stiffness should be higher than the cardiac muscle.

Otherwise, the scaffold could undergo a rupture during the movements of diastole and systole. The results showed in Figure 5 are, therefore, consistent. A close relationship between drilling, Young's modulus, flexibility could be found.

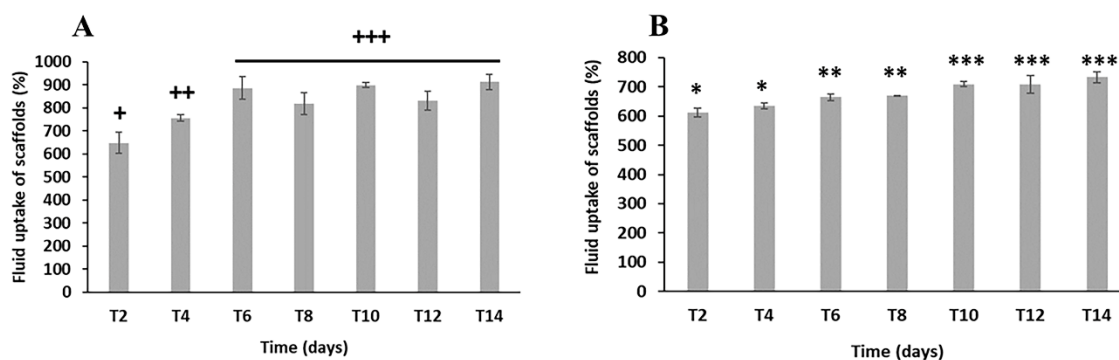
Mucoadhesion is a measure of fracture resistance between two different surfaces. The fracture resistance of the 1.5 N.cm^{-2} (0.015 MPa), after 180 sec of contact, between scaffold with mucin disc can be enough to support the diastole and systole movement.

In this circumstance, a material designed to thicken the ventricle wall artificially and preserved contractility and significantly protected the cardiac tissue from injury at the anatomical and functional levels.

1.4.5 Swelling efficiency

The swelling of scaffold consists of penetration of solvent leads to wet of the scaffold, which is due to the diffusion of solvent molecules through the polymer matrix and local relaxation of polymer segments (NANDA et al., 2013). The swelling (%) of hydrogel scaffold formulations in PBS (pH 7.4) were obtained, as shown in Figure 6 (A-B). Figure 6A is swelling characteristics related to fluid retained both by the whole scaffold structure (matrix and porous), while Figure 6B is swelling characteristics by the scaffold material itself (matrix).

Figure 6. Fluid uptake of scaffolds (%) fluid retained both by the whole scaffold structure (A) and by the scaffold material itself (B) in PBS 7.4 at 37 °C according to the cross-linking agent. Different symbols mean that statistical differences were found between different times ($p < 0.05$) for A or B test ($n = 3$); the bars charts represent means and standard deviation values

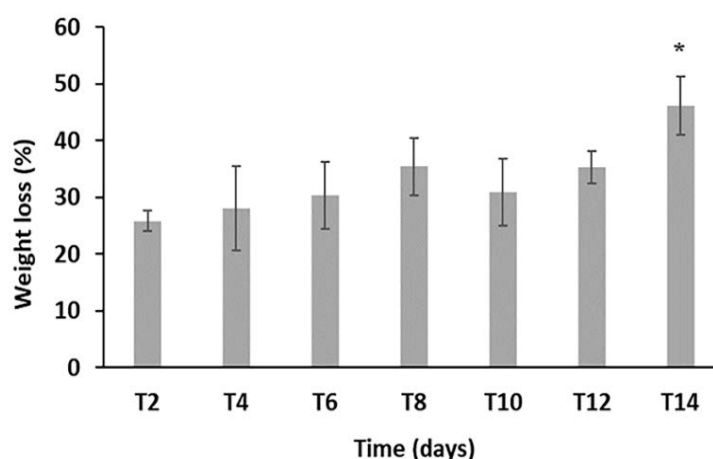


The hydration of scaffolds is important in indicating how cell culture medium may be absorbed during culture and how the scaffold may behave *in vivo*. Crosslinking is known to reduce the hydrophilic nature of the material since groups involved in the binding of water are consumed during the crosslinking process (amino and carboxylic acid groups) with crosslinking agents (GROVER; CAMERON; BEST, 2012; HANANI; SHAHITHA; HUSSAIN, 2014). The uptake of PBS 7.4 into scaffold is found to be dependent on time (Figure 6 A-B). For the scaffold itself, the hydrophilic nature of the material is likely to affect the quantity of PBS taken up by the PANI-scaffold. The fluid uptake values showed in Figure 6B, indicate that the most significant water amount is in the matrix of the scaffold, that is, absorbed by material no into porous.

1.4.6 *In vitro* disintegration study

The biodisintegration of the frameworks intended for tissue engineering is a complex phenomenon whose rate depends on different intrinsic and morphological factors, such as pore size, pore morphology, crystallinity, kind of crosslinking, surface area, hydrophilicity, and percentage of porosity (HANANI; SHAHITHA; HUSSAIN, 2014; QASIM et al., 2017). Figure 7 shows the weight loss (%) of PANi-scaffold for 14 days. The result obtained was, on average, 33.1 ± 3.84 % of the end of this test. The mass loss was considered independent of the time ($p > 0.05$), except after 14 days (Figure 7).

Figure 7. Weight loss (%) in PBS at 37 °C according to a cross-linking agent. * Means that statistical differences were found in different times ($p < 0.05$) ($n = 3$); the bars charts represent means standard deviation values.



1.4.7 Porosity, interconnectivity and pore size

Cardiac scaffolds should contain appropriate porosity and pore size, and have an interconnected structure for cell infiltration, enabling high densities of seeded cells and vascularization (MARTINS et al., 2014). Table 2 shows the morphological characteristics of PANi-scaffold. The scaffold showed the high interconnectivity between the pores (71.06%) with anisotropic features (degree of anisotropy = 0.76).

The freeze-drying technique has been used widely to obtain 3D porous structures (XIA; VILLA; WEI, 2015). The scaffold fabricated under a directional and a rapid freezing rate demonstrated anisotropic pore structure. In this work, the pore size and shape may have been controlled by the plastic compression technique, freezing rate, and ice growth direction.

Table 2. Morphological characteristics of PANi-scaffold

	PANi-scaffold
Total VOI* volume (mm⁻³)	6.02
Pore interconnectivity (%)	71.06
Volume of open pores (%)	71.09
Closed porosity (%)	0.05
Degree of anisotropy	0.76

*VOI (Volume of Interest) do scaffold

The software CT-An was used to calculate the morphometric parameters of the scaffold. The VOI was determined by tridimensional (3D) analyze of the scaffold and indicates the volume of VOI. This measure was used to calculate the morphometric parameters interweave by the walls of the pores, i.e., the part of the inner surface of the VOI in which the walls of the pores in the interior and on the surface of the scaffold are intersecting.

1.4.8 Permeability Measurement

The permeability of a scaffold is determined by a combination of microstructural factors including porosity, pore size, geometry, and distribution, pore interconnectivity, fenestration size, orientation of pores with respect to flow direction, and hydrophilicity of polymers (VARLEY et al., 2016).

The permeability coefficient of PANi-scaffold was $1.10 \cdot 10^{-10} \text{ m}^2$. The close result was obtained by O'Brien et al. (2007) (O'BRIEN et al., 2007), that produced collagen-glycosaminoglycan scaffold by lyophilization and obtained a permeability coefficient of the $1.387 \pm 0.516 \times 10^{-10} \text{ m}^2$ for scaffolds with equal pore size $151 \mu\text{m}$. Besides that, the permeability coefficient can be used as a quantitative tool to predict the barrier performance of porous media, and also estimate parameters as anisotropy or isotropy. The result is coherent with the degree of anisotropy showed in Table 2.

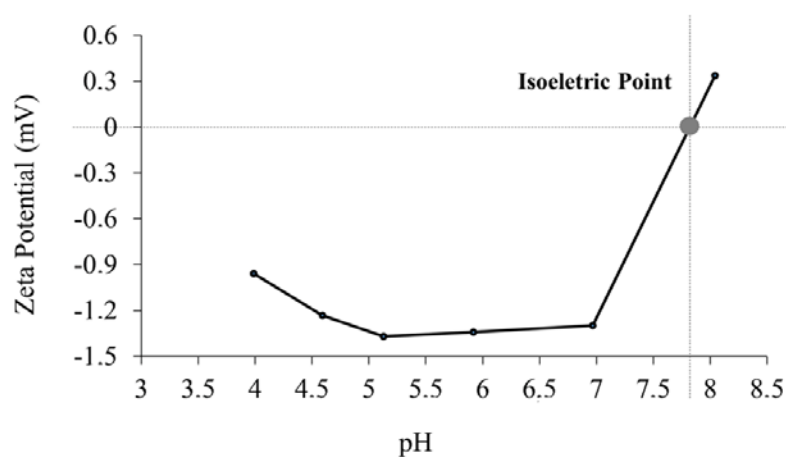
1.4.9 Surface zeta potential

Over the last few decades zeta potential measurements have become an important characterization method for surface functionality or stability of dispersed particles. The focus of zeta potential analysis is gaining information on the surface charge of a material.

Zeta potential measurements have an important characterization method for surface functionality or stability of planar and porous samples as the scaffolds. In this case, the focus of zeta potential analysis is gaining information on the surface charge of the scaffolds. Surface zeta potential gives information about the nature and dissociation of reactive functional groups, about polarity, hydrophilicity or hydrophobicity of the solid surface, and about ion or water sorption too (KASALKOVA et al., 2013).

The isoelectric point (IEP) can be measured by determination of zeta potential vs. pH (Figure 8). The IEP is defined as the point at which the electrokinetic potential equals zero, and it is an essential characteristic for coverings, for material for the study of living cell adhesion (KASALKOVA et al., 2013). Figure 8 shows the surface zeta potential of PANi-scaffold as pH-dependent. As it is clear, IEP of PANi-scaffold was obtained pH 7.8. Moreover, this result indicates that the main mucoadhesion mechanism of the PANi-scaffold (Figure 4) occurred by diffusion-interpenetration. According to this theory, the mucoadhesion involving the interpenetration and entanglement between the polymer chains and the mucous chains (SHAIKH et al., 2011).

Figure 8. Surface zeta potential of PANi-scaffold



1.4.10 Scanning electron microscopy (SEM)

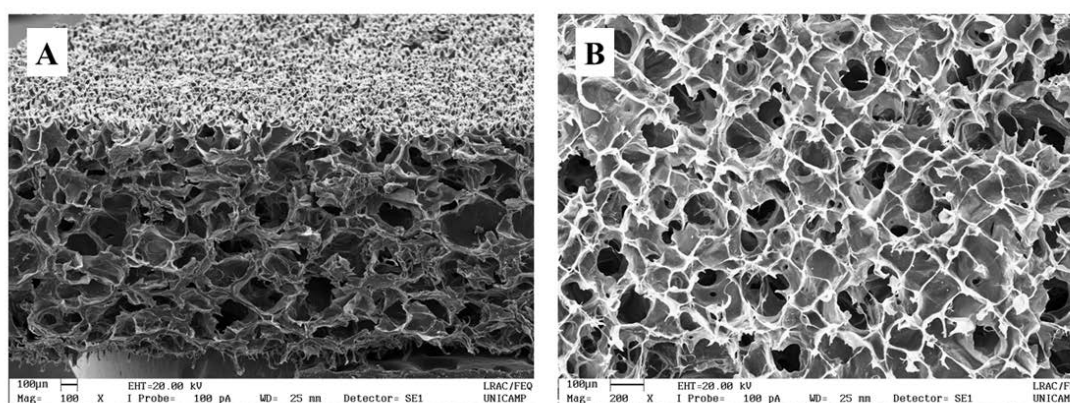
SEM images (Figure 9) of the different types of the cross-section, of the PANi-scaffold, showed a continuous irregular porous but rather uniformly distributed interconnected pores. The pores diameter estimated from SEM microphotographs, by the manual measurement the scale bar of the instrument that has been previously calibrated. The pore dimensions estimated from SEM microphotographs were 100 – 150 μm . This agrees with the size required for cell migration and nutrient flow, due the myocardial cells have dimensions in the range of 10–100 μm (MARTINS et al., 2014).

Exposure to organic solvents, application of mechanical stress, or thermal treatments to convert the *B. mori* silk fibroin from the random coil and/or silk I

conformation to β -sheet (CHEN et al., 2001; HU et al., 2012). The use of PANi, PA (crosslinking agent) associated to plastic compression and freeze-drying technique generated the sheets conversion of silk fibroin in the structure of the scaffold (Figure 9 A- B). The sheets formation can be viewed in Figure 9B, and it is common in the structure surface of the scaffold when the same is added of fibroin (ALVES et al., 2018).

Azhar F.F., Olad A., and Salehi R. (2014) (FARSHI AZHAR; OLAD; SALEHI, 2014); and Baheiraei et al. (2015) (BAHEIRAEI et al., 2015) produced scaffolds with chitosan–gelatin/ nanohydroxyapatite–polyaniline, and aniline pentamer-modified polyurethane/PCL blend, respectively. The SEM images obtained by them was similar with PANi-scaffolds images in this work. Thus, the morphological observation by SEM, of PANi-scaffolds, indicated the homogeneous structure and compatible with cardiac features.

Figure 9. SEM of PANi- scaffold (A-B). Magnification of A is 250x, and B is 500x.



1.4.11 Electrical conductivity

The heart beats as a result of coordinated mechanical responses to electrical signals that travel through excitable cardiac tissue, mediated by ion efflux through cell membranes. In the case of MI, the scarred, infarcted area may disrupt the proper electrical signal flow in the heart. This may lead to dysfunctional contractions and inefficient blood supply. It is thus desirable that an engineered cardiac patch will support the propagation of electrical signals in order to regain contractility of the damaged tissue (SHAPIRA; FEINER; DVIR, 2015).

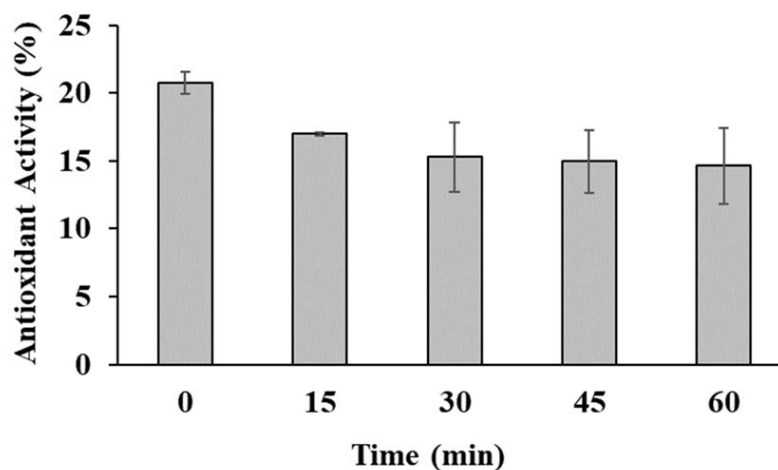
The electrical conductivity of the PANi-scaffold was measured using the standard probe method. The result was recorded to be on the order of $2 \cdot 10^{-6} \text{ S.cm}^{-1}$ for dry PANi-scaffold and $6 \cdot 10^{-4} \text{ S.cm}^{-1}$ for hydrated PANi-scaffold. In both situations, the PANi-scaffold is the range of semiconductor materials ($10^2 - 10^{-6} \text{ S.cm}^{-1}$) (BIDEZ et al., 2005). Thus, there were significant changes in the conductivity of the scaffolds that have been incubated. Scaffolds cardiac tissue engineering of the aniline pentamer-modified polyurethane/PCL blend, obtained by (BAHEIRAEI et al., 2015), showed an electrical conductive value close to $10^{-5} \text{ S.cm}^{-1}$.

In regenerative medicine, the conductivity ranges of the semiconductor polymers (micro-current) is sufficient to direct cell proliferation and possibly differentiation. Although it has been stated that native myocardial conductivity ranges from 0.0016 S.cm^{-1} (longitudinal) to $5 \cdot 10^{-5} \text{ S.cm}^{-1}$ (transverse) (BAHEIRAEI et al., 2015). It is at this point that PANi-scaffolds have the chance to be applied to cardiac tissue regeneration.

1.4.12 *In vitro* antioxidant activity

The antioxidant activity of PANi has significant implications for their inclusion as biomaterials in biological media. This property may be beneficial in tissues suffering from oxidative stress, as myocardial infarction, where the ability to lower excessive levels of reactive radical species is desirable (GIZDAVIC-NIKOLAIDIS et al., 2004; WANG et al., 2007). The antioxidant activity as a function of time of the PANi-scaffold is shown in Figure 10. It is possible to observe that occurs an initial peak (20.77%) at time = 0, but after that occurs a decrease of antioxidant activity of the PANi-scaffolds (average of $15.45 \pm 1.06 \%$).

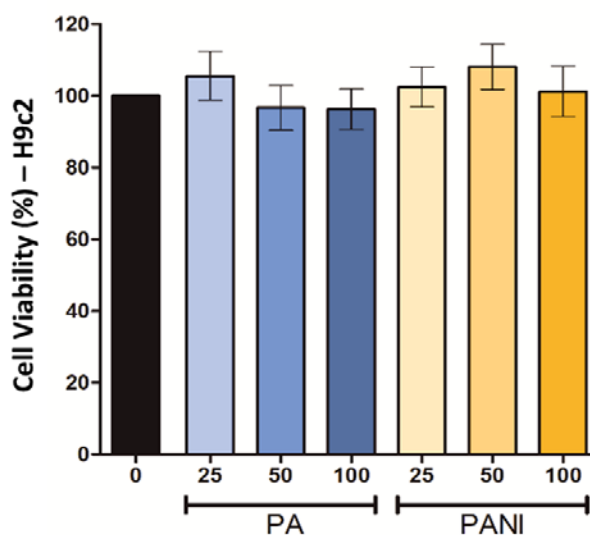
Figure 10. Antioxidant activity as a function of time of the PANi-scaffold



1.4.13 Cell viability

In the present study, was performed a preliminary evaluation of the biocompatibility of PANi-scaffolds and PA-scaffold by MTT assay (Figure 11). After 24 h of exposure, in different concentrations, all of the scaffolds supported above 90% cell viability for H9c2 cell lines, which suggested good affinity and biocompatibility for cells. Scaffold containing PANi, as a conducting polymer, showed absolutely non-toxic effects in vitro. It being not possible at these concentrations to determine the IC_{50} .

Figure 11. Results of MTT analyses, exposure to PANi-scaffold and PA-scaffold (without PANi) in H9c2 cells for 24h.

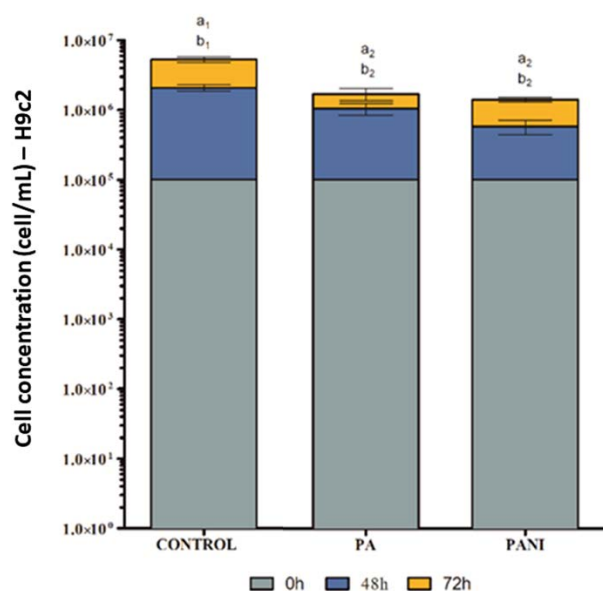


1.4.14 Image cytometer

Regarding cell multiplication (which was initially plated with the same number of cells) the preliminary results show that after 48h these presented differentiated growth, with lower cell growth in the treatments. Both treatments (PA and PANI) showed no significant difference between them (Figure 12). Nonetheless, after 72 h, the cells in PANI treatment showed the same growth as the control, indicating normality cell cycle carrying. This behaviour was probably due to the residual acidic contaminants that are present on the surface of the polymer and have been released for some time, this has led to cellular changes.

Bidez et al. (2005) investigated the adhesion and proliferation properties of H9c2 cardiac myoblasts on a polyaniline-conducting substrate. The results obtained by them were the same after 100 h of exposure (BIDEZ et al., 2005).

Figure 12. Results on cell growth (H9c2) after exposure to PANi-scaffold and PA-scaffold (without PANi) at 48 and 72h.



1.5 Conclusion

To stabilize the PANi has selected a biocompatible amphiphilic polymer that would bring together several properties of interest for stabilization and increase the water solubility of PANi. So, the PVP was polymer chose due to good solubility in water as well as in organic solvents, good affinity to various polymers, high hygroscopicity,

proper for film formation, good adhesiveness to various substrates, and excellent chelate/complex formation property. These properties were fundamental to the incorporation and stabilization of PANi in the scaffold by both routes shown in Figure 1. The results of FTIR and DSC give support to affirm that PVP as a stabilizer exist on the surface of the PANi to form a solid dispersion.

The DSC curve (Fig 4) to PANi-PVP showed two endothermic events, one of them with onset at 70o C and end set at 110o C degree, which was associated to the elimination of residual water of the mixture. On the other endothermic event is an exclusive Tg with onset and end set respectively at 150o and 220o C degree. The existence of a single Tg in the blend of two or more polymers confirms the homogeneity of the PANi / PVP blend, which resulted in increased water solubility of PANi, due to the obtention of solid dispersions. The other hand, in PANi-scaffold DSC two discrete events of Tg, can be observed. These are indicating that the polymers mixture is not completely miscible. A discrete separation or displacement of the polymer fibres, especially the collagen fibres, may have occurred during the compacting process.

Given that the chemical groups as quinoid (1480 cm⁻¹) and benzenoid (1565 cm⁻¹) ring of the PANi molecules, and C = O (1664 cm⁻¹) and C – N stretching present in the PVP molecules were preserved, and that no one other signals of a new chemical bond was found in the FTIR PANi-PVP. The spectra of UV-Vis (Fig 2) and FTIR for PANi-PVP (Fig. 3) corroborate with results found in the DSC (Fig. 4), indicating that the PVP as a stabilizer agent exists on the surface of the PANi as a solid dispersion or a suitable dopant.

There is a strong correlation between miscibility, polymers concentration in the PANi scaffold formulation with the biomechanical properties related to compression, traction, and Young's modulus. The results showed in Figure 5 are, therefore, consistent. A close relationship between drilling, Young's modulus, flexibility could be found. The traction strength (Figure 5) is a measure of the biomechanical stress that undergo the cardiac muscle in the vertical direction, i.e., following the skeletal striated muscle orientation

Poor conductivity could limit the ability of the patch to contract effectively as a unit. Besides that, constructing a specific microenvironment with conductive polymers can promote the guide the cells in its proliferation. The electrically conductive result was 6.10⁻⁴ S/cm² for hydrated PANi-scaffold, thus, classified as a semiconductor

material ($102 - 10^{-6} \text{ S/cm}^2$) with potential application to cardiac regeneration. Another factor that influences the cell adhesion and proliferation is the isoelectric point of the surface scaffold; it achieved at pH 7.8 by PANi scaffold.

The swelling efficiency assay of the scaffolds was done under adverse condition relative to the physiological water content in the heart area. Even so, the scaffold was able to absorb 900% more water concerning its initial mass. This result suggests that under physiological conditions, the scaffold could remain for at least twice as long without undergoing structural biodesintegration, which was about 40% in 14 days. The water content increases the weight of the scaffold, and this is an essential factor in containing the left ventricular expansion during the diastole.

All physiomechanical properties, as well as the wettability and disintegration time, has a straight correlation with morphometric parameters (Table 2) of the PANi-scaffold. The permeability has a close relationship with scaffold's morphology, especially the degree of anisotropy (Table 2), the cell viability (Fig. 11) and cell proliferation (Fig 12). The analyze by μCT 3D showed small variation in the scaffold's VOI indicating that the volume of open-pore and pore-interconnectivity were uniform, these results showing that both were constant, confirm that the formulation and the technique by plastic compression were uniform and robustness.

Just as the polymers were selected to mimic the extracellular matrix and they were designed so that the cells could adhere to the scaffold surface and proliferate into the scaffold and migrate using the pore size and the connection between them.

The scaffold manufacture favoured the free circulation of fluids (nutrients and oxygen) to the cells and at the same time as removing the catabolites produced by the cells and depleting the reactive oxygen species.

Thus, the microenvironment created by the scaffold was always favourable to the proliferation of healthy cells that can be capable of repairing the tissue damage caused by myocardial infarction.

This hypothesis, which predicts the functional recovery of the heart stimulated by scaffold described, is being evaluated. In vivo study with laboratory animals with previously induced infarction is being developed by our team.

1.6 Final Remarks and Future View

In this work, we have successfully fabricated electroactive dense lamellar scaffolds with interconnected pores and controlled porosity using collagen, fibroin solution, and hyaluronic acid, by plastic compression. Combination of conducting polymer (polyaniline) with natural polymers, appears to be appropriate to construct of a 3D structure able to be harbouring native cells, to stimulate the growing, spreading, and organization for the formation of new tissue. The PANi-scaffold has biomechanical and physico-chemical properties supported the viability and proliferation of cardiomyocytes. With a better understanding of the purposes and advancement of scientific knowledge related to the engineering of cardiac tissues, a significant and positive development is happening in this field of study, aiming at the promotion of inverse cardiac remodelling.

1.7 References

- ALVES, T. F. R. et al. Dense Lamellar Scaffold as Biomimetic Materials for Reverse Engineering of Myocardial Tissue: Preparation, Characterization and Biomechanical Properties. **Journal of Material Science & Engineering**, v. 07, n. 05, 2018.
- BAHEIRAEI, N. et al. Synthesis, characterization and antioxidant activity of a novel electroactive and biodegradable polyurethane for cardiac tissue engineering application. **Materials Science and Engineering C**, v. 44, p. 24–37, 2014.
- BAHEIRAEI, N. et al. Preparation of a porous conductive scaffold from aniline pentamer-modified polyurethane / PCL blend for cardiac tissue engineering. **Society for Biomaterials**, p. 1–9, 2015.
- BIDEZ, P. R. et al. Polyaniline, an electroactive polymer, supports adhesion and proliferation of cardiac myoblasts. **Journal of Biomaterials Science**, Polymer Edition, v. 17, n. 1, p. 199–212, 2005.
- CHATTOPADHYAY, D.; MANDAL, B. M. Methyl Cellulose Stabilized Polyaniline Dispersions. **Langmuir**, v. 12, n. 6, p. 1585–1588, 1996.
- CHEN, X. et al. Conformation transition kinetics of regenerated Bombyx mori silk fibroin membrane monitored by time-resolved FTIR spectroscopy. **Biophysical Chemistry**, v. 89, n. 1, p. 25–34, 2001.
- DHANDAYUTHAPANI, B. et al. Polymeric scaffolds in tissue engineering application: A review. **International Journal of Polymer Science**, v. 2011, n. ii, 2011.

FARSHI AZHAR, F.; OLAD, A.; SALEHI, R. Fabrication and characterization of chitosan–gelatin/nanohydroxyapatite–polyaniline composite with potential application in tissue engineering scaffolds. **Designed Monomers and Polymers**, v. 17, n. 7, p. 654–667, 2014.

FUNK, R.H.W.; MONSEES, T.K. Effects of Electromagnetic Fields on Cells: Physiological and Therapeutical Approaches and Molecular Mechanisms of Interaction. **Cells Tissues Organs**, n. 182, p. 59–78, 2006.

GIZDAVIC-NIKOLAIDIS, M. et al. The antioxidant activity of conducting polymers in biomedical applications. **Current Applied Physics**, v. 4, p. 347–350, 2004.

GOMES, E. C.; OLIVEIRA, M. A. S. Chemical Polymerization of Aniline in Hydrochloric Acid (HCl) and Formic Acid (HCOOH) Media . Differences Between the Two Synthesized Polyanilines. **American Journal of Polymer Science**, v. 2, n. 2, p. 5–13, 2012.

GROVER, C. N.; CAMERON, R. E.; BEST, S. M. Investigating the morphological , mechanical and degradation properties of scaffolds comprising collagen , gelatin and elastin for use in soft tissue engineering. **Journal of the Mechanical Behavior of Biomedical Materials**, v. 10, p. 62–74, 2012.

HAN, Y.; LO, Y. H. Imaging Cells in Flow Cytometer Using Spatial-Temporal Transformation. **Scientific Reports**, v. 18, n. 5, p. 13267, 2015.

HANANI, F.; SHAHITHA, F.; HUSSAIN, J. In vitro degradation study of novel HEC / PVA / collagen nano fi brous scaffold for skin tissue engineering applications. **Polymer Degradation and Stability**, v. 110, p. 473–481, 2014.

HU, X. et al. Regulation of Silk Material Structure by Temperature-Controlled Water Vapor Annealing. **Biomacromolecules**, v. 12, n. 5, p. 1686–1696, 2012.

HUSSIN, H. et al. Synthesis of water-soluble polyaniline by using different types of cellulose derivatives. **Polymers and Polymer Composites**, v. 25, n. 7, p. 515–520, 2017.

JAWAD, H. et al. Myocardial tissue engineering: a review. **Journal of tissue engineering and regenerative medicine**, v. 1, p. 327–342, 2007.

KASALKOVA, N. et al. Electrokinetic Potential and Other Surface Properties of Polymer Foils and Their Modifications. **Polymer Science**, n. iv, 2013.

KESSEL, S. et al. Real-time viability and apoptosis kinetic detection method of 3D multicellular tumor spheroids using the Celigo Image Cytometer. **Cytometry Part A**, v. 91, n. 9, p. 883–892, 2017.

KREDIET, C. J. et al. Rapid, precise, and accurate counts of symbiodinium cells using the guava flow cytometer, and a comparison to other methods. **PLoS ONE**, v. 10, n. 8, p. e0135725, 2015.

- LEÓN-MANCILLA, B. H. et al. Physico-chemical characterization of collagen scaffolds for tissue engineering. **Journal of Applied Research and Technology**, v. 14, n. 1, p. 77–85, 2016.
- MARTINS, A. M. et al. Electrically Conductive Chitosan/Carbon Scaffolds for Cardiac Tissue Engineering. **Biomacromolecules**, v. 15, p. 635–643, 2014.
- MIHIC, A. et al. A conductive polymer hydrogel supports cell electrical signaling and improves cardiac function after implantation into myocardial infarct. **Circulation**, v. 132, p. 772–784, 2015a.
- MIHIC, A. et al. A Conductive Polymer Hydrogel Supports Cell Electrical Signaling and Improves Cardiac Function After Implantation into Myocardial Infarct. **Circulation**, v. 25, p. 772–784, 2015b.
- MO, Z. LI et al. Heterogeneous preparation of cellulose-polyaniline conductive composites with cellulose activated by acids and its electrical properties. **Carbohydrate Polymers**, v. 75, n. 4, p. 660–664, 2009.
- NANDA, S. et al. Preparation and Characterization of Poly (vinyl alcohol) - chondroitin Sulphate Hydrogel as Scaffolds for Articular Cartilage Regeneration. **Indian Journal of Materials Science**, v. 2013, n. 1–8, 2013.
- O'BRIEN, F. J. et al. The effect of pore size on permeability and cell attachment in collagen scaffolds for tissue engineering . **Royal College of Surgeons in Ireland**, v. 15, n. 1, p. 3–17, 2007.
- QASIM, S. B. et al. In- vitro and in -vivo degradation studies of freeze gelated porous chitosan composite scaffolds for tissue engineering applications. **Polymer Degradation and Stability**, v. 136, p. 31–38, 2017.
- QAZI, T. H. et al. Development and characterization of novel electrically conductive PANI – PGS composites for cardiac tissue engineering applications. **Acta Biomaterialia**, 2014.
- RADISIC, M.; CHRISTMAN, K. L. Materials science and tissue engineering: Repairing the heart. **Mayo Clinic Proceedings**, v. 88, n. 8, p. 884–898, 2013.
- RAI, R. et al. Biomimetic poly(glycerol sebacate) (PGS) membranes for cardiac patch application. **Mater Sci Eng C Mater Biol Appl** 33, 3677, 2013.
- RIAZ, T. et al. FTIR analysis of natural and synthetic collagen. **Applied Spectroscopy Reviews**, v. 53, n. 9, p. 703–746, 2018.
- SARVARI, R. et al. Novel three-dimensional, conducting, biocompatible, porous, and elastic polyaniline-based scaffolds for regenerative therapies. **RSC**, p. 1–54, 2016.
- SHAIKH, R. et al. Mucoadhesive drug delivery systems. **Journal of Pharmacy and Bioallied Sciences**, v. 3, n. 1, p. 89–100, 2011.

- SHANMUGASUNDARAM, N. et al. Collagen- chitosan polymeric scaffolds for the in vitro culture of human epidermoid carcinoma cells. **In Vitro**, v. 22, p. 1943–1951, 2001.
- SHAO, L. et al. Synthesis and characterization of water-soluble polyaniline films. **Synthetic Metals**, v. 161, n. 9–10, p. 806–811, 2011.
- SHAPIRA, A.; FEINER, R.; DVIR, T. Composite biomaterial scaffolds for cardiac tissue engineering. **International Materials Reviews**, v. 00, n. 0, p. 1–19, 2015.
- VAN MEERLOO, J.; KASPERS, G. J. L.; CLOOS, J. Cell sensitivity assays: The MTT assay. **Methods in Molecular Biology**, v. 731, p. 237–245, 2011.
- VARLEY, M. C. et al. Cell Structure , Stiffness and Permeability of Freeze-dried Collagen Scaffolds in Dry and Hydrated States. [s.l.] **Acta Materialia Inc.**, 2016.
- WANG, J. et al. Antioxidant activity of polyaniline nanofibers. **Chinese Chemical Letters**, v. 18, p. 1005–1008, 2007.
- XIA, Z.; VILLA, M. M.; WEI, M. A Biomimetic Collagen-Apatite Scaffold with a Multi-Level Lamellar Structure for Bone Tissue Engineering. **Journal of Materials Chemistry B. Materials for biology and medicine.**, v. 14, n. 2, p. 1998–2007, 2015.
- YE, G.; QIU, X. Conductive biomaterials in cardiac tissue engineering. **Biotarget**, n. 5, p. 1–7, 2017.
- ZEGHIOUD, H. et al. Preparation and characterization of a new polyaniline salt with good conductivity and great solubility in dimethyl sulphoxide. **Journal of the Serbian Chemical Society**, v. 80, n. 11, p. 1435–1448, 2015.
- ZHANG, Z.; LI, G.; SHI, B. Physicochemical properties of collagen, gelatin and collagen hydrolysate derived from bovine limed split wastes. **JOURNAL-SOCIETY OF LEATHER ...**, v. 90, p. 23–28, 2006.

CONSIDERAÇÕES FINAIS

- A concepção deste projeto possibilitou o desenvolvimento de *scaffolds* lamelares densos, compostos de biopolímeros, para engenharia reversa do tecido cardíaco.
- Os resultados de propriedades fisiomecânicas e físico-químicas indicam que os *scaffolds* lamelares denso contendo proantocianidina, como agente reticulante (*PA-scaffold*), apresentam potencial aplicação na recuperação do tecido infartado.
- Os *scaffolds* lamelares densos contendo polianilina (*PANi-scaffold*) apresentaram adequada capacidade condutora, além de propriedades fisiomecânicas e físico-químicas biomiméticas ao tecido cardíaco.
- Esta pesquisa contribui para o avanço do conhecimento no campo dos biomateriais e a interdisciplinaridade das ciências específicas, as quais abrangem os conhecimentos da engenharia de tecidos.

Próximas Etapas

- Avaliar a capacidade antioxidante, dos *scaffolds* lamelares denso, e a eficácia na regeneração da função do músculo cardíaco infartado através de marcadores bioquímicos e hematológicos, bem como o mecanismo de ação de estresse oxidativo;
- Avaliar, *in vivo*, os parâmetros de contratilidade do ventrículo esquerdo e da disfunção cardíaca pelo envolvimento do fator de transcrição nuclear NF-KB após o infarto do miocárdio;
- Avaliar, *in vivo*, o aumento da espessura da área do ventrículo infartado e a diminuição de área de fibrose relacionada ao infarto;
- Avaliar, *in vivo*, a remodelação ventricular mais favorável pela verificação da expressão de citocinas como TNF $-\alpha$, IL-6 e IL-1 β .

Anexo A – Artigos Submetidos

Manuscript Details

Manuscript number	MSEC_2019_1562
Title	Design and evaluating of biomimetically inspired dense lamellar scaffold for cardiac tissue regeneration; Development, biomechanical characterization, and in vitro cellular activities.
Article type	Research Paper

Abstract

The regenerative medicine is an emerging field that aim is healing damaged tissue. The choice of crosslinking agent is one of the most important require for the development of 3D scaffolds devices. This study aimed to investigate the effects of proanthocyanidins (PA) and glutaraldehyde (GA) associated with plastic compression method on the properties of the dense lamellar scaffold with a stiffness above of the range of the heart muscle. The biomechanical and physical-chemical properties of the scaffolds were evaluated. The antioxidant activity was investigated by DPPH method; viability and proliferation cellular were evaluated by MTT and imaging cytometer (H9c2 cells). The effect of the crosslinking agents modified the biomechanical properties, but did not modify the mucoadhesion properties. PA-scaffold has the ability to bind water's molecule and to reduce the space between polymeric chains. PA-scaffold and GA-scaffold showed, respectively, 44% and 17% of antioxidant activity. Both crosslinking agents did not influence the viability and proliferation of H9c2 cells. Considering the anisotropic structure, the biomechanical properties, cellular compatibility, and protective action against reactive oxygen species, this study may provide a way to improve the inverse remodeling of heart tissue, after infarct acute of the myocardium.

Keywords regenerative medicine; cardiac scaffold; dense lamellar scaffold; proanthocyanidin; glutaraldehyde; plastic compression.

Corresponding Author Marco Chaud

Corresponding Author's Institution Sorocaba University